Journal of Hazardous Materials 501 (2026) 140929

Contents lists available at ScienceDirect

Journal of Hazardous Materials

journal homepage: www.elsevier.com/locate/jhazmat

Review

Gas-solid reaction processes for the removal of hydrogen halides from flue gases: A review

Carmela Chianese, Alessandro Dal Pozzo, Valerio Cozzani *

LISES – Laboratory of Industrial Safety and Environmental Sustainability, Department of Civil, Chemical, Environmental and Materials Engineering (DICAM), University of Bologna, Via Terracini 28, Bologna 40131, Italy

HIGHLIGHTS

- Experimental data on hydrogen halides removal by different sources are systematized.
- Reactivity trends as a function of sorbent, halide and operating conditions are reconstructed.
- Open issues in the modelling of gas-solid reactions for acid gas removal are discussed.
- Studies on HF, HBr and on simultaneous sorption of halides are identified as research priorities.

GRAPHICAL ABSTRACT

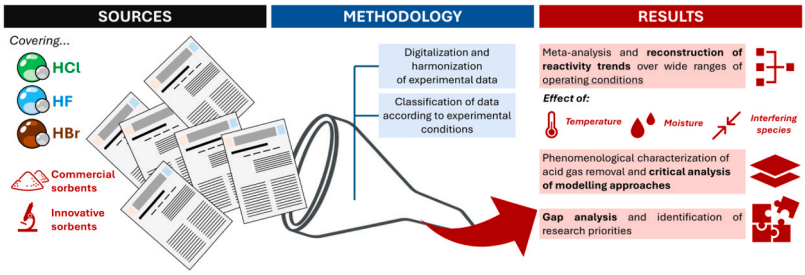

ARTICLE INFO

Keywords:
Hydrogen halides
HCl
HF
HBr
Acid gas removal
Flue gas treatment
Dry sorbent injection

ABSTRACT

The management of hydrogen halides (HX) in industrial flue gases has gained renewed attention due to increasingly stringent emission regulations worldwide. Dry treatment processes that utilize the injection of solid sorbents are effective methods for separating HX from flue gases in various sectors. Their environmental and economic sustainability critically depends on their optimization, requiring an improved understanding of the fundamental physicochemical phenomena governing the gas-solid reaction process. Thus, a comprehensive review of experimental studies on the use of calcium-, sodium-, and magnesium-based sorbents for dry HX treatment is proposed, tracking the state of the art to identify knowledge gaps, guide future research, and support current industrial practice. Data from different sources are systematically examined to elucidate the influence of conditions such as temperature, humidity, and gas composition on sorbent performance. Distinct reactivity profiles among sorbents are highlighted, with Na-based reactants exhibiting superior HCl removal efficiency at low temperatures, Ca-based reactants benefiting from moisture and surface area enhancements, and dolomitic sorbents emerging as the most effective for high-temperature applications. Critical challenges in the modelling of gas-solid reactions for HX removal are analyzed, focusing on the limitations of conventional approaches, such as the inability to fully capture incomplete sorbent conversion in Ca-based reactants. The investigation of sorbent performance towards HF and HBr, key pollutants in emerging flue gas treatment markets, and the characterization of competitive and synergistic phenomena involved in the simultaneous removal of multiple halides are identified as the main research needs to advance dry sorption in industrial flue gas cleaning.

* Corresponding author.
E-mail address: valerio.cozzani@unibo.it (V. Cozzani).

https://doi.org/10.1016/j.jhazmat.2025.140929
Received 22 May 2025; Received in revised form 21 December 2025; Accepted 23 December 2025
Available online 24 December 2025

1. Introduction

1.1. Hydrogen halides emissions in flue gases

Hydrogen halides (HX, where X stands for F, Cl, Br, I) are a class of hazardous materials that are present in gaseous form in several industrial flue gas streams, more frequently due to the combustion of a fuel or to the thermal decomposition of a raw material that contains the corresponding halogen. Quantitatively speaking, the anthropogenic emissions of hydrogen chloride (HCl) are the most relevant among halides, leading to an estimated global annual rate in the range of 1661–3200 kt_{Cl}/y [1]. The main source of HCl emissions is the incineration of industrial and urban waste [2,3]. Specifically, HCl can be released from the combustion of alkali salts in food waste [4] and Cl-containing plastics [5], such as polyvinyl chloride, PVC [6], which exhibits a chlorine content >6 wt% [7]. HCl is also present in medical waste: during their combustion, HCl gas can evolve from Cl-bearing plastics and physiological saline solutions [8].

Biomass combustion can also give rise to HCl emissions [9], depending on the chlorine concentration in the biomass fuel, which is typically low in wood and higher in herbaceous biomass, fruit, and crop residues [10]. HCl is a typical contaminant also in other thermal treatment of waste and biomass, as it is present, e.g., in syngas derived from biomass gasification [11,12] or plastic pyrolysis [13]. Biogas from landfill gas collection or sewage sludge digestion contains HCl as a trace pollutant [14]. Furthermore, coal-fired power plants are estimated to contribute to *ca* 25 % of the global HCl emissions [1], as hard and brown coals have a world average Cl content of 340 and 120 ppm, respectively [15]. In the pyrometallurgical recovery of spent Li-ion batteries, the use of chlorinating agents is expected to be a source of HCl emissions [16].

Hydrogen fluoride (HF) is also a typical pollutant in flue gases from waste incineration. Its presence is often associated with specific waste streams, such as, e.g., materials containing polytetrafluoroethylene (PTFE) as automotive shredder residues [17], or sewage sludge rich in per- and polyfluoroalkyl substances [18]. Beyond waste incineration, HF emissions are prevalent in other industrial sectors. HF is commonly found in flue gases from the ceramic tile industry [19], where it is released from the decomposition of fluorine-bearing clays [20]. Alongside HCl, HF is a flue gas contaminant in copper smelting [21] and glass manufacturing, where it might arise from the thermal decomposition of F-containing raw materials and the inclusion of specific chemical additives [22]. In the aluminum industry, HF is present in the effluent gases from the electrolytic production of primary aluminum [23,24] and it can be released by thermal pre-treatment of aluminum waste (e.g., PTFE-coated cookware) during secondary aluminum production [25].

Hydrogen bromide (HBr) is a highly specific pollutant, and its emissions typically evolve from the thermal treatment of brominated compounds [26]. As brominated resins are extensively used as flame retardants, electronic waste (WEEE) and waste printed circuit boards (WPCBs) usually contain brominated compounds [27]. An estimation of the amount of the yearly production of brominated resins is provided by Ghosh et al. [28] (200 kt worldwide at the time of the study), while Beccagutti et al. [29] provide figures concerning the Br content in WEEE. Relevant HBr emissions are thus present in the incineration of brominated wastes and in pyrometallurgical processes, which represent a growing sector for the recovery of valuable critical elements from WEEE and WPCBs [30].

Table 1 provides a summary of the main industrial sectors where emissions of gaseous hydrogen halides occur and the related typical ranges of HX concentrations in the untreated flue gas.

The uncontrolled emission of hydrogen halides is harmful for human health and the ecosystem, as these compounds are toxic substances, precursors of environmental acidification [28,40] and contributors to photochemical pollution [41]. In fact, HCl has been the first major pollutant to be regulated through pollution control legislation in history, dating back to the Alkali Act enacted by the British Parliament in 1863 to limit the venting of hydrochloric acid in soda ash production [42]. Significant progress has been made over the decades to curb the emissions of hydrogen halides [43] and, nowadays, the concentration of HX compounds at the stack of facilities such as waste-to-energy (WtE) plants is typically orders of magnitude lower than that in the untreated flue gas [44]. However, interest in HX removal is rising again for at least two reasons.

Table 1
Main industrial sectors affected by the emission of hydrogen halides.

Sector/activity	Typical concentration in raw flue gas (mg/Nm^3)			Source
	HCl	HF	HBr	
Waste incineration				
Municipal solid waste	500–2000	5–20	trace	[31–33]
Industrial waste	3000–10000	50–1000	trace	[32]
Medical waste	2500	5–20	trace	[8,34,35]
Sewage sludge	500–1500	5–100	-	[18,32]
WEEE / batteries	50–1000	5–100	50–3000	[29]
Coal combustion	5–100	-	-	[36]
Biomass combustion	100–1000	-	-	[37]
Non-ferrous metals Smelting	Trace	30–70	-	[38,25]
Ceramic manufacturing	30–50	30–150	-	[39]

First, current environmental policies worldwide are setting new, ambitious standards for air pollution control. A relevant example is the European Union (EU) Action Plan towards "Zero Pollution" for air, water, and soil [45], coupled with the continuous improvement required by Best Available Techniques (BAT) updates in industrial emissions policy [46]. Similarly, starting from the introduction of ultra-low emission (ULE) standards for coal-fired power plants in 2014 [47], China has inaugurated a season of ambitious emission control policies across all industrial sectors. For instance, the Chinese flat glass industry is now subject to some of the strictest acid gas emission standards worldwide [48], and the significant increase in waste incineration capacity has been coupled with a significant tightening of emission control requirements [49].

Second, a significant driver for current research is the need to optimize the flue gas cleaning process from a holistic point of view, focusing not only on the minimization of the emissions at the stack, but also on the reduction of the environmental impact across the entire life cycle of flue gas treatment [50]. Suboptimal processes consume excess feed rates of reactants and generate high amounts of solid residues, which are classified as hazardous waste for the presence of trace pollutants such as heavy metals and dioxins, and due to the high leaching potential of solid halides [51,52].

This review aims at tracking the state of the art concerning the heterogeneous gas-solid reaction processes involved in HX abatement in dry treatment technologies, specifically addressing the underlying fundamental physicochemical phenomena crucially influencing yields and conversions of the full-scale industrial systems.

Dry treatment processes based on the reaction of HX with Ca-, Na-, and Mg-based sorbents, as discussed in the following, are the most widespread technologies for HX abatement across industrial sectors. Despite the apparent simplicity of such reaction processes, several fundamental aspects still need to be fully understood. The comparative reactivity of the different categories of sorbents toward the different halides (and combination thereof) has not been characterized by any single study over the full range of operating temperatures of industrial interest. Furthermore, a representative description of the influence of moisture and interfering species typically present in the flue gas (SO_2, CO_2) is still an unresolved challenge limiting the accuracy of conventional modelling approaches.

Therefore, the present study collects and systematizes the relatively fragmented literature on the topic to: i) combine experimental evidences from different sources to provide reactivity data on the widest combinations of hydrogen halides, sorbents, and operating conditions

(temperature, humidity, flue gas composition), ii) analyze the open issues in the phenomenological characterization of the reaction process and the modelling approaches adopted to target them, and iii) identify the key gaps that ongoing research in the field should aim to address.

1.2. Dry hydrogen halide removal processes

Processes for the removal of acid pollutants from flue gas streams can be classified into either "wet processes" or "dry processes", including semi-dry techniques [53].

Wet processes, based on the scrubbing of flue gases with water or basic solutions [54], in order to promote the physical and chemical absorption of hydrogen halides, have been in the past the most widespread technology, due to the high removal efficiency and low operating costs. However, wet scrubbing presents relevant drawbacks, namely the production of acidic or basic wastewater streams, carrying trace contaminants, which require physicochemical treatment before safe discharge into public sewage systems [55], and the cooling and saturation of the flue gas released into the atmosphere, which hinders atmospheric dispersion and creates plume visibility issues [56].

In recent years, dry and semi-dry treatments were increasingly considered as alternatives to wet processes, in particular in Europe [57, 58]. Dry sorbent injection (DSI) processes consist of the direct introduction into the flue gas ductwork of a pulverized basic sorbent [59]. In semi-dry techniques, the sorbent is sprayed in the form of a water suspension, which quickly evaporates in the hot flue gases [60]. In both cases, the sorbent reacts with acid pollutants via a heterogeneous reaction process. At the core, the reaction is an acid-base neutralization that can be summarized as follows:

$$\textbf{\textit{Base}} + \textbf{\textit{Acid}} \rightarrow \textbf{\textit{Salt}} + \textbf{\textit{Water}} \quad (1)$$

The resulting salts are solid reaction products that are collected downstream in gas-solid separators (typically, fabric filters [61]. The filter is an integral part of the DSI technique, as the reaction takes place both in the duct upstream of the filter and on the layers of solid particles deposited on the filter itself, thus increasing the overall contact time between sorbent and gaseous reactant [62]. DSI methods are widely employed in industrial processes and are listed among the best available techniques (BAT) for flue gas treatment in the BAT Reference Documents of the European Commission for a variety of industrial sectors. The benefits of DSI include low investment costs and low impact on plant layout, ease of operation, possibility of combination with dioxins, mercury, and fine particles removal [63].

Nevertheless, dry processes present a relevant drawback. To ensure safe compliance with emission standards and to achieve high removal efficiency, a large excess in sorbent feed, up to more than 4–5 times the stoichiometric demand, is typically fed to the process [53]. The overconsumption of reactants and the resulting overproduction of solid process residues constitute both an unnecessarily high operating expenditure and a non-negligible source of indirect environmental impact [55].

Under the concurrent drivers of increasingly stringent emission limits, on one hand, and soaring costs for the procurement of sorbents and the management of solid process residues, on the other hand, plant operators and technology suppliers face the pressing need to optimize the DSI process and enhance sorbent utilization. Therefore, a better understanding of the fundamentals of the gas-solid reaction process is required to go beyond an operational practice that is currently mostly empirical [33] and to allow for a fully aware optimization of the design and control of acid gas treatment systems.

1.3. Structure of the review

This review is structured as follows. Section 2 provides some methodological notes and preliminary scientometric data concerning the documents collected. Section 3 presents the different types of sorbents studied in the literature with regard to HX removal via gas-solid reactions. Section 4 reviews the experimental setups and conditions adopted by investigators. A critical discussion of the most relevant experimental findings is carried out in Section 5 with reference to the removal of single hydrogen halides (HCl, HF, and HBr) and in Section 6 with reference to studies addressing the simultaneous removal of different halides, also considering the most relevant interfering acidic species (SO_2 and CO_2). Section 7 discusses the comparative performance assessment of sorbents. The modelling approaches developed in the literature for the interpretation of experimental findings are reviewed in Section 8. Lastly, Section 9 summarizes the most relevant findings, and in Section 10, the conclusions and future perspectives are stated.

2. Methodology

2.1. Inclusion criteria

The present review analyzes methodological approaches, models and experimental findings reported in scientific publications addressing the removal of hydrogen halides, available in international peer-reviewed journals indexed in the Scopus database. The approach used in the systematic review is in accordance with the PRISMA Flow Diagram [64]. Relevant publications were searched using the combination of keywords listed in Table 2, identifying a corpus of 230 papers encompassing research published from the 1980s to the present day. Fig. 1 illustrates the flow chart of the methodology applied for the bibliographic search, also reporting the number of records identified, screened, excluded, and included in the review.

2.2. Scientometric analysis

Fig. 2 illustrates the timespan of the body of literature considered for the present review. The removal of hydrogen halides for flue gas cleaning has been an active field of research since the late 1970s, but the distribution of scientific articles has been irregular over the years. Such variability, which also exhibits differences across countries, may be attributed to the divergent evolution of environmental regulations.

In North America, the relevant research effort on the topic from the 1980s up to the early 2000s can be directly linked to intense regulatory activity over those decades, starting with the 1990 US Clean Air Act (CAA) Amendments [65], requiring the creation of technology-based standards for emission control and dedicated CAA rules for municipal waste combustors (first extension in 1995 and revision in 2006). The publications dating back to that period (see Fig. 2) served as a scientific and technical base for the implementation of standards, as most of the research was funded or directly performed by the US Environmental Protection Agency.

Analogously, in Europe, a relevant research activity preceded the first publication of the EU reference documents on the best available techniques for emission control in the WtE sector (2006), large combustion facilities (2006), and industrial sectors such as glass and ceramic tile manufacturing (2008). However, after a decade of relative inactivity, a renewed interest in acid gas removal is present in recent years. Although industrial flue gas treatment systems have been able to comply

Table 2
Generation of search strings by the combination of three-level keywords.

Primary words (pollutant)	Secondary words (process)	Tertiary words (sorbent)
"Hydrogen chloride", HCl	removal	calcium
"Hydrogen fluoride", HF	(ad)sorption	sodium
"Hydrogen bromide", HBr	treatment	magnesium
	abatement	lime
	reaction	dolomit*
	neutralization	
	injection	

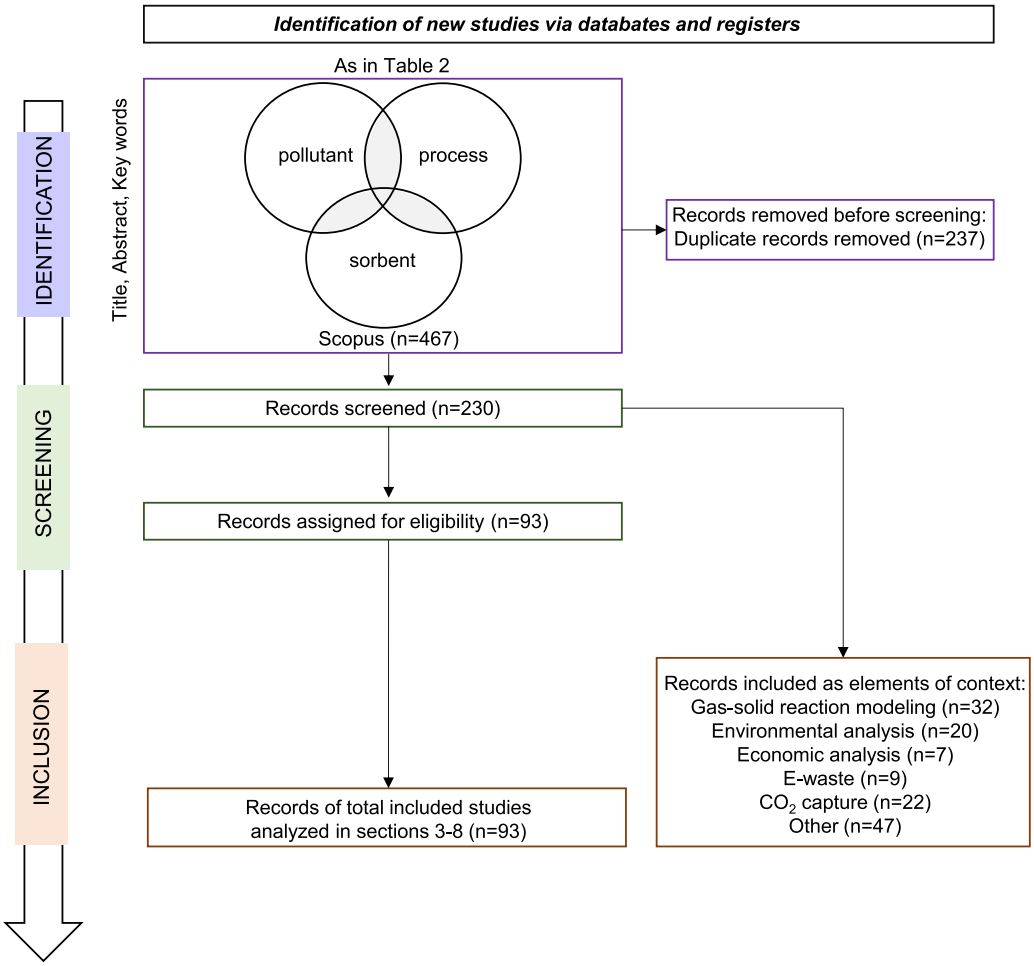

Fig. 1. PRISMA Flow Chart applied in the systematic literature search.

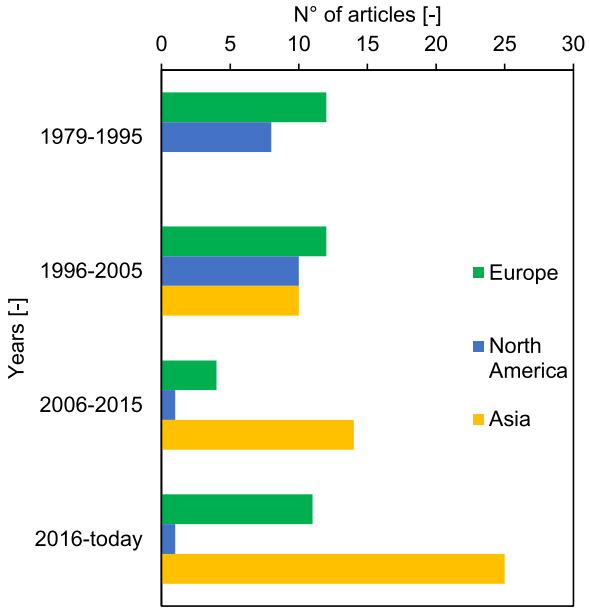

Fig. 2. Year of publication and geographical distribution of the affiliation of the authors of the publications included in the study.

with extremely tight emission standards on hydrogen halides for years [43], the concept of integrated pollution control, which is a cornerstone in the EU policy on industrial emissions (Industrial Emissions Directive), has recently imposed a paradigm shift from the mere compliance with emission limit values at the stack to a holistic minimization of the overall environmental impact of an industrial process. Nowadays, close attention is paid to the reduction of the cross-media effects of flue gas treatment [50,66,67]. Therefore, a renewed focus on the optimization of flue gas cleaning processes, in order to rationalize reactant usage and process waste generation, has rekindled the interest for a deeper understanding of the chemical and physical fundamentals of HX abatement [68,69].

As shown in Fig. 2, publications authored by scientists with affiliations in the Asian continent have seen a remarkable increase over the years. The introduction in 2014 of the so-called "ultra-low emissions" (ULE) standards policy in China for existing and new coal-fired power plants [70], together with a general strengthening of emission standards across industrial sectors [48], is often cited as the motivation for undergoing research on acid gas removal in the introduction of scientific publications from Chinese research institutions.

Fig. 3 shows the relations between the different research groups active in the field. The analysis, performed using the *VOSviewer* software, correlated articles by citations, using organizations as reference units, encompassing both universities and research institutes. As shown in the figure, in recent years, Chinese universities have performed most of the research in the field, although significant research activity is also carried out in Europe, where the University of Bologna (Italy) and the Czech Academy of Science (Czech Republic) emerge as the most active centers of investigation on the topic.

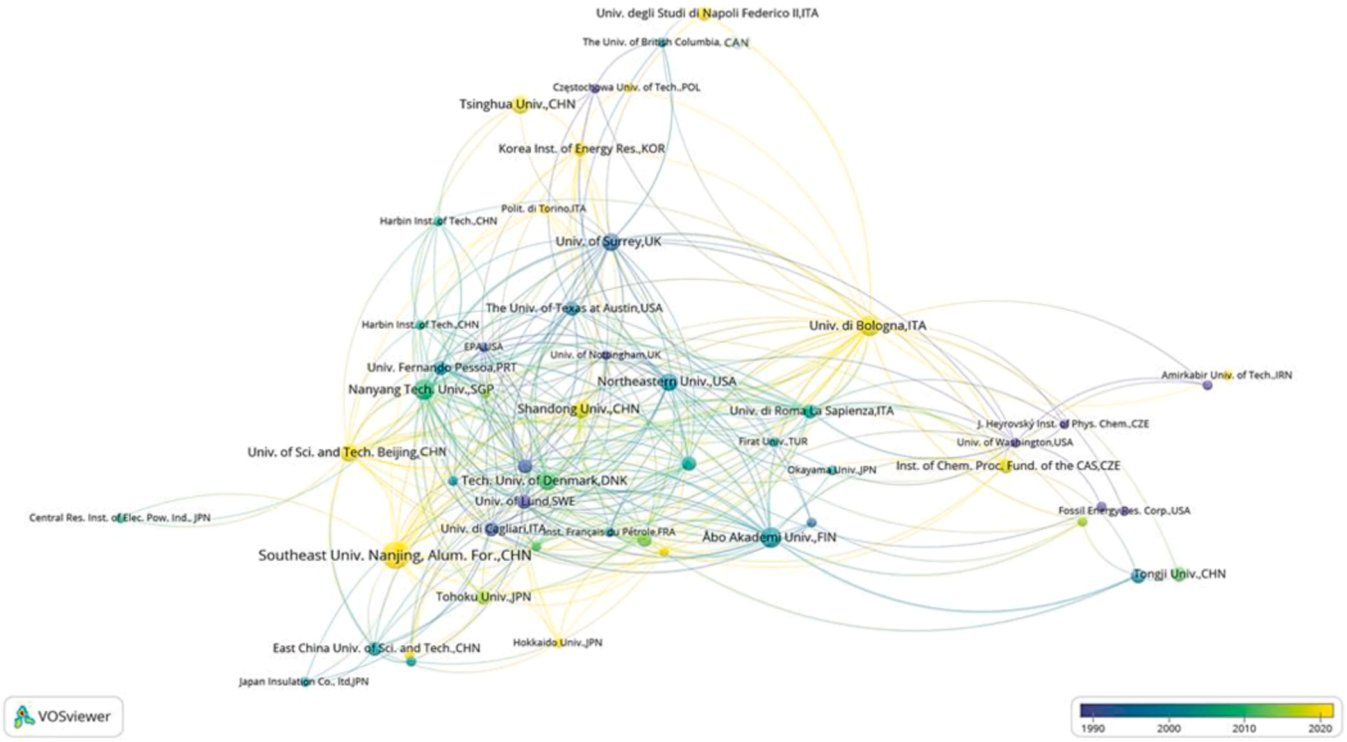

Fig. 3. Scientometric mapping of research institutions active in the acid gas removal field, classified per year of the most recent publication.

3. Sorbents

Various sorbents for acid gas removal have been extensively investigated in the literature and adopted in current industrial practice. They can be grouped in two broad categories: *commercial sorbents*, i.e., sorbents that are already on the market and employed for flue gas treatment at full-scale facilities, and *innovative sorbents*, i.e., sorbents that have been synthesized by research groups and to date tested only at laboratory or pilot scale.

3.1. Commercial sorbents

Commercial sorbents can be further divided into calcium-, sodium-, and magnesium-based sorbents.

Calcium-based sorbents. Ca-based compounds have been the first reactants to be considered for dry acid gas removal. Earlier acid gas abatement efforts, focused first on SO_2 emission control in coal-fired power plants [71] and then also on HCl [72], were based on the high-temperature injection of raw limestone (chemically, calcium carbonate, $CaCO_3$) directly in the combustion chamber. From the late 1980s, the use of calcium hydroxide, $Ca(OH)_2$, was introduced in flue gas treatment, obtained from the calcination and subsequent hydration of limestone. Commonly known as hydrated lime or slaked lime, $Ca(OH)_2$ is more reactive than calcium carbonate, mainly due to the increased basic strength [73] and the higher porosity [74]. Commercial hydrated lime samples typically exhibit a BET surface area in the range 10–25 m^2/g [75,76], although specific products with $S_{BET} > 40\ m^2/g$ are now available on the market [77].

Depending on the injection temperature, the species reacting with hydrogen halides can be either $Ca(OH)_2$ or calcium oxide (CaO), if injection takes place at a temperature higher than 400°C. Similarly, when calcium carbonate is injected, the reacting compound may be $CaCO_3$ or CaO if the injection takes place at a temperature higher than 650°C [78].

Several studies regarding the gas-solid reaction between Ca-based sorbents and HCl have assumed calcium chloride ($CaCl_2$) as the solid-phase product, either in anhydrous or dihydrate form:

$$Ca(OH)_{2\ (s)} + 2{\cdot}HCl_{(g)} = CaCl_{2\ (s)} + 2{\cdot}H_2O_{(g)} \quad (2)$$

$$Ca(OH)_{2\ (s)} + 2{\cdot}HCl_{(g)} = CaCl_{2} \cdot 2{\cdot}H_2O_{(s)} \quad (3)$$

$$CaO_{\ (s)} + 2{\cdot}HCl_{(g)} = CaCl_{2\ (s)} + H_2O_{(g)} \quad (4)$$

However, studies focusing on the identification of the reaction product via analytical techniques pointed out the formation of calcium hydrochloride (CaOHCl), a compound characterized by Allal et al. [79], as an intermediate or as the final solid product of the reaction, depending on operating conditions. Chin et al. [80] found that the chlorination product of CaO is initially CaOHCl, but over an extended reaction period (800 min) CaOHCl ultimately transforms into $CaCl_2$. Partanen et al. [81]determined that the only chlorination product of CaO at T > 650 °C for a shorter reaction time (15 min) is CaOHCl, while in the case of a longer exposure (150 min), $CaCl_2$ is formed. Jozewicz and Gullett [78] reported the formation of different products depending on the reaction temperature: a mixture of $CaCl_2$•2 H_2O and CaOHCl at 500 °C and only CaOHCl at 200 °C. In the temperature range of main interest for DSI applications (120–180 °C), Dal Pozzo et al. [82] reported only CaOHCl as the reaction product. Accordingly, sample evidence from the chemical analysis of solid residues collected from full-scale dry flue gas treatment systems [83–87] confirm that CaOHCl is the primary solid product of the reaction between $Ca(OH)_2$ and HCl at low temperatures, which proceeds as follows:

$$Ca(OH)_{2\ (s)} + HCl_{(g)} = CaOHCl_{(s)} + H_2O_{(g)} \quad (5)$$

Conversely, experiments carried out in a thermogravimetric analyser (TGA) found that, at temperatures higher than 500 °C, CaOHCl in the presence of CaO converts to $CaCl_2$ [82,88], confirming that in the high temperature range the stable product of reaction with HCl is $CaCl_2$. A wider discussion on the characterization of the reaction products in the $Ca(OH)_2$/HCl system is provided by Dal Pozzo et al. [82].

When calcium hydroxide reacts with HF and HBr, the following stoichiometric equations are assumed [89,90]:

$$Ca(OH)_{2\ (s)} + 2{\cdot}HF_{(g)} = CaF_{2(s)} + 2{\cdot}H_2O_{(g)} \quad (6)$$

$$Ca(OH)_{2\ (s)} + 2{\cdot}HBr_{(g)} = CaBr_{2(s)} + 2{\cdot}H_2O_{(g)} \quad (7)$$

No evidence of the formation of oxidized products is reported in the literature to date.

Sodium-based sorbents. The first studies on the use of sodium carbonate (Na_2CO_3) for acid gas abatement date back to the 1980s, as documented by Mocek et al. [91] and Kimura and Smith [92]. However, it was not until the mid-1990s that Solvay S.A. launched the NEUTREC process [93], Na-based sorbents gained widespread commercial adoption, primarily in WtE plants. The NEUTREC process is a typical DSI technique, involving the injection of $NaHCO_3$ into the flue gas stream at an optimum temperature of 200 °C and the subsequent separation of solid reaction products using a fabric filter or an electrostatic precipitator [94,95].

When introduced in the flue gas at a temperature higher than 130 °C, sodium bicarbonate undergoes an almost instantaneous decomposition to sodium carbonate [96]:

$$2{\cdot}NaHCO_{3\ (s)} = Na_2CO_{3\ (s)} + CO_{2\ (g)} + H_2O_{(g)} \quad (8)$$

This process, also known as thermal activation, has a pivotal role in enhancing the reactivity toward acid pollutants. The release of CO_2 and H_2O generates a porous structure that increases the specific surface area, improving in turn the efficiency of the reactions with acid gases [97]

The nascent sodium carbonate reacts with hydrogen halides to form the corresponding sodium salt according to the following reactions [98,99]:

$$Na_2CO_{3\ (s)} + 2{\cdot}HCl_{(g)} \rightarrow 2{\cdot}NaCl_{(s)} + CO_{2\ (g)} + H_2O_{(g)} \quad (9a)$$

$$Na_2CO_{3\ (s)} + 2{\cdot}HF_{(g)} \rightarrow 2{\cdot}NaF_{(s)} + CO_{2\ (g)} + H_2O_{(g)} \quad (9b)$$

$$Na_2CO_{3\ (s)} + 2{\cdot}HBr_{(g)} \rightarrow 2{\cdot}NaBr_{(s)} + CO_{2\ (g)} + H_2O_{(g)} \quad (9c)$$

Magnesium-based sorbents. Sorbents derived from dolomite rock have been introduced in the last few years for specific use in high-temperature furnace injection, to overcome the limitations of limestone [100]. Their chemical composition typically includes calcium hydroxide, $Ca(OH)_2$, magnesium oxide, MgO, and/or magnesium hydroxide, $Mg(OH)_2$ [101]. The advantage of these reactants, often referred to as dolomitic sorbents, is due to the presence of the Mg compounds, exhibiting a high Tammann temperature that explains enhanced resistance to sintering [102].

When injected in a combustion chamber, at temperatures higher than 800 °C, the hydroxides undergo decomposition, releasing water vapor and forming meso- and macropores in the material [103]:

$$Ca(OH)_2{\cdot}(MgO)_x{\cdot}(Mg(OH)_2)_{1-x\ (s)} \rightarrow CaO{\cdot}MgO_{(s)} + (2-x)H_2O_{(g)} \quad (10)$$

The development of the porous structure promotes the reactivity of the sorbent towards acid pollutants. The possible reactions with HCl are the following [103]:

$$CaO_{(s)} + 2{\cdot}HCl_{(g)} \rightarrow CaCl_{2\ (s)} + H_2O_{(g)} \quad (11)$$

$$MgO_{(s)} + 2{\cdot}HCl_{(g)} \rightarrow MgCl_{2\ (s)} + H_2O_{(g)} \quad (12)$$

Nonetheless, it is generally assumed that MgO is inert towards HCl in the temperature range of interest (800–1000°C). The thermodynamic analysis carried out by Dal Pozzo et al. [100] indicates that, at temperatures exceeding 900 °C, only reaction 11 shows a negative Gibbs free energy of reaction. Correspondingly, Zhou et al. [104] found no magnesium chloride in the solid residues resulting from HCl removal with dolomitic lime.

Therefore, in the acid gas removal process started by the activated dolomitic sorbent following reaction 10, it is postulated that CaO is the active compound reacting with HCl (as well as with other acid pollutants present in the flue gas, as SO_2), while MgO acts as a sintering-resistant structural component, preventing the collapse of the porous structure that develops during reaction 10, as proposed by Biganzoli et al. [103].

3.2. Innovative sorbents

To enhance the efficiency of acid gas removal, a wide body of research has been devoted to novel formulations of Ca-, Na-, and Mg-based sorbents that overcome the limitations of commercial materials. The main goals are: i) enhancing sorption kinetics by increasing the specific surface area of the sorbent, and ii) reducing sintering by the incorporation of a support. Relevant examples of synthetic sorbents formulated in the literature are listed in Table 3, classified by the synthetic approach.

The simplest synthesis method is represented by the mere *wet mixing* of precursors in water or aqueous solutions. Upon drying, the resulting solid phase is crushed and sieved. For Ca-based compounds, adding an organic solvent to water to form an aqueous hydration solution increases the surface area of the resulting hydrated lime [75]. Recently, Wang et al. [87] described the simple synthesis of high-surface-area calcium hydroxide through the hydration of CaO powder in a solution of ethanol and deionized water, with the volumetric ratio 3:4 producing the particles with the highest BET area at over 66 m^2/g. If both soluble and insoluble precursors are used, wet mixing results in a rather uniform deposition of the soluble compound on the surface of the insoluble substrate, allowing, e.g., the preparation of mixed Na/Ca sorbents [105] or Ca/Al sorbents [106].

Impregnation has been frequently adopted to deposit Ca- or Na-based compounds from an alkaline solution on a support, typically alumina. For example, Liang et al. [107] coated commercial activated alumina balls with $Ca(OH)_2$, NaOH or Na_2CO_3 by wetness impregnation. Na_2CO_3-coated alumina balls exhibited the highest HCl binding capacity, as impregnation resulted in the formation of Na_2CO_3 fibrous structures, reducing diffusional limitations.

Co-precipitation is a widely used method for the preparation of particles of micrometric and nanometric size. In the context of Ca- or Na-based sorbents, a cation solution and an anion solution are generally mixed at a controlled pH to precipitate either a hydroxide or a carbonate that can be subsequently calcined [108]. Co-precipitation has often been employed also to mix the sorbent with inert supports (mainly, Mg or Al) with the aim of stabilizing the porous structure of the solid [109,110]. Layered double hydroxides (LDHs) are a popular class of sorbent materials that are in generally synthesized through co-precipitation. LDHs, sometimes denoted as hydrotalcite-like sorbents, are lamellar compounds where positively charged mixed metal hydroxide layers are intercalated with interlayer regions containing charge-compensating anions and water molecules [111]. Kameda and coworkers in 2010 [112] explored the use of magnesium-aluminum LDHs for the neutralization of several acid pollutants, including gaseous HCl. The synthesis protocol started from magnesium nitrate, ammonium nitrate, and sodium carbonate, and involved NaOH for pH correction. The resulting LDHs were intercalated with CO_3^{2-} ions (CO_3•Mg-Al LDH), but could be converted into structures intercalated with OH^- ions (OH•Mg-Al LDH) by calcination at 500 °C. The performance of Mg-Al LDHs in removing HCl was found to increase as the Mg/Al molar ratio increased [113], and OH•Mg-Al LDH exhibited a higher removal efficiency than CO_3•Mg-Al LDH [114]. Interestingly, the authors demonstrated that HCl sorption on the synthesized LDHs is reversible and that the sorbents may be regenerated in aqueous Na_2CO_3 [113] or under a CO_2 flow [115]. Similarly, Cao and coworkers focused on the synthesis of Ca-Al and Ca-Mg-Al LDHs [116,117]. They calcined the sorbent synthesized through co-precipitation in order to remove structural water in the interlayer galleries and decompose the carbonate anions present in the metal hydroxide layers [116]. The resulting material exhibited a specific surface area 10 times higher than that of reference calcium oxide, leading to a high removal efficiency once exposed to HCl.

Table 3
Routes for the preparation of innovative sorbents and relevant examples.

Synthesis method	Description	Sorbent	References
pelletizing	• Pelletizing of alkali and alkali earth metals with binders (bentonite or sodium silicate) and texturing agents. • Drying of pellets at 100 °C for 2 h. • Calcination at 550 °C in air for 6 h.	ECl1: $NaHCO_3$, $CaCO_3$, $Ca(OH)_2$, $Mg(OH)_2$;	[124]
impregnation	• Impregnation of alkali or alkali earth compounds on Al_2O_3. • Crushing and sieving of the sorbent.	ECl2: $Ca(OH)_2$, Al_2O_3	[124]
	• Dissolution of $Ca(OH)_2$, NaOH and Na_2CO_3 powders in deionized water. • Impregnation of activated alumina balls (AAB) in the solution prepared above. • Ultrasonic shocking for 1 h, immersion for 17 h, and drying at 200 °C for 24 h.	$10Na_2CO_3$-AAB	[107]
hydrothermal synthesis	• Mixing of $NaHCO_3$, $Ca(OH)_2$, $Mg(OH)_2$ with binders and texturing agents. • Calcination at 550 °C for 6 h.	$NaHCO_3$, $Ca(OH)_2$, $Mg(OH)_2$,	[125]
	• Mixing of alumina-sol, amorphous silica, and lime in autoclave with distilled water. • Heating at 200 °C for 15 h. • Filtration and drying of the sorbent at 110 °C for 24 h.	$[Ca_3Al_2\text{-}(SiO_4)(OH)_8]$	[126]
dip-coating	• Mixing of soda ash and 2-propanol. • Soaking of honeycomb support in the solution prepared above for 1 min • Drying of the solution.	Soda ash with honeycomb support	[127]
co-precipitation	• Mixing of $Mg(NO_3)_2$, $Al(NO_3)_3$, and Na_2CO_3 at 30 °C. • Dropwise addition of NaOH to keep pH= 10.5. • Stirring for 8 h • Filtering of the precipitated sorbent and washing with deionized water. • Drying at 40 °C under reduced pressure.	CO_3·Mg-AL LDH	[112]
	• Mixing of $Mg(NO_3)_2{\cdot}6\ H_2O$, $Ca(NO_3)_2{\cdot}4\ H_2O$, and $Al(NO_3)3{\cdot}9\ H_2O$ in deionized water. • Precipitaion of 2 solutions $NaHCO_3$ and Na_2CO_3. • Titration, filtering, and washing of the solutions. • Drying for 24 h.	Ca−Mg−Al HTlc material	[117]
	• Mixing of $Mg(NO_3)_2{\cdot}6\ H_2O$, $Ca(NO_3)_2{\cdot}4\ H_2O$, and $Al(NO_3)_3{\cdot}9\ H_2O$ with water at 60 °C. • Dropwise addition of the solution above to a solution of Na_2CO_3 and $NaHCO_3$. • Titration to keep the pH value at 10. • Aging of the suspension. • Washing of the sorbent with deionized water. • Drying at 85 °C for 1440 min	CaMgAl-HTLc	[116]
	• Mixing of $Mg(NO_3)_2{\cdot}6\ H_2O$, $Ca(NO_3)_2{\cdot}4\ H_2O$, and $Al(NO_3)_3{\cdot}9\ H_2O$ with water at 60 °C. • Dropwise addition of the solution above to a solution of Na_2CO_3 and $NaHCO_3$. • Titration to keep the pH value at 10. • Stirring of the slurry at 65 °C for 24 h. • Filtering and washing with deionized water until pH reached 7. • Drying of the precipitate at 95 °C for 12 h. • Addition of the sorbent to a $KF{\cdot}2\ H_2O$ solution. • Primary drying of the precipitate at 150 °C. • Secondary drying at 95 °C for 12 h. • Calcination at 550 °C for 5 h.	KF/CaMgAl-HTLc	[128]
	• Mixing of $Mg(NO_3)_2$ and $Al(NO_3)_2$ with Na_2CO_3 to keep pH value to 10. • Filtering of the slurry and washing with deionized water. • Calcination at 700 °C in air for 4 h.	Na-Mg-Al HTLc	[129]
	• Mixing of $Mg(NO_3)_2 \cdot 6\ H_2O$ and $Al(NO_3)_2{\cdot}\ 9\ H_2O$ with NaOH and Na_2CO_3 into ultra-pure water at 60 °C to keep pH value to 11–11.5 • Stirring of the sorbent at 60 °C for 2 h. • Growing of crystals at 80 °C for 20 h. • Washing, drying, and sieving of the sorbent.	CO_3·Mg-AL LDH	[130]
ball milling	• Mixing and milling of raw slag with NaOH powder. • Heating of the mixture at 600 °C for 6 h. • Cooling of the fused mixture at room temperature. • Milling and mixing with $Al(OH)_3$ powder. • Addition of the mixture into distilled water. • Heating at 120 °C for 24 h. • Filtering and washing of the sorbent with water. • Drying at 60 °C overnight.	$CaCO_3$, $Ca_3Al_2(SiO_4)_{0.8}(OH)_{8.8}$, $Na_8Al_6Si_6O_{24}(OH)_2$	[131]
	• Mixing of CaO with NaOH. • Milling with agate grinding balls at 400 rpm for 1 h.	NaOH-modified CaO	[123]
	• Calcination of $CaCO_3$ to obtain CaO. • Mixing of CaO with deionized water. • Drying at 75 °C for 12 h. • Powdering of the sorbent with a mortar and a pestle. • Mixing of the powder with deionized water. • Milling with zirconia balls at 100, 200, and 400 rpm for 3 h. • Drying at 75 °C for 12 h.	Modified $Ca(OH)_2$	[121]
	• Dissolution of metal salts/organic solvents with deionized water. • Mixing of the solution with CaO. • Doping with ball milling.		
wetmixing +calcination	• Mixing of of $H_3AlO_3{\cdot}xH_2O$ and $CaAl_2O_4$ with deionized water. • Stirring at 50 °C. • Calcination of the slurry at 850 °C for 5 h. • Crushing and sieving of the sorbent.	85Al-15Ca	[106]

(*continued on next page*)

Table 3 (*continued*)

Synthesis method	Description	Sorbent	References
	• Mixing of $CaCO_3$ with phenol resin and. • Pellet formation by molding method. • Calcination at 500 °C in nitrogen for 1 h.	Ca-C	[132]
	• Mixing of Na_2CO_3, alumina-sol, and γ-alumina powder. • Drying and calcination in air.	$NaAlO_2$	[133]
wet mixing+drying	• Hydration of CaO with deionized water. • Addition of sodium alkali into industrial CaO and $CaCO_3$. • Drying of the solution.	CaO+$CaCO_3$+sodium alkali	[105]
	• Mixing of CaO powder with ethanol solution. • Stirring at 70 °C. • Drying at 105 °C for 12 h. • Crushing and sieving of the sorbent.	Ethanol-modified CaO	[87]
	• Mixing of CaO powder with ethanol solution in a 70 °C water bath. • Drying at 105 °C for 12 h.	Ethanol-modified CaO	[134]

Mechanochemistry, i.e., chemical synthesis enabled by the application of mechanical force [118], has been gaining increasing interest as a clean, safe, and solvent-free synthesis route for sorbents [119]. *Ball milling*, as a key mechanochemical technique, utilizes high-energy grinding to reduce the particle size of sorbents to nanoscale grains. For example, Wysocki and Szymanek [120]compared the use of an impact mill and an electromagnetic mill for the micronization of sodium bicarbonate. Zhou et al. [121] prepared $Ca(OH)_2$ particles by ball milling that presented up to a 52 % higher specific surface area and a 5 times smaller crystallite size compared to $Ca(OH)_2$ obtained from the common route of CaO hydration. In addition, ball milling is a suitable method to synthesize composite sorbents, e.g., by combining a sorbent compound and a support [122], due to an excellent macro-scale mixing and micro-scale chemical bond reconstruction. Shen et al. [123] highlighted the effectiveness of doping mechanically modified sorbents with additional agents during ball milling. In particular, they showed that the addition of 5 wt% NaOH did not negatively affect the porosity of CaO and enhanced its alkalinity, ultimately improving its HCl removal performance.

4. Experimental configurations and operating conditions

Table 4 presents the configurations employed in the literature analyzed for the investigation of the heterogeneous gas-solid dry removal process of hydrogen halides. The reactions involved in the process have been studied at different reactor scales. A few authors carried out TGA sorption tests, typically performed on 1–10 mg of sorbent, while the majority opted for fixed-bed reactors, which were operated at sorbent loads of 10–1000 mg. Although in the industrial DSI systems the first contact between sorbent and acid pollutants occurs in entrained flow [135], fixed beds have been a popular choice for their ease of operation and the reproducibility of test conditions. In addition, the fixed bed environment still provides a similarity with industrial DSI systems, where the downstream fabric filter acts both as a solid separator and a fixed bed reactor, as the deposited sorbent forms a filter cake where most of the acid gas capture takes place [136]. Notably, reactor configurations extend to pilot-scale apparatuses with versatile setups, resembling industrial systems. For instance, Zach et al. [137]employed a 27 cm-wide heated cylindrical reactor housing candle filters, equipped with a sorbent feeder and a 15-kW burner upstream for the generation of HCl- and SO_2-rich flue gas via the combustion of impregnated wood pellets. Eventually, some research groups also carried out experimental campaigns at full-scale facilities, e.g., by executing test runs of sorbent injection in the combustion chamber of WtE plants [100,103], or by proposing a new reactor design and installing it in an existing flue gas treatment line [138].

The monitoring of sorption performance in the experimental setups listed in Table 4 was typically conducted via off-gas analysis. Earlier studies employed pH measurement on the solution obtained from downstream absorption of off-gases to detect residual hydrogen halides [74,139], but in more recent research, direct measurement by online gas analysis has become widespread, with Fourier-transform infrared spectroscopy (FT-IR) representing the most frequent analytical choice. Gas analysis is often complemented with solid analysis, conducted offline, to characterize the sorbent before and after reaction with gas halides. The X-ray diffraction (XRD) is used to investigate chemical speciation, the BET (Brunauer-Emmett-Teller) measurements are used to quantify surface area, and scanning electron microscopy (SEM) is applied to elucidate morphology changes in the solid during reaction.

A much higher variety can be observed in the experimental design when it comes to operating conditions. Table 5 reports the experimental conditions investigated in the literature, in terms of amount of sorbent, gas flow rate, and composition, temperature, and moisture. Particular attention should be paid to the broad span of acid-to-sorbent ratios employed by different studies, ranging, e.g., for Ca-based reactants from 4 mg of sorbent for 18 mg/h of HCl flow [140] to 3000 mg of sorbent for 2.45×10^{-2} mg/h of HCl flow [141].

In the following sections, results from different studies will be compared in order to draw general observations on the characterization of gas-solid reactions for hydrogen halide removal. Time series reported by different authors, like, e.g., breakthrough curves or sorbent conversion trends over time, cannot be compared "as is" because of the broadly different sorbent loads and gas compositions. Therefore, time series of fixed bed runs published by different authors were normalized according to the acid-to-sorbent ratio adopted by the authors and reported in the following figures as a function of t/τ, where τ is the theoretical time for the complete conversion of the sorbent, defined as:

$$\tau = \frac{m_{sorb}}{\dot{V} \bullet C_{HX,in} \bullet \frac{\nu_{sorb}}{\nu_{HX}} \bullet \frac{MW_{sorb}}{MW_{HX}}} \tag{13}$$

where m_{sorb} is the sorbent mass in the fixed bed, $\dot{V}$ the gas flowrate, $C_{HX,in}$ the inlet concentration of the hydrogen halide in the gas, ν and MW the respective stoichiometric coefficient and molar mass of the sorbent and halide. By definition, when $\frac{t}{\tau} = 1$ enough hydrogen halide has passed through the sorbent bed to convert it completely according to stoichiometry (100 % removal efficiency).

5. Sorption of single hydrogen halides

5.1. Sorption of hydrogen chloride (HCl)

As shown in Table 5, the removal of hydrogen chloride is by far the most studied in the literature, as HCl is present in most flue gas treatment applications (see again Table 1). Exploring the performance of different sorbents in the gas-solid reaction with HCl requires a comprehensive analysis of the influence exerted by operating conditions, and in particular by temperature and humidity of the gas stream.

5.1.1. Influence of temperature

Several researchers investigated the effect of temperature on HCl abatement. In the case of Ca-based sorbents, Fig. 4 reports sorbent conversion curves obtained by various investigators at different temperature intervals, in dry conditions (no moisture in the inlet gas mixture). Fig. 4a collects studies performed on $Ca(OH)_2$ in the low- to mid-temperature range, which is of interest for typical DSI applications. Despite differences in the experimental conditions adopted by the different authors (see Table 5), a remarkable agreement can be noticed, pointing out a positive effect of temperature on the sorbent conversion rate in dry gas in the temperature range between 50 and 300 °C, in line with an Arrhenius-type dependence of kinetic and diffusive stages of the reaction process. Notably, the trend of sorbent conversion exhibits declining rates with time and, over long-time intervals, reaches a plateau, which is lower at lower reaction temperatures. This phenomenon, indicated as "incomplete ultimate conversion" by some authors [33,143], will be discussed in detail in Section 8.

Fig. 4b compares the findings of Partanen et al. [145] and Lin and Chyang [160] for the reaction between CaO and HCl in the high temperature range (650–850 °C), which is of interest for direct furnace injection. Both studies indicate 650 °C as the optimal reaction temperature. At higher temperatures, the solid reactant is converted faster in the early stages of reaction, but then the conversion rate slows down abruptly. Other authors who do not report time series also evidenced that the final HCl uptake of Ca-based sorbents decreases rapidly at temperatures higher than 650 °C [164,166,167]. Sun et al. [168] and Tan et al. [159] observed a maximum of reactivity at 550 °C and 500 °C, respectively. Weinell et al. [74] reported maximum conversions in the range 500–600 °C, depending on the type of lime. For short reaction times, the rapid initial growth in conversion is indicative of a kinetic control of the reaction. At the beginning of the reaction, with open porosity and no solid product deposited on the sorbent yet, internal diffusional limitations are negligible. Subsequently, the overall reaction rate diminishes as control shifts from chemical reaction to mass transfer of the gaseous reactant [169]. Such a shift is more abrupt at higher temperatures as a consequence of a reduction in porosity due to the thermal sintering of CaO particles [170]. In addition, Partanen et al. [145] considered that the melting point of $CaCl_2$ is 772 °C and speculated that the formation of a molten product phase can produce agglomeration of sorbent particles, hampering high conversion rates.

Studies that utilized very high concentrations of HCl in the inlet gas are grouped in Fig. 4c. Li et al. [153] showed a monotonic increase of conversion rate with temperature in the range 148–400 °C. Conversely, Daoudi and Walters [142] investigated the temperature interval 465–650 °C, identifying 600 °C as the optimal reaction temperature.

Compared to Ca-based sorbents, limited data are available in the literature on the temperature dependence of HCl removal by Mg-based sorbents. In a relevant patent for a dolomitic sorbent derived from the calcination and hydration of dolomite rock (see Eq. 10 for reference), Moreschi and Marras [101] tested its performance for HCl abatement in fixed bed runs, obtaining a removal efficiency over a $t/\tau = 2$ of 65–68 % at 800 °C and of 69–72 % at 1050 °C (inlet HCl concentration equal to 1433 mg/Nm^3). Notably, whereas for purely Ca-based sorbents, solid conversion plummeted at temperatures higher than 650 °C, the conversion of dolomitic lime, having a Mg/Ca ratio in the range 0.53–0.65, slightly increases with temperature in the high temperature range. This is due to the stabilizing effect of the Mg fraction that prevents severe sintering of the Ca fraction, which is mainly active for HCl absorption. Similarly, Shemwell et al. [164] investigated the reaction of several organic and inorganic Ca-based sorbents (calcium formate, calcium magnesium acetate, calcium propionate, calcium oxide, calcium carbonate) with 2425 ppm HCl in the temperature range 600–1000 °C. Only the sorbent containing Mg (calcium magnesium acetate, Mg/Ca ratio = 2) exhibited a conversion of the Ca fraction higher than 25 %, with a peak of 48–53 % at the highest tested temperature (1000 °C).

Regarding Na-based sorbents, Dal Pozzo et al. [98] and Fellows and Pilat [139] studied the effect of temperature on the $NaHCO_3$-HCl reaction process in the temperature range of main interest for DSI applications (100–300 °C). After normalization for the different HCl-to-sorbent ratios according to Eq. 13, Fig. 5 shows a remarkable agreement between the sorbent conversion curves obtained in the two studies, which both highlight a trend of increasing reactivity with temperature in the interval of interest, as expected from an Arrhenius-type dependence of reaction and diffusion rates. However, this effect appears to level off in the range 235–288 °C [139]. Dal Pozzo et al. [98] found that the sorption capacity of activated Na_2CO_3 decreases significantly at 300 °C. As elucidated by SEM images, the drop in reactivity can be attributed to the significant reduction of surface area in the activated sorbent at 300°C compared to lower temperatures. Tang et al. [171] also reported a decrease in porosity caused by thermal sintering at temperatures above 300 °C for Na_2CO_3. Therefore, the loss of surface area associated with sintering appears to occur at temperatures lower than the Tammann temperature of the material (~426 °C), which is often assumed as the onset temperature for sintering phenomena. Conversely, Verdone and De Filippis [155], in investigating the reaction of sodium bicarbonate with 3000/6000/9000 ppm HCl in the range 200–600 °C, observed increasing reaction rates up to 400 °C, albeit their experiments ran for short reaction times ($t/\tau < 0.5$). Lastly, Ma et al. [172] performed FBR runs with sodium bicarbonate and 400 ppm HCl in the range 200–500 °C, identifying 300 °C as the optimal reaction temperature and attributing this to a trade-off between the temperature dependency of both kinetics and sintering.

5.1.2. Influence of humidity

In addition to temperature, the humidity of the gas stream is a key operating parameter for the gas-solid removal of hydrogen halides, as in industrial flue gas treatment applications, a non-negligible water content is typically present in the gas phase. The effect of moisture in the gas stream on the efficiency of HCl removal has been addressed by various authors across a wide range of temperatures. For Ca-based sorbents, Jozewicz et al. [173] and Weinell et al. [74] were the first investigators to test the influence of moisture on the binding capacity of lime and limestone for HCl. They found that, at temperatures below 150 °C, the sorbent conversion is very low (< 10 %) in the absence of water but increases significantly with increasing water vapor concentration. At 100 °C, complete conversion was actually achieved for a 15 vol% water content in the gas. The influence of moisture gradually disappears at increasing temperatures, and above 200 °C, the sorbent conversion was found to be apparently independent of the water content in the gas. Similar results were reported by Fonseca et al. [151], showing that the conversion of $Ca(OH)_2$ after 20 min of reaction with 600 ppm HCl in the temperature range 50–130 °C is very low (around 5 %), but it can be greatly enhanced by the addition of water vapor. With a 6 H_2O concentration in the gas, conversion after 20 min reached values of 40 % at 90 °C and 65 % at 50 °C. The increased lime conversion at low temperatures and high water content was ascribed to three potentially concurring phenomena: i) the formation of an aqueous film of adsorbed water molecules that facilitates the dissolution of the gaseous HCl, creating a liquid-phase interface where neutralization occurs more efficiently [173]; ii) the rearrangement of the crystal lattice of the sorbent, exposing new surface and active sites for reaction [74]; and iii) the partial dissolution and reprecipitation of the layer of solid product, the deliquescent $CaCl_2$ salt, which reduces diffusional resistance to the reaction progress [152]. Notably, relative humidity (RH), i.e., the ratio between the actual amount of water vapor in the gas and the saturation value at a given temperature, and not the absolute water content in the gas phase, appears to be the determining factor governing the increase of reactivity. This is shown in Fig. 6, where the experimental data on lime conversion obtained by the different authors are plotted as a function of RH. At higher RH values, the adsorption of water on the sorbent surface is favored and its diffusivity is enhanced, giving reaction interfaces the characteristics of both solution-like and dry-like environments [174].

Table 4
Overview of reactor configurations and analytical techniques adopted in the literature for the study of hydrogen halide removal.

Reactor configuration	Temperature range	Dry/ Wet	Solid analytical techniques	Gas analytical techniques	Reference	Notes
Laboratory scale						
TGA	310–670 °C	dry	XRD and titration	-	[142]	
	170,200,230,300 °C	dry	XRD	FT-IR	[143]	
	120 °C	dry	XRD	-	[144]	
	650, 850 °C	dry	SEM, EDXA, XRD	-	[145]	
	200 °C	dry	XRD	-	[146]	
Fixed-bed reactor	150–400 °C	dry	Titration	-	[147]	
	800 °C	dry	BET	Titration in NaOH solution	[148]	
	300–700 °C	dry	BET	-	[149]	
	107, 153, 190, 235,288 °C	dry	-	pH measurement with a pH electrode, titration in NaOH solution	[139]	
	350–600 °C	dry	-	Chloride measurement with chloride-selected electrode	[150]	
	60–1000 °C	dry	EDAX, BET	pH measurement with a pH electrode	[74]	
	100–600 °C	dry	DSC	-	[78]	
	50–120 °C	dry	SEM, X-ray sedimentometry, mercury porosimetry	pH measurement with a pH electrode	[151]	
	120 °C	dry	-	FT-IR	[152]	
	148, 175, 203, 248, 275, 300, 330, 356, 400 °C	dry	-	FT-IR	[153]	
	300–950 °C	dry	BET, XRD, XRF, AAS	$AgNO_3$ titration in NaOH solution, HCl gas infrared analysis	[126]	
	150,200,250,275,300,350 °C	dry	BET, SEM, XDS, XRD,	Ion chromatography, AA	[140]	
	550 °C	dry	-	$AgNO_3$ titration in NaOH solution	[154]	
	200–600 °C	dry	BET	pH measurement with a pH meter	[155]	**multilayer fixed bed*
	600–800 °C	dry	-	HCl gas infrared analysis	[156]	
	22,54 °C	dry	-	UV-IR analysis	[157]	**packed tower*
	-	dry	-	FT-IR	[158]	
	150 °C	-	EMPA, XRD	Ion chromatography	[99]	
	500,600,700 °C	dry	-	$AgNO_3$ titration in NaOH solution	[159]	**dual-layer granular bed*
	500 °C	dry	BET	Io chromatography	[96]	
	650–850 °C	dry	-	FT-IR	[160]	
	150 °C	dry	XRD, SEM, BET	pH measurement with pH electrode	[107]	
	700 °C	dry	TGA, FE-SEM, HR-TEM, EDS, BET, contact angle goniometry	FT-IR	[161]	**reaction enhanced-regenerative catalytic system (RE-RCS)*
	200 °C	dry	XRD, EDS-SEM	-	[162]	**$Ca(OH)_2$ single crystal as sorbent*
	120–180 °C	dry	XRD, TGA	FT-IR	[82]	
	120,150,180,210,300	dry	BET	FT-IR	[98]	
	25 °C	dry	FT-IR, ICP-AES, BET, XRD, ESEM, TEM-EDX	FT-IR	[163]	
	100,200,270, 350, 400 °C	dry	BET	Ion chromatography	[132]	**fixed bed microreactor*
	400 °C	dry	-	Ion chromatography	[133]	
	130,160,190 °C	dry	XRD	Ion chromatography	[112]	
	300–700 °C	dry	XRD, BET	online flue gas analysis	[117]	
	350–650 °C	dry	XRD, SEM, BET, TGA	HCl gas infrared analysis	[116]	
	600 °C	dry	XRD, TGA, SEM, EDS, BET	HCl gas infrared analysis	[128]	
	400–600 °C	dry	ICP-OES, TGA, BET, SEM, EDS	Ion chromatography	[129]	
	300,400,500 °C	dry	XRD, BET	HCl gas infrared analysis	[127]	
	800 °C	dry	XRD	pH measurement with a pH meter	[131]	
	150 °C	dry	XRD, BET, SEM	laser HCl gas online detection	[123]	
	750–900 °C	dry	FESEM-EDS, BET, XRD, XPS, ICP-OES	Ion chromatography	[106]	
	150 °C	dry	XRD, BET, BJH, FESEM, EDX	HCl gas online detection	[87]	
	25 °C	dry	SEM	Ion chromatography	[141]	
	350 °C	dry	XRD, BET, SEM, DLS	Ion chromatography	[121]	
	150,250,350,450 °C	dry	XRD, TEM, DLS, BET	HCl gas infrared analysis	[134]	
	300–700 °C	dry	ICP-OES, XRD, SEM, TGA	HCl gas infrared analysis	[130]	
fluidized- bed reactor	650–1050 °C	dry	-	HCl gas infrared analysis	[164]	
	450–760 °C	dry	XRD, SEM.	Chloride measurement with chloride-selected electrode	[105]	
Pilot scale						

(*continued on next page*)

Table 4 (*continued*)

Reactor configuration	Temperature range	Dry/ Wet	Solid analytical techniques	Gas analytical techniques	Reference	Notes
absorber-reactor	175,250,380 °C	wet-dry	-	Gas sampling	[165]	
fixed-bed	170–225 °C	dry	-	Portable gas analysis, ion chromatography	[137]	
Commercial facility						
dry sorbent reaction accelerator (SRx)	180 °C	dry	SEM, EDS	Mercuric thiocyanate method, FT-IR	[138]	

Accordingly, the positive effect of water on the HCl uptake of Ca-based sorbents fades at higher temperatures, at which the typical range of moisture in industrial flue gases (5–20 vol%) corresponds to very low RH values. Mura and Lallai [150] reported that a 5 vol% water content does not affect the HCl removal performance of calcined limestone in the temperature range comprised between 400 and 600°C.

Partanen et al. [145] compared the HCl uptake of calcined limestone at 850 °C in dry gas and with 14 H_2O, finding that the maximum conversion of calcined limestone to $CaCl_2$ is almost halved in a moist atmosphere. The authors attributed the results to the negative effect of water on the thermodynamic equilibrium of Eq. 2.

Some researchers investigated the reaction between $Ca(OH)_2$ and HCl using single crystals of solid sorbent exposed to the acid gas, obtaining insights into the role of moisture in the reaction [162,175]. Iizuka et al. [162] presented SEM images of a cross-section of a lime crystal exposed to HCl-rich gas for 24 h, at 0 % and 10 % humidity, and performed elemental mapping to detect chlorine. No chlorine was detected in runs with 0 % humidity, whereas chlorine was detected all over the side face and subsurface of the sample in runs with 10 % humidity. Thus, coherently with previous results, the presence of H_2O was found to accelerate the chlorination reaction, probably due to the formation of an aqueous phase that disrupts the crystal structure of the solid, enabling the progression of the reaction. Kaiser et al. [89] suggested that the formation of hydrates (see reaction 3) generates a film of water on the reaction surface, which favors the absorption of gaseous reactants.

For Na-based sorbents, no evidence of the role of moisture on HCl removal is reported. Verdone and De Filippis [155] found no effect of the water content in the gas mixture on the HCl sorption performance of sodium bicarbonate in the interval 300–600 °C. Zhang et al. [1] found that the presence of water has a negative effect on the HCl absorption by sodium carbonate at 550 °C.

5.2. Sorption of hydrogen fluoride (HF)

Gas-solid reactions for the removal of HF have received much less attention in the scientific literature compared to HCl. Only two relevant publications were retrieved, providing at least a qualitative comparison of the temperature dependence of solid conversion and reaction rate reported by different investigators for Ca-based sorbents (Fig. 7). The absence of the required information on flue gas flowrate and/or mass of sorbent precluded the calculation of τ, and the data are merely reported as a function of the experimental time. Nonetheless, Fig. 7 evidences a positive effect of temperature on the reactivity of CaO. Kossaya et al. [149] explored the HF binding capacity of CaO in the range 300 – 700 °C, reporting a conversion of calcium oxide into fluoride that is almost negligible at 300 °C and as high as 40 % at 700 °C after 1 h of exposure to HF gas. Final CaO conversion remarkably increases with temperature, also in the tests by Byer et al. [148], reaching values as high as 90 % for the experimental runs carried out at 800 °C.

Notably, the reduction of sorbent conversion rate at temperatures higher than 600–650 °C reported by several authors for the reaction with HCl (Section 5.1) was not observed by Byer et al. [148] for the reaction with HF. Such findings appear in line with a thermogravimetric study by Partanen et al. [176], which reported conversions to CaF_2 close to 100 % for CaO at 850 °C, compared to a much lower performance when exposed to HCl.

For Mg-based sorbents, Moreschi and Marras [101] reported the removal efficiency of dolomitic lime in fixed bed runs against single hydrogen halides, finding that for t/τ higher than 2 the abatement yield of HCl (inlet concentration of 1433 mg/Nm^3) increased from 65 % to 68 % at 800 °C to 69–72 % at 1050 °C and that of HF (inlet concentration 45 mg/Nm^3) increased from 79 % to 85 % at 800 °C to 83–87 % at 1050 °C, thus confirming a marked increase of reactivity with temperature even in the high temperature range.

Recent research [157,158,161] has focused on the utilization of different sorbents, such as NaF and CaO/SiO_2, as alternative sorbents to be employed in HF removal.

5.3. Sorption of hydrogen bromide (HBr)

As outlined in Table 1, HBr represents the third most important hydrogen halide in the framework of flue gas treatment. While the combustion of chlorinated waste results almost quantitatively in the release of HCl and the generated HCl undergoes only limited thermal decomposition to form Cl_2 [177], HBr may experience a significant conversion to Br_2 in the flue gas [178]. In view of the design of flue gas cleaning systems for dedicated thermal processes for brominated waste treatment, there is a consensus that thermal treatment should be operated in order to minimize HBr conversion to Br_2 [179–181], as HBr could be removed by means of solid sorbents, similarly to HCl and HF. Ruzovic et al. [90] performed a thermodynamic assessment of the $HCl/SO_2/HBr/Na_2CO_3$ system, predicting complete conversion of HBr to NaBr in the presence of sodium bicarbonate (0.05 mol% with respect to the flue gas molar flow rate) at 127–287 °C, a temperature range compatible with typical DSI applications. However, it is worth pointing out that, to date, no dedicated experimental campaign addressing the removal efficiency of Ca- or Na-based sorbents toward HBr is available in the literature.

6. Competitive reactions

The vast majority of studies in the literature primarily focus on the removal of a single pollutant using a solid sorbent. However, in real industrial scenarios, flue gases might contain a variety of halides and other interfering contaminants, depending on the composition of the fuels or raw materials utilized in the industrial process, thus requiring DSI systems to perform simultaneous abatement. The concurrent removal of pollutants triggers interactions, which may manifest as synergistic or competitive effects.

6.1. Competition between hydrogen halides

Very few studies addressed the simultaneous removal of different halides. Schmal et al. [182] reported that, for the typical raw gas composition of municipal solid waste incinerators (HCl = 800 mg/Nm^3, HF = 10 mg/Nm^3), a calcium hydroxide injection at a molar Ca/Cl ratio equal to 1 reduces the emissions of HCl by up to 50 % and those of HF by up to 80 %. More recently, Wysocki and Szymanek [120] tested the in-duct injection of $NaHCO_3$ after alternative activation approaches in a

Table 5
Summary of operating conditions adopted in literature for the study of hydrogen halide removal.

Solid reactant	Mass of sorbent	Acid gas	Gas flow rate	Gas composition	Temperature (°C)	RH (%)	Reference
Na-based sorbents							
$NaHCO_3$	0.1 g	HCl	1.1 L/min	415 ppm at 153 °C and 760 ppm at 235 °C	107, 153, 190, 235, 288	0	[139]
$NaHCO_3$	2.0 g	HCl	-	3000, 6000, 9000 ppm	200–600	0	[155]
NaF	107–345 g	HF	1.7–11.7 L/min	2–15 % mol	22, 54	0	[157]
NaF	-	HF	-	-	-	-	[158]
$NaHCO_3$	0.015 mg	HCl	0.8–2.4 L/min	100–700 ppm in N_2 + 15 % CO_2 + 10 % H_2O	500	0.02	[96]
$NaHCO_3$	0.050 mg	HCl	0.17 NL/min	1000, 2500 ppm	120, 150, 180, 210, 300	0	[98]
$NaHCO_3$	-	HCl	200, 300 L/min	0–490 mg/m^3 + 7–10 % O_2	170–225	-	[137]
Ca-based sorbents							
$Ca(OH)_2$	1.56 g	HCl	1.98 L/min	630 ppm in N_2	150, 250, 400	2, 0.3, 0.04	[147]
CaO	0.150 g	HF	0.76 L/min	0.625,1.25,2.5,5 %	550, 650, 750, 800	-	[148]
CaO on γ-alumina	-	HF	1.20 L/min	17 % in N_2	300–700	-	[149]
$CaCO_3$	0.010 g	HCl	0.50–3.00 L/min	0.5–5 % mol	310–670	0	[142]
$Ca(OH)_2$, $CaCO_3$	0.025 g	HCl	1.00 L/min	1000 ppm in N_2	60–1000	0, 1, 4, 5, 15, 25, 32	[74]
$CaCO_3$	0.050 g	HCl	-	2000 ppm + 5 % or 30 % CO_2	350–600	0.05–0.01	[150]
$Ca(OH)_2$, CaO	0.100 g	HCl	23 L/min (STP)	1000 ppm + 5 % O_2 in N_2	100–600	0	[78]
$Ca(OH)_2$	0.020 g	HCl	4.02 NL/min	150–1000 ppm in N_2	50–120	0, 4, 8, 9, 10, 17, 20, 36, 51	[151]
$Ca(OH)_2$	0.018,0.035 g	HCl	1.50 L/min (STP)	250,500,1000,2000,3500 ppm	120	0, 1, 3.5, 9, 19	[152]
CaO	0.028 g	HCl	12.50 L/min	1.74 % in N_2	148, 175, 203, 248, 275, 300, 330, 356, 400	-	[153]
CaO	0.004 g	HCl	40 L/min (STP)	5000 ppm + 5 % O_2 in N_2	150, 200, 250, 275, 300, 350	0	[140]
$Ca(OH)_2$	0.010 g	HCl	0.15 L/min	914 mg/m^3 + 9 % O_2	170, 200, 230, 300	-	[143]
$Ca(OH)_2$	-	HCl	1133, 1500 NL/min	250, 1000 ppm	175, 250, 380	0	[165]
$Ca(HCOO)_2$, $CaMg_2(CH_3COO)_6$, $Ca(C_2H_5COO)_2$, CaO, $CaCO_3$	-	HCl	4.00 L/min (STP)	2425 ppm in N_2	650–1050	0	[164]
$Ca(OH)_2$	0.001–0.010 g	HCl	0.90 L/min (STP)	240 ppm	120	9	[144]
$CaCO_3$, $CaMg(CO_3)_2$	0.040 g	HCl	1.40 L/min (at 0 °C and 0.01 MPa)	HCl 2000 ppm + 5 % O_2 + 0 or 14 % CO_2	650, 850	0, 0.004	[145]
$Ca(OH)_2$	0.010 g	HCl	0.15 L/min	2094 ppm+ 9 % O_2	200	0	[146]
CaO	0.5 g	HCl	0.80 L/min (STP)	2000 ppm in N_2	600–800	0	[156]
$CaCO_3$	31 g	HF	0.02,0.08,0.16 L/min	0.574, 2.239, 4492 mol/m^3	150	-	[99]
$Ca(OH)_2$	-	HCl	-	1000 ppm + 10 % CO_2+ 10 % O_2 in N_2	500, 600, 700	0.02, 0.05	[159]
$Ca(OH)_2$	1200–1833 g/min	HCl	660000 NL/min	728, 1123 ppm	180	0	[138]
CaO	0.056 g	HCl	0.10 L/min (STP)	491 ppm + 0 or 11 % CO_2 + 0 or 10 % O_2	650–850	0	[160]
CaO on SiO_2 support	15 g	HF (as CF4)	-	3000 ppm	700	8	[161]
$Ca(OH)_2$	0.050, 0.100 g	HCl	0.18 NL/min	1250, 2500 ppm in N_2	120, 150, 180	0	[82]
$CaCO_3$	0.3–0.5 g	HCl	0.05 L/min	500 ppm in N_2	25	0	[163]
$Ca(OH)_2$	-	HCl	-	1000 ppm in N_2 + 5 % O_2	200	0, 0.7	[162]
$Ca(OH)_2$	3 g	HCl	0.50 L/min	548 ppm in N_2	25	0	[141]
Innovative sorbents							
$[Ca_3Al_2\text{-}(SiO_4)(OH)_8]$	1 g	HCl	0.50 L/min	1000 ppm in N_2	300–950	0	[126]
Ca-C	2 g	HCl	0.54 L/min	1820 ppm in N_2	100, 200, 270, 350, 400	0	[132]
CaO+$CaCO_3$+sodium alkali	-	HCl	-	1050–1460 mg/m^3 (mixed with air)	450–760	0	[105]
ECl1: $NaHCO_3$, $CaCO_3$, $Ca(OH)_2$, $Mg(OH)_2$; ECl2: $Ca(OH)_2$, Al_2O_3	-	HCl	-	1000 mg/m^3	550	0	[154]
$NaHCO_3$, $Ca(OH)_2$, $Mg(OH)_2$, $NaAlO_2$	-	HCl	-	1000 mg/m^3	350–650	0	[125]
	4.0–6.8 g	HCl	0.20 L/min	200 ppm+ 20 % CO+ 5 % CO_2+ 8 % H_2	400	0.02	[133]
CO_3·Mg-Al HTLc	0.4–3.0 g	HCl	0.10 L/min	1500–10000 ppm	130, 160, 190	0.6 mL/min of water	[112]
Ca−Mg−Al HTLc	1 g	HCl	0.50–1.30 L/min	500–1000 ppm	300–700	0	[117]
10Na_2CO_3-AAB	23 g	HCl	20 mL/min	50 %	150	0	[107]
CaMgAl-HTLc	0.500 g	HCl	0.50 L/min	450–1500 mg/g	350–650	0	[116]
KF/CaMgAl-HTLc	0.500 g	HCl	0.90 L/min	500 ppm in N_2	600	0	[128]

(*continued on next page*)

Table 5 (*continued*)

Solid reactant	Mass of sorbent	Acid gas	Gas flow rate	Gas composition	Temperature (°C)	RH (%)	Reference
Soda ash with honeycomb support	0.200 g	HCl	0.10 L/min (STP)	2030 ppm in N_2	300, 400, 500	0	[127]
Na-Mg-Al HTLc	0.814 g	HCl	-	200 ppm in N_2	400–600	0	[129]
$CaCO_3$, $Ca_3Al_2(SiO_4)_{0.8}(OH)_{8.8}$, $Na_8Al_6Si_6O_{24}(OH)_2$	0.300 g	HCl	0.50 L/min	1000 ppm in N_2	800	0	[131]
NaOH-modified CaO	0.100 g	HCl	1.00 L/min	150 ppm in N_2	150	0	[123]
85Al-15Ca	-	HCl	0.25 L/min	0.02 % + 10 % CO+ 10 % CO_2+ 10 % H_2+ 0.02 % NaCl + 0.01 % KCl in N_2	750–900	0.006, 0.01	[106]
Ethanol-modified CaO	0.100 g	HCl	1 L/min	150 ppm	150, 300, 450, 600	0	[87]
Modified $Ca(OH)_2$	-	HCl	-	150 ppm in N_2	350	0	[121]
Ethanol-modified CaO	0.100 g	HCl	1.00 L/min	150 ppm in N_2	150, 250, 350, 450	0	[134]
CO_3·Mg-Al HTLc	-	HCl	0.50 L/min	400 ppm in N_2	300–700	0	[130]

synthetic flue gas carrying 20 mg/Nm^3 HCl and 45 mg/Nm^3 HF, reporting up to 60 % HCl removal and less than 15 % HF removal. Moreschi and Marras [101] tested the full-scale injection of dolomitic lime (see formulation in Eq. 10) in two WtE plants where both HCl and HF were present in the flue gas, reporting a superior abatement yield for HF (83 % and 99 % compared to 41 % and 32 % for HCl, respectively, in the two plants). Other recent studies explored the use of Ca- or Mg-doped porous adsorbents for the simultaneous capture of HCl and HF [21,52,183] showing comparable removal efficiencies toward the two halides, with a slight preference for HF. Given the paucity of literature on the topic, further research is needed to confirm the relatively higher affinity of Ca-based and Mg-based sorbents toward HF and Na-based sorbents toward HCl. Notably, no studies on the simultaneous sorption of HCl or HF and HBr are available in the literature.

6.2. Competition with sulfur dioxide (SO_2)

The other main acid pollutant that is usually found in combustion flue gases, together with hydrogen halides, is sulfur dioxide (SO_2). A wealth of research focused on gas-solid reactions for SO_2 abatement: the reader is referred to recent dedicated reviews for detailed discussion [184,185]. Here, SO_2 capture is discussed solely in the context of simultaneous removal with hydrogen halides, to elucidate competitive and/or synergistic interactions.

Matsukata et al. [4] studied the simultaneous sorption of SO_2 and HCl (both at the concentration of 1000 ppm in N_2) by calcined limestone at 750 °C, finding that the presence of HCl increased the conversion of CaO to $CaSO_4$, as confirmed by Xie et al. [186] and by Lawrence et al. [187], who observed the enhancement of sulfation even at 680 °C. Partanen et al. [145,188] reported that HCl promotes SO_2 adsorption at 650 °C and 850 °C, but the increased conversion of CaO to $CaSO_4$ significantly reduces the conversion to $CaCl_2$ compared to the sorption of HCl alone. Similarly, Lin and Chyang [160] found that increasing the reaction temperature from 650 °C to 850 °C improves the SO_2 uptake efficiency of calcined limestone but suppresses HCl capture.

A possible explanation for the enhanced CaO sulfation in the presence of HCl in this temperature range is the formation of a molten phase, as the $CaCO_3$–$CaSO_4$–$CaCl_2$ system exhibits a eutectic point at ~580 °C [81,145]. As it will be discussed in Section 8, diffusion plays a relevant role in the gas-solid reaction mechanism, and diffusivity through layers of solid products is typically low. The melting of the reaction products can reduce diffusional resistance, enabling the reaction process to progress. However, this mechanism cannot explain the suppressed chlorination of CaO in the presence of SO_2, as the molten phase should increase the mobility of both Cl^- and SO_4^{2-} ions. Lin and Chyang [160] proposed that at T > 750°C, the apparent inhibitory effect on chlorination might be due to the consumption of nascent $CaCl_2$ by its subsequent reaction with SO_2, leading to the re-release of HCl and explaining the concurrent enhanced sulfation.

Moving to lower temperatures, Zhou et al. [121] explored the effect of different concentrations of SO_2 and SO_3 on the HCl uptake efficiency at 350 °C of $Ca(OH)_2$ prepared by simple hydration or via ball milling. Setting the inlet HCl concentration at 150 ppm and testing SO_2 or SO_3 concentrations respectively at 500/1000/1500 ppm and 50/100/150 ppm, they found a marked suppression of HCl sorption with the increase of SO_x load. The final HCl absorption was reduced up to 82 % in the presence of 1000 ppm SO_2 and up to 86 % with 150 ppm SO_3. The authors showed that in the late stages of absorption, the affinity of $Ca(OH)_2$ towards the acid pollutants follows the order SO_3 > HCl > SO_2, likely due to the lower SO_2 diffusivity. However, in the early kinetically-controlled stages of reaction, both SO_x compounds can react with CaOHCl, the favored product of lime chlorination in the low to mid-temperature range (see Section 3.1), hindering HCl uptake.

In the low-temperature range of interest for DSI processes (100–200 °C), Ca-based sorbents exhibit a remarkably high selectivity for HCl over SO_2 [134], but HCl capture is still affected by the competition with SO_2. By conducting thermogravimetric tests at 200 °C, Chin et al. [146] demonstrated that the overall conversion of $Ca(OH)_2$ after more than 10 h exposure to acid gases is almost halved for a $Ca(OH)_2$-HCl-SO_2 system compared to a $Ca(OH)_2$-HCl system. Building on previous experimental evidence on sulfation [189], the authors postulated that the reaction with SO_2 forms a dense layer of solid product on the lime surface that hinders the continuation of the absorption process. The problem is exacerbated if O_2 is present in the gas mixture. In an N_2 atmosphere, the thermodynamically favored product of sulfation is $CaSO_3 \bullet \frac{1}{2}H_2O$, and HCl appears capable of attacking sulfite layers to form $CaCl_2$ [80]. Conversely, in the presence of O_2, sulfation generates $CaSO_4$ in either anhydrous or hydrate form, which is resistant to reaction with HCl [80]. Kaiser et al. [89] also speculated on the different porosity of S-containing and Cl-containing product layers, suggesting that the more porous nature of $CaCl_2$ layers promotes SO_2 removal by Ca-based sorbents compared to what is observed in the absence of HCl.

Wang et al. [87] investigated the effect of SO_2 concentrations in the range 0–1600 ppm on the HCl sorption of high-surface-area $Ca(OH)_2$ (T = 150 °C, HCl = 150 ppm). A 31 % reduction in HCl removal efficiency was observed at the highest SO_2 concentration. The authors proposed that the presence of SO_2 hinders HCl uptake through: i) on a physical level, the clogging of sorbent pores by the sulfite product $CaSO_3$, which has a higher molar volume than CaOHCl, and ii) on a chemical level, the competition for the same type of alkaline active sites. In addition, Liu et al. [134] advanced the notion of a "shielding effect" of sulfide product layers toward HCl capture. SO_2 not only occupies alkaline sites on $Ca(OH)_2$ surface, but also induces a local negative electrostatic potential that prevents the attraction of Cl atoms with a negative charge in nearby Ca sites.

Regarding the competitive absorption of HCl and SO_2 on sodium-based sorbents, a limited body of research is available in scientific literature. Dal Pozzo et al. [98] compared the reactivity of $NaHCO_3$ toward the two acid pollutants separately, showing that SO_2 uptake is comparatively lower in the temperature interval 120–300 °C and much

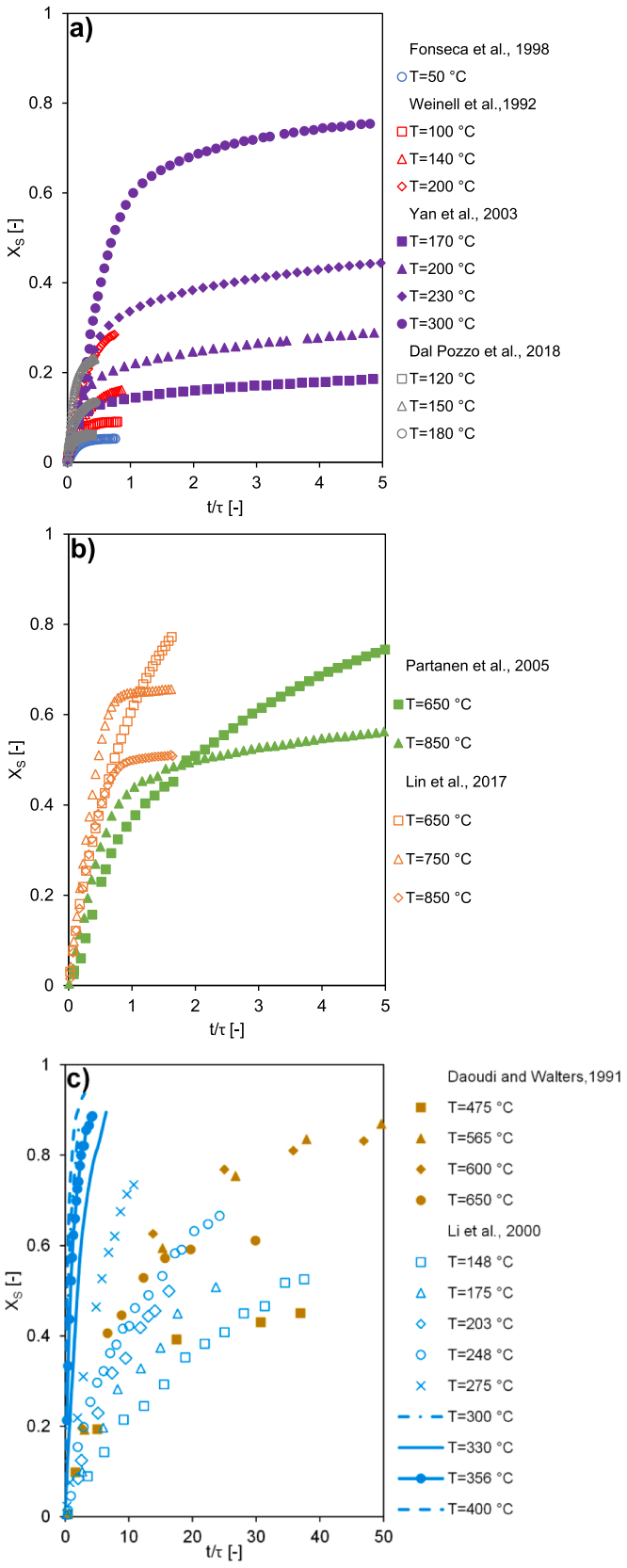

Fig. 4. Ca-based sorbent conversion X_S in HCl removal with respect to normalized reaction time. a) Data collected in the low temperature range (50–200 °C) with a HCl medium inlet concentration of 600 ppm [151] and 1000 ppm [74,82,143]. b) Data collected in the high temperature range (650–850 °C) with HCl medium inlet concentrations of 2000 ppm [145] and 500 ppm [160].c) Data collected at high HCl concentrations (>15000 ppm).

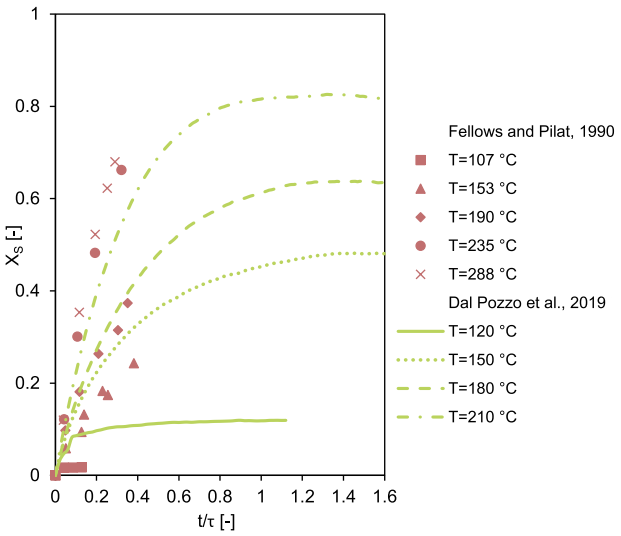

Fig. 5. Na-based sorbent conversion X_S in HCl removal with respect to normalized reaction time. Data collected with an HCl medium inlet concentration of 500 ppm for Fellows and Pilat [139] and 2500 ppm for Dal Pozzo et al. [98].

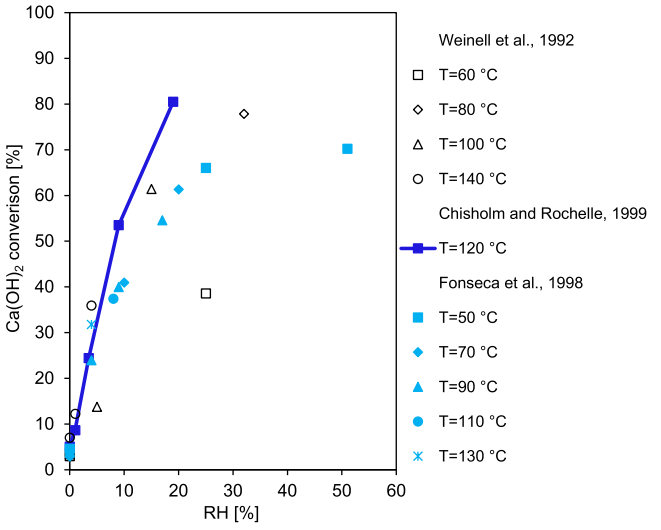

Fig. 6. Effect of the Relative Humidity (RH) on $Ca(OH)_2$ conversion upon exposure to HCl. Conversion values recorded after 20–40 min of reaction. Experiments conducted with a HCl inlet concentration of ~~6~~00 ppm for Fonseca et al. [151] and 1000 ppm for the others.

more affected by the incipient sintering of the sorbent at the higher end of the tested temperature range. Zach et al. [137] tested the simultaneous sorption of HCl and SO_2 with sodium bicarbonate in a pilot-scale apparatus. They postulated that HCl reacts preferentially with $NaHCO_3$, rapidly consuming the available surface of the sorbent and forcing SO_2 to diffuse deeper into the sorbent particles for the reaction to occur. The preferential reactivity toward HCl was also verified at HCl concentrations in the raw gas lower than SO_2.

Ma et al. [172] studied the competitive sorption of HCl and SO_2 over sodium bicarbonate at 300 °C, observing a slight decrease of HCl uptake (< 18 %) when SO_2 was also present in the feed gas. No consistent trend with SO_2 concentration was found, as the hindering of HCl sorption was the highest at 200 ppm SO_2, the lowest at 400 ppm SO_2, and in the middle at 600 ppm SO_2. Through density functional theory (DFT) calculations, the authors showed that SO_2 affects the electron exchange in HCl adsorption on Na_2CO_3, weakening the bonding capacity between Na

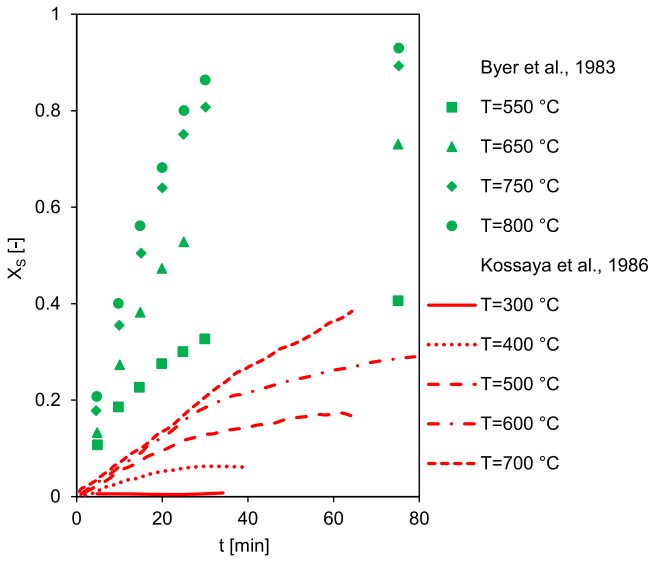

Fig. 7. Ca-based sorbent conversion in HF removal with respect to reaction time. HF inlet concentration: 625 ppm [148]; 17,000 ppm [149].

and Cl atoms. They further suggested that sulfation of the chlorination products might occur. However, previous studies found that the sulfation of NaCl presents markedly slow kinetics [190].

6.3. *Competition with carbon dioxide (CO_2)*

In real combustion flue gases, the abatement of hydrogen halides always takes place in the presence of CO_2. Calcium oxides and hydroxides react with CO_2 to form calcium carbonate, a reaction that is actively exploited for CO_2 separation from flue gases in the calcium looping process [109] or for CO_2 mineralization in accelerated carbonation processes [191]. When Ca-based sorbents are injected for acid gas abatement purposes, their carbonation is a competitive reaction that interferes with the removal of halides and generates an over-consumption of solid reactant [192].

With the surge of interest toward CO_2 capture in the framework of decarbonization, the most recent research is focusing on how HCl affects CO_2 uptake by Ca-based sorbents. For example, several authors explored how the presence of HCl affects the CO_2 carrying capacity of different Ca-based sorbents in calcium looping cycles: CaO-Fe_2O_3 sorbent [193], carbide slag [194], carbide slag stabilized with alumina [195], carbide slag stabilized with magnesium compounds [196]. Vice versa, only a few studies investigated how CO_2 affects HCl removal.

In general, the absorption of CO_2 is a much slower process compared to HCl removal, and high temperatures (600–700 °C) are needed to boost the kinetics of dry carbonation [158,197]. In their study on the chlorination of calcined limestone in the temperature range 400–600 °C, Mura and Lallai [150]noted that at 400 °C the addition of 30 vol% CO_2 in the gas did not affect HCl uptake, while at 600 °C the conversion of CaO to $CaCl_2$ decreased from 72 % to 48 % in the presence of CO_2. Operating with 11 vol% CO_2 in the gas, Lin and Chyang [160] did not observe a negative effect of CO_2 on the reaction between CaO and HCl at 650 °C, but reported an appreciable decrease in HCl uptake in the presence of CO_2 at 750 and 850 °C. Focusing on HCl removal efficiency rather than final HCl uptake, Duo et al. [198] noticed instead that, for the reaction of CaO with 900 ppm HCl at 400 °C, a breakthrough concentration of 200 ppm was observed at a much lower sorbent conversion value (32 % instead of 71 %) when the CO_2 concentration in the feed gas was set at 10 vol% instead of 2 vol%.

More recently, several studies conducted in the medium-high temperature range (400–800 °C) have focused on the performance of Ca-based or Mg-based hydrotalcite-like sorbents, synthesized as discussed

in section 4.2. Wu et al. [128] prepared CaMgAl-layered double oxides (LDOs) exhibiting the highest HCl removal performance at 600 °C. They noted that a moderate CO_2 concentration (~6 %) in the gas induced a 10 % reduction of the HCl binding capacity of the sorbent, an effect attributed to the interference of gaseous CO_2 with both the decomposition of carbonates to oxides in the LDOs and the conversion into metal chloride during the HCl removal process. Similarly, Kameda et al. [113] found that the presence of CO_2 decreased the removal rate of HCl for a MgAl-LDH sorbent intercalated with carbonate ions, likely because of the exchange reaction between intercalated CO_3^{2-} and gas-phase CO_2, which in turn inhibits the desired exchange between intercalated CO_3^{2-} and HCl. Cao et al. [130] also identified that CO_2 plays a competitive role in the removal of HCl for Ca-Mg-Al-CO_3 hydrotalcites tested in the interval 300–700 °C. At 300 °C, the sorbent exposed to 400 ppm HCl exhibited a more than 30 % lower HCl uptake when 10 vol% CO_2 was present in the feed gas. However, they found an opposite effect on Mg-Al-hydrotalcites, for which the presence of CO_2 magnified the HCl uptake capacity. Cao et al. [130] ascribed this phenomenon to the capacity of CO_2 to regenerate intercalated anions in the Mg-based LDH, generating in turn more active sites for HCl binding.

Coming to the temperature range of higher interest for DSI applications (T < 250 °C), there is a notable lack of studies on the competitive absorption of HCl and CO_2. Chin et al. [146] performed a comparative study in TGA of the weight gain of hydrated lime exposed to HCl (540 ppm) with or without CO_2 (8 vol%) in the feed gas at 200 °C. It was evidenced that CO_2 reacts more rapidly than HCl with lime in the first instants of exposure, but carbonation quickly dies out, managing only a very limited sorbent conversion. On the other hand, the presence of CO_2 has a detrimental effect on the overall conversion of lime, as the simultaneous absorption of HCl is also hindered. The authors attributed this effect to the higher tendency of CO_2 to form an impermeable solid product layer, causing pore blockage in the sorbent [146].

Few studies investigated the effect of CO_2 on the HCl absorption of Na-based sorbents. Liang et al. [199] analysed the performance of a CuO-doped Na_2CO_3-based sorbent in the temperature interval 100–190 °C, finding that increasing CO_2 content in the feed gas decreased HCl uptake. Zhang et al. [1] studied the HCl removal efficiency of a fixed bed of sodium carbonate at 550 °C, in N_2 dry gas or in a 25 vol% CO_2/N_2 atmosphere. A 40 % reduction in the amount of absorbed HCl over the duration of the experiment was recorded in the presence of CO_2. Complementing the fixed bed runs with thermodynamic calculations, the authors concluded that excess CO_2 promotes the carbonation of NaCl, the product of the reaction between Na_2CO_3 and HCl, at temperatures higher than 400 °C.

7. Comparative performance of sorbents

7.1. Comparative performance of commercial sorbents

As discussed in Sections 5 and 6, most studies in the literature focus on the performance of a single sorbent type, investigating the effect of operating conditions such as temperature, humidity, and flue gas composition on its behavior. Clearly enough, it is of paramount industrial interest to finalize the characterization of the sorbents carrying out a comparative assessment of their removal efficiency.

In the temperature range of main interest for DSI applications (120–250 °C), there is a wide consensus in both the technical and scientific literature that the HCl removal performance of commercial sodium bicarbonate is higher than that of calcium hydroxide [192,200]. For instance, the findings obtained in terms of sorbent conversion in the reaction of HCl with $Ca(OH)_2$ and $NaHCO_3$ at the same temperatures, respectively by Dal Pozzo et al. [82] and by Dal Pozzo et al. [98], are compared in Fig. 8. The figure evidences the different reactivity of the two classes of commercial sorbents, since the conversion data are obtained in comparable operating conditions (same reactor setup, temperature, gas flow rate, mass and particle size of sorbent, acid gas concentrations).

In the case of calcium hydroxide, after an initial rapid absorption phase, the rate of reaction tends to decrease and conversion reaches an asymptotic value, highlighting the “incomplete conversion” that will be discussed in Section 6.2. Conversely, in the case of sodium bicarbonate, the solid conversion in the temperature range between 150 and 180 °C constantly increases. At a fixed ratio t/τ of 0.4, sodium bicarbonate conversion reaches a value 4 times higher than that of calcium hydroxide.

Similarly, studies carried out at full-scale facilities, such as those based on operating data recorded for some Italian municipal solid waste incinerators by Dal Pozzo et al. [201], or the DSI tests at a pilot 200 kW coal-fired boiler carried out by Tan et al. [202], confirmed the higher HCl removal efficiency of $NaHCO_3$ in the temperature intervals 160–180 °C and 260–320 °C, respectively.

The current industrial practice already incorporates such findings, at least in the WtE sector. The ideal operating temperature range for Ca $(OH)_2$ DSI is widely considered to be 120–160°C [82], with efficiency improving as temperature decreases due to the increased relative humidity (coherently with the findings discussed in Section 5.1.2). In contrast, the typical range of operating temperatures for $NaHCO_3$ injection in the flue gas is above 140 °C, which is widely considered as the minimum temperature for fast thermal activation [96], with a slight improvement in performance due to kinetic effects as temperature increases. An upper operating limit of 300 °C is also identified in the current practice. Above this temperature, the sintering of Na-based sorbents becomes prominent, as highlighted in Section 5.1.1. Cao et al. [117] tested both CaO and $NaHCO_3$ sorbents for HCl removal at 550 °C. At this temperature, after 75 min of reaction, a sharp drop of reactivity for sodium bicarbonate is evident, indicating a higher vulnerability to sintering compared to CaO.

Eventually, it is worth recalling that sorbent performance is also significantly influenced by particle size and porosity, which might differ from case to case. Commercial Ca-based sorbents are typically marketed with a d_{90} lower than 30 μm and a BET surface area lower than 25 m^2/g. However, as mentioned in Section 3.1, modified $Ca(OH)_2$ products with surface areas over 40 m^2/g are receiving increasing attention in the flue gas treatment market, and full-scale test runs have shown their superior reactivity compared to conventional calcium hydroxide [203].

Na-based sorbents can have significantly lower surface areas, as commercial sodium bicarbonate is basically non-porous [98]. Still, the high reactivity of the porous sodium carbonate formed after thermal activation in the flue gas typically allows achieving HCl emission control with a very low stoichiometric excess ratio (1.1–1.4) compared to Ca-based sorbents, where ratios higher than 2 or 3 are frequently used in industrial practice [204].

Nonetheless, hydrated lime is widely used in DSI systems due to its high availability and lower cost compared to $NaHCO_3$ [204]. Eventually, the selection of the most suitable sorbent (or combination thereof) is strongly affected by plant-specific conditions, considering both process variables (flue gas compositions, integration with other FGT units) and specific cost factors (local costs for the supply of reactants and the disposal of process residues). For the WtE sector, several detailed studies addressing the comparative assessments of the cost-effectiveness of using Ca- or Na-based sorbents in DSI systems are reported elsewhere [205–207].

Notably, comparative analyses on the performance of Ca- and Na-based sorbents toward HF and HBr are not available in the open literature.

Mg-based sorbents are typically adopted in current industrial practice as dedicated reactants for high-temperature injection, as confirmed by experimental evidence. Partanen et al. [81] showed the superior HCl binding capacity of dolomite compared to limestone at 850 °C, reporting a final sorbent conversion of 75 % compared to 60 % after 3 h exposure in TGA to a 2000 ppm HCl gas flow. Moreschi and Marras [101] evidenced that the HCl and HF abatement of dolomitic sorbents increases

when shifting to temperatures higher than 1000 °C, whereas Ca-based sorbents typically present their maximum performance around 600 °C, as discussed in Section 5.1.1.

7.2. Comparative performance of innovative sorbents

As discussed in Section 3.2, in the past decade, several researchers focused on enhancing the removal efficiency of solid sorbents through the development of new formulations and advanced synthetic methods. However, although the influence of operating parameters on the performance of such novel reactants is typically well documented, only a limited number of authors have compared the efficiency of synthetic sorbents with benchmark commercial sorbents.

Fig. 9 reports two representative examples of studies clearly evidencing the superior performance of novel reactants over conventional ones, for Ca-based and Na-based synthetic sorbents, respectively. Cao et al. [117] compared the performance of a Ca-Mg-Al mixed oxide sorbent to conventional CaO in the treatment of HCl, while Tsubouchi et al. [127] compared the removal of HCl by conventional, unsupported Na_2CO_3 and honeycomb-supported Na_2CO_3. In both cases, experimental findings are reported in the form of curves of HCl breakthrough over a fixed bed of sorbent. Table 5 reports the experimental conditions applied in experimental runs.

In both cases, breakthrough curves allow observing a clear distinction in the performance between the novel sorbent and the benchmark. Notably, both synthetic sorbents demonstrate a significantly higher HCl removal rate. The initial phase of nearly 100 % HCl removal lasts at least 4 times longer than for the benchmark. In the case of the Ca-Mg-Al mixed oxides synthesized by Cao et al. [117], the superior performance can be ascribed to a tenfold specific surface area compared to conventional CaO, leading to the observed higher reactivity. In the case of Tsubouchi et al. [127], the superior performance derives from the use of a support for the sorbent. The honeycomb structure uniformly disperses the powdered sodium carbonate, minimizing particle agglomeration and improving gas-solid contact. In addition, the support mitigates the sintering effects that are frequently observed in unsupported sodium carbonate (see Section 5.1.1). From a more general point of view, Fig. 9 confirms that the use of comparative breakthrough curves appears to be a commendable approach to document the superior performance of a novel sorbent compared to a benchmark, as it allows to appreciate both the rate of HX absorption and the ultimate HX uptake capacity. A few other authors reported the average HCl removal efficiency of their synthesized sorbents against commercial benchmarks over a reference reaction time (see Table 6).

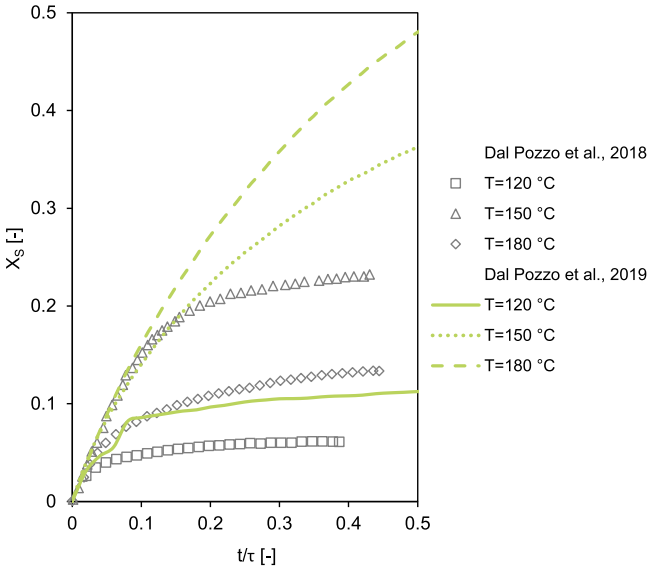

Fig. 8. Sorbent conversion in HCl removal (inlet concentration:1000 ppm) with respect to normalized reaction time. Dots refer to $Ca(OH)_2$ as sorbent, while lines refer to $NaHCO_3$.

It can thus be inferred that various synthetic sorbents reported in the literature in recent years show a higher removal efficiency compared to conventional reactants [63]. This could potentially translate into a significant reduction of sorbent consumption in DSI systems. However, it should be noted that some of the synthetic approaches adopted in the literature (see Table 3) involve the use of multiple chemicals and energy-intensive processing steps. This might be critical for the cost-effectiveness of synthetic sorbents, given that reference conventional sorbents are rather inexpensive commodities. Conducting a preliminary techno-economic analysis is therefore advisable to assess the viability of novel reactants and synthesis routes. It is equally important to evaluate whether the improved performance of synthetic sorbents outweighs their potentially higher environmental impact throughout the supply chain. While comparative life cycle assessment (LCA) studies on the environmental footprint of commercial Ca- and Na-based sorbents are available [55,66,208], similar analyses for synthetic sorbents are still lacking. Addressing this gap is crucial to assess the overall sustainability of these advanced materials.

8. Mechanisms of the reaction process

8.1. Reaction steps

The experimental evidence concerning hydrogen halide removal by solid sorbents, summarized in Sections 6 and 7, can be interpreted considering the underlying physicochemical phenomena controlling the overall reaction process. Non-catalytic gas-solid reactions are characterized by many elemental physical and chemical steps that can take place sequentially or simultaneously [144]. These steps include: i) gas film diffusion of the gaseous reactant from the bulk gas phase to the exterior surface of the sorbent particles (external mass transfer); ii) intra-particle transport through macro- and micro-pores (internal mass transfer); iii) diffusion through the layers of solid reaction products, and iv) adsorption on the sorbent surface and subsequent chemical reaction with the sorbent. The relative importance of these reaction process steps is greatly influenced by both operating conditions (temperature, humidity, gas composition) and structural properties of the solid sorbent, including particle size, pore size distribution, and tortuosity [209]. In addition, the gas-solid reaction system is inherently unsteady, and the controlling regime might change as the reaction proceeds [210]. Gas-solid reactions that produce a solid product, as in the case of the sorption of hydrogen halides, typically present two subsequent reaction regimes [211]: i) an initial fast stage governed by chemical kinetics, until a compact product layer covers the available reaction surface; and ii) a slower stage limited by product layer diffusion, as the compact product layer acts as a barrier between the gaseous and the solid reactants. In this context, product layer diffusion is typically rate-limiting compared to diffusion in the pores [212].

8.2. Conventional gas-solid reaction models applied to the sorption of hydrogen chloride

Table 7 summarizes the literature studies addressing the adaptation of conventional models for gas-solid reactions [213] to HX/solid sorbent system.

As shown in the table, a wide array of non-specific gas-solid heterogeneous reaction models were applied to the modelling of HCl sorption, with some studies focusing also on SO_2 removal. A single study focused on HF removal [148], while, to the knowledge of the authors, no studies addressing the modelling of HBr removal are present in the literature. A schematic representation of the conventional gas-solid reaction models is depicted in Fig. 10.

The early studies addressing the reaction mechanism of HCl removal

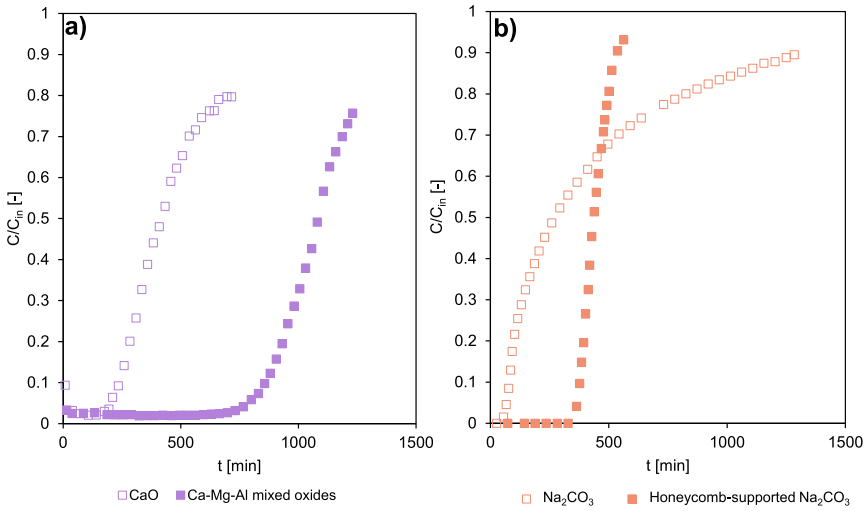

Fig. 9. a) Breakthrough curves for CaO and Ca-Mg-Al mixed oxides with respect to reaction time [117]. b) Breakthrough curves for powder soda ash and honeycomb-supported soda ash over reaction time [127]. Full dots refer to the synthetic sorbent, empty dots refer to the reference conventional sorbent used as a benchmark. Experimental conditions are reported in Table 5.

mostly relied on the application of the *shrinking core model* (SCM, Fig. 10a) [217]. Starting from experiments designed to minimize external mass transfer limitations [142,143], the SCM has been applied under the assumptions of chemical reaction control (governing parameter: kinetic constant k_s) or product layer diffusion control (governing parameter: PL diffusivity D_s). As the limiting step in the process can change as the reaction progresses, versions of the SCM with combined kinetic and diffusive control have been proposed [198]. The main limitation of this approach is the use of idealized geometries (spherical particles) and the exclusion of sorbent porosity.

To extend the SCM to porous solids, the *grain model* (GM, Fig. 10b) has frequently been adopted by describing the solid phase of a porous particle as a matrix of non-overlapping, non-porous grains. This implies coupling a diffusion resistance model for the particle (i.e., gas film and pore diffusion of the gases from the bulk gas phase to the inner grain surface) with an unreacted shrinking core model for the grain (i.e., diffusion through the product layer of the grain and reaction at the surface of the fresh reactant core) [150]. A common limitation of several applications of the GM [74,142,151,155] is the assumption of uniform grain size. Actually, sorbent particles exhibit a distribution of pore sizes, which the GM can approximate by considering populations of grains of different initial size, e.g., deriving a set of size distributions of grains from the size distribution of pores measured via mercury porosimetry, as in Dal Pozzo et al. [82]. In addition, studies employing the GM often neglect how the PL growth also affects sorbent porosity, causing pore clogging and reducing internal gas diffusion.

As highlighted in Table 7, most studies on HCl removal adopted the GM or modified versions of the GM to interpret experimental data, reporting product layer diffusion as the controlling stage. Resulting estimates of the diffusion coefficient of the gaseous reactant through the product layer D_S [m^2/s] obtained by different investigators, albeit using different modelling approaches, are reported in Fig. 11, for Ca-based (panel a) and Na-based (panel b) sorbents, as a function of inverse temperature. In this representation, it is evident that the Arrhenius-type dependence of D_S with temperature. An exception is represented by D_S values derived at temperatures lower than 100 °C in the presence of moisture (see, e.g., Fonseca et al. [151]), for the reasons discussed in Section 5.1.2.

The *random pore model* (RPM, Fig. 10c) has found significant applications in the study of gas-solid reactions for acid gas removal, particularly in cases where structural changes in the porous sorbent dramatically reduce the reaction rate, e.g., for SO_2 sorption [215,218], due to its ability to account for structural changes during reactions, capturing the dynamic nature of pore structure and altering reaction kinetics accordingly. However, possibly due to the detailed knowledge of the dynamic structural properties of the sorbent required for its application, the RPM has been adopted in a single study addressing HCl removal [199].

Despite the extensive research conducted to date regarding gas-solid reactions and their modelling, notable gaps remain in properly describing the overall reaction process occurring during acid gas removal. The conventional models for non-catalytic gas-solid reactions typically fail to describe the incomplete conversion of solid sorbents [33]. In particular, the above-mentioned models have shown limitations in the prediction of the incomplete conversion of calcium-based sorbents observed in several experimental studies [74,143,151,152]. In fact, a wealth of experimental evidence, summarized in Fig. 12, indicates that the reactions of Ca-compounds with HCl stop before the complete conversion of the solid calcium sorbent and that the final calcium conversion depends on temperature [219].

Distinct trends characterize different temperature ranges in Fig. 12. At temperatures below 300 °C, studies conducted in dry gas revealed an increase in the ultimate conversion with temperature [74,82,143]. Conversely, as discussed in Section 5.1.2, studies reporting the results of experiments in moist gas found that the ultimate conversion of the sorbent decreases with temperature, as a consequence of the increase in the relative humidity [151,152]. In the range 400–600 °C, above the

Table 6
Comparative HCl abatement performance of synthetic sorbents versus commercial benchmarks in terms of average removal efficiency in relevant literature studies. Experimental conditions are reported in Table 5.

Sorbent	Average HCl removal efficiency (%) over 60 min of reaction time	Reference
Ca-Mg-Al mixed oxides *(synthetic sorb.)*	97.9	[117]
CaO *(benchmark)*	93.5	
$NaHCO_3$ *(benchmark)*	97.0	
Na_2CO_3 supported on alumina *(synthetic sorb.)*	98.0	[107]
$Ca(OH)_2$ *(benchmark)*	15.0	
Honeycomb-supported Na_2CO_3 *(synthetic sorb.)*	67.0	[127]
Na_2CO_3 *(benchmark)*	10.0	
Ethanol-modified CaO *(synthetic sorb.)*	97.8	[87]
CaO *(benchmark)*	14.2	

dehydration temperature of $Ca(OH)_2$, authors testing the HCl uptake of calcium oxides and carbonates report an increase in the ultimate conversion with temperature [142,150]. A notable lack of experimental data is present in the range between 300 and 400 °C. At temperatures higher than 600 °C, sorbent conversion decreases with temperature [145,160], as thermal sintering becomes relevant (see Section 5.1.1).

As a matter of fact, even if researchers have gathered ample evidence of incomplete sorbent conversion, as summarized in Fig. 12, a consensus on the theoretical explanation of this phenomenon is not yet present. The early studies that first observed the incomplete solid conversion in the sulfation of lime and limestone attributed it to the blockage of the porous structure of the sorbent [220,221]. Yan et al. [143] hypothesized that the pore plugging mechanism might also explain the incomplete conversion of calcium hydroxide particles exposed to HCl. As the molar volume of the solid product $CaCl_2$ is larger than that of the reactant $Ca(OH)_2$, the gas-solid reaction may lead to an expansion of the solid, thus clogging the pores. Eventually, the void fraction of the sorbent particles may be entirely filled before complete sorbent conversion is reached.

Simons and Garman [221] derived an expression to estimate the theoretical maximum solid conversion at which complete closure of the intraparticle voids occurs:

$$X_{s,max} = \frac{\varepsilon_p}{(1-\varepsilon_p)(\alpha-1)} \tag{18}$$

where ε_p is the initial void fraction of the sorbent and α is the volumetric expansion factor, i.e., the ratio of the molar volume of the solid product to that of the solid reactant. For instance, the conversion of $Ca(OH)_2$ to $CaCl_2$ in anhydrous or dihydrate form leads to α equal to 1.54 and 2.39, respectively. In contrast, the formation of NaCl from Na_2CO_3 entails α equal to 1.29. Therefore, according to Eq. 18, a Na_2CO_3 particle with an initial porosity $\varepsilon_p = 0.3$ can be fully converted to NaCl, while a $Ca(OH)_2$ particle with the same initial porosity can only achieve a maximum theoretical conversion of 80 % or 30 %, whether the solid product is anhydrous or dihydrate $CaCl_2$, offering a first possible explanation of the evidence concerning the incomplete conversion issues in Na-based sorbents [96].

However, the pore plugging theory for incomplete conversion derived from Simons and Garman [221] assumes that the phenomenon depends solely on properties of the solid reactant and product (Eq. 18), hence it cannot explain why the ultimate conversion is affected by operating conditions, e.g., by temperature, as shown in Fig. 12. Furthermore, the theory fails to account for the very low maximum conversions (i.e., 10 %) observed at low temperatures for porous sorbents (see Fig. 12, data reported by [74,170]), where the volume expansion associated with chloride formation would be too small to fill the pores.

Therefore, Yan and coworkers in 2003 [143] proposed an alternative mechanism to explain the incomplete conversion of the solid sorbent. They suggested that the growth of solid product layers might occlude the pore mouths, i.e., the outer pores of sorbent particles, preventing or severely limiting access of the gaseous reactant to the internal pores and the core of sorbent particles [143]. Yet, this idea conflicts with the findings of researchers who investigated the elemental composition of cross-cut sorbent particles after exposure to HCl. Weinell et al. [74] and Partanen et al. [145] analysed by energy dispersive X-ray (EDX) spectroscopy the distribution of chlorine inside a 70 μm $Ca(OH)_2$ particle reacted with 1000 ppm HCl at 200 °C and inside a 200 μm CaO particle reacted with 1000 ppm HCl at 850 °C, respectively. Both studies found Cl to be evenly distributed along the cross-section of the reacted particles, as shown in Fig. 13, thus suggesting a rather uniform solid conversion across the radial coordinate.

In addition, another set of tests, based on single-crystal (SC) measurements, appears to disprove pore clogging as the most relevant cause for the incomplete ultimate conversion of the solid. SC have been used as model systems to study the reaction between sorbent and gaseous reactant on a simple and clearly defined surface geometry, not influenced by the complex texture and porosity patterns of sorbent particles [162]. Koch et al. [175] exposed calcium hydroxide SCs, grown from aqueous solutions of $CaCl_2$ and NaOH in a desiccator, to 220 ppm HCl in moist gas (10 H_2O) at 100 °C. After 150 min, cross-sections of the SCs were analyzed by EDX, revealing that the surface of the SC remained plane after the reaction. The reaction product was located within the parent $Ca(OH)_2$ crystal, showing that the reaction front penetrated inside the crystal instead of expanding outwards. Therefore, the authors concluded that no pore closure could occur during $Ca(OH)_2$ reaction with HCl as a consequence of product layer growth [175].

Sun et al. [168] also investigated how the solid surface is affected by reaction in the CaO-HCl system, with a different experimental design, shown in Fig. 14. They pressed CaO powder into cylindrical tablets, sintered them at 1200 °C for 2 days to remove the inner pore volume, then applied a strip of platinum paint on the tablet surface. Pt paint acted as an inert marker to elucidate the prevailing mechanism in

Table 7
Modelling studies addressing the application of non-specific gas-solid heterogeneous kinetic models to acid gas reaction with solid sorbents.

Gas	Sorbent	Model	Notes	Reference
HCl	CaO	SCM	Assumes mixed chemical reaction and product layer (PL) diffusion control, neglects pore diffusion.	[140]
HCl	CaO	SCM	Determines an apparent kinetic rate, neglects PL growth.	[142]
HCl	$Ca(OH)_2$	SCM	Assumes chemical reaction control, neglects PL growth.	[143]
HCl	$Ca(OH)_2$	SCM	Assumes lumped kinetics, with a kinetic constant dependent on temperature and gas composition.	[147]
HCl	Mixed Ca/Na-based sorbent	SCM	Assumes mixed chemical reaction and PL diffusion control.	[125]
HCl	Na-Mg-Al LDH	SCM	Adapts SCM to account for layered structure and ion exchange, assuming uniform particles.	[129]
HCl+SO_2	$Ca(OH)_2$	SCM	Parallel-reaction SCM with moisture-dependent PL diffusion coefficients.	[152]
HCl	$Ca(OH)_2$, $CaCO_3$	GM	First application of the GM to HCl removal. Assumes spherical particles and uniform grain size.	[74]
HCl	$CaCO_3$	GM	Coupling of a GM using mixed chemical reaction and PL diffusion with pore diffusivity from RPM.	[150]
HCl	$Ca(OH)_2$	GM	GM with mixed chemical reaction and PL diffusion. PL diffusivity as a linear function of moisture.	[151]
HCl	Na_2CO_3	GM	GM model nested in an integral fixed-bed reactor model, including gas film and pore diffusion.	[155]
HCl	Mixed Ca/Na-based sorbent	GM	Steady-state and isothermal assumptions; simplified flow conditions in a high-temperature gas stream	[214]
HCl	$Ca(OH)_2$	GM	Coupling of conventional GM with a crystallization and fracture submodel. Accounts for sorbent structural change; still assumes steady-state and neglects dynamic behavior.	[33]
HCl	$Ca(OH)_2$	GM	Extension of the model introduced in [33]. Considers a distribution of grain size, modelled based on the experimental pore size distribution of the reactant.	[82]
HCl	Mixed Ca/Na-based sorbent	RPM	Application of RPM to HCl removal with mixed chemical reaction and PL diffusion control.	[199]
SO_2	CaO	RPM	Compares different formulations to include the evolution of pore diffusivity over time.	[215]
SO_2	Na_2CO_3	RPM	Application to slab pellet geometry. Includes variation of pore diffusivity over time.	[216]

SCM: shrinking core model; GM: grain model; RPM: random pore model.

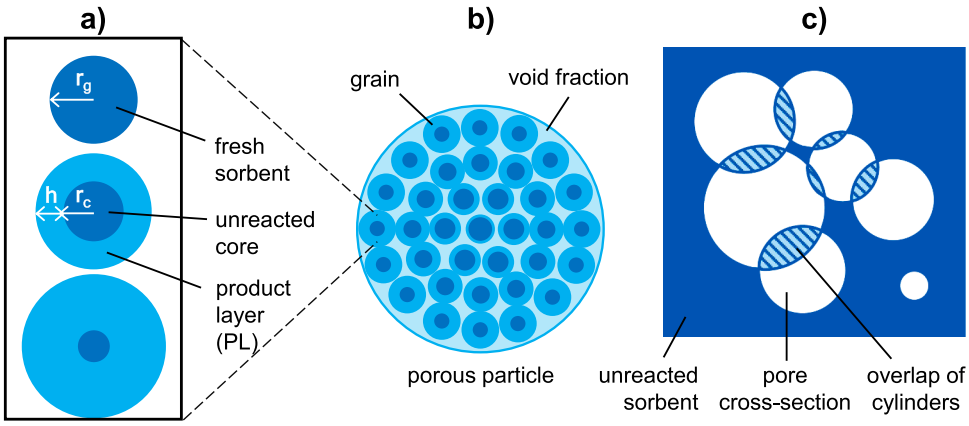

Fig. 10. Schematization of the models for gas-solid reactions: a) shrinking core model (SCM), b) grain model (GM), where each grain reacts according to the SCM, c) random pore model (RPM).

solid-state diffusion through the product layer, i.e., determining whether the inward migration of reactant ions from the gas phase or the outward migration of reactant ions from the solid phase is faster. After 30 days of exposure to a flow of 50 ppm HCl in N_2 at 500 °C, the authors observed that the position of the Pt layer at the exterior surface of the CaO tablet remained unchanged and the $CaCl_2$ product layer grew beneath the Pt layer, hence showing a preferred "inward growth" mode, in agreement with the evidence from the SC experiments by Koch et al. [175].

On the whole, the experimental findings reported in the literature point out that the incomplete conversion of the solid reactant derives from the evolution of the product layer and its influence on the overall reaction rate.

8.3. *Specific gas-solid reaction models addressing sorbent incomplete conversion*

As discussed above, conventional heterogeneous gas-solid reaction models fail in providing a sound approach to the incomplete conversion of the solid sorbent. Thus, a few studies introduced modeling approaches specifically addressing the incomplete sorbent conversion, linking it to phenomena occurring within the product layer.

Duo et al. [219,222] advanced a thermodynamic explanation concerning how the product layer formation affects the maximum achievable solid conversion for Ca-based sorbents reacting with acid gases. Their approach, named *crystallization and fracture (CF) model*, starts from the assumption – later proved by scanning electron microscopy (SEM) images [189,223]– that at the beginning of the reaction, the solid product, rather than forming a uniform thin layer on the pristine sorbent surface, nucleates in clusters of molecules according to a crystallization process. The process involves four main steps: (i) nucleation of product molecules at the interface between the product layer and unreacted sorbent; (ii) growth of nuclei into larger crystals that form a thickening product layer; (iii) displacement of the product layer during growth, potentially causing fractures due to volume expansion; and (iv) termination of the reaction when the energy required for further crystallization and fracture exceeds the free energy of the reaction. Notably, step (iv) is consistent with the experimental observations of an incomplete sorbent conversion that is a function of temperature and concentration of the gaseous reactant.

Antonioni et al. [33] integrated the CF model in the grain model framework by converting the increase of the energy threshold for nucleation into a reduction factor of the overall reaction rate. The grain model modified by the incorporation of the CF submodel to fit different experimental datasets for the reaction between $Ca(OH)_2$ and HCl [74, 143,205] highlighted a log-linear decrease with temperature of the mechanical resistance of the product layer, in agreement with the typical behavior of the elastic modulus of several materials [224]. Therefore, it may be concluded that the CF modification of the grain model appears capable of describing the phenomenological nature of the problem, although it introduces complexity in the modelling framework.

A simpler approach to account for incomplete sorbent conversion is to introduce in the model a variation of the diffusivity in the product layer with sorbent conversion [209]. Different empirical expressions for the time dependency of PLD have been proposed in the literature, especially with reference to the reaction between lime and SO_2 [89,225] that, in principle, may also apply to the reaction with hydrogen halides. In this context, Montagnaro et al. [212] introduced a fractal formulation of PLD that takes into account not only the dependency on the reaction time, but also an inverse correlation with the concentration of the gaseous reactant, in agreement with the CF theory [226].

Although the proposed approaches were successful in the interpretation of experimental data obtained at the laboratory scale, the scale-up of such models to develop a sound modelling of the full-scale gas-solid reaction process for full-scale flue gas cleaning is still lacking. To date, process design, optimization, and control in the industrial environment are typically carried out by applying empirical data-driven models [227, 228]. Such models present increasing accuracy due to the progress in data analytics and the wealth of process data usually available in facilities such as WtE plants [229]. Yet, they inherently require plant-specific tuning [55]. Although some empirical models calibrated on industrial process data have shown a rather broad validity [230], also taking advantage of hybrid modelling strategies [203], the progress in first principles approaches constitutes the way forward towards a generalization and more robust DSI process modelling. In particular, from a perspective, the advanced reaction models discussed in this section could be nested into computational fluid dynamics codes describing the entrained flow of sorbent particles in the flue gas to provide a detailed simulation of DSI operation [135].

9. Discussion

The review carried out allowed tracking the state-of-the-art of research on gas-solid reactions for the removal of hydrogen halides from flue gases. In light of the work carried out, the most relevant findings can be summarized as follows:

- **Performance of commercial sorbents.** Calcium-, sodium-, and magnesium-based materials are the commercial sorbents most widely applied in flue gas treatment. In particular, in the low temperature range that is typical of most DSI industrial applications (120–250 °C), Na-based sorbents exhibit higher HCl removal efficiency than Ca-based sorbents, and their reactivity increases with temperature. The reactivity of Ca-based sorbents can be enhanced by

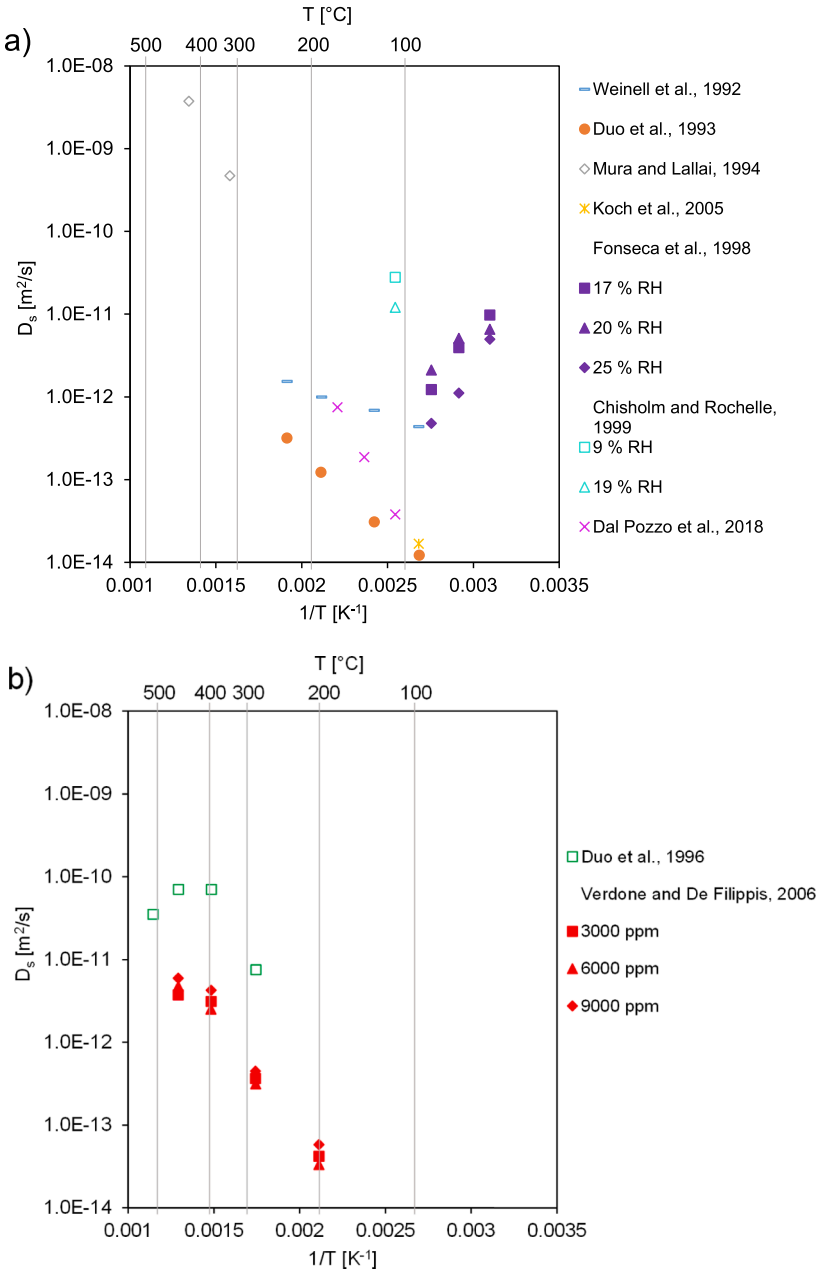

Fig. 11. Product layer diffusivity values reported in the literature for the reaction between: a) Ca-based sorbents and HCl; b) Na-based sorbents and HCl.

increasing their specific surface area (e.g., via hydration in aqueous solutions containing alcohols or ball milling) or by operating the process near the saturation temperature of the flue gas (i.e., at high relative humidity).

In the high-temperature range of interest for reactant injection in furnaces or boilers (600–1000 °C), the performance of Na-based sorbents is severely limited by thermal sintering. Dolomitic sorbents emerge as the most suitable class of reactants for high-temperature applications thanks to the structural action of their Mg components.

- **Performance of innovative sorbents.** Developed with the aim of magnifying specific surface area, they can exhibit significantly higher reactivity (at least 3 times longer breakthrough times in comparative experiments) compared to commercial hydrated lime and sodium bicarbonate. However, to date, scarce attention has been dedicated to the costs of the materials used and to synthesis techniques. Additionally, most of the proposed innovative sorbents are developed at laboratory scale, demonstrating a technology readiness level (TRL) equal to or lower than 4. This underscores the need of an extended experimental validation before they may be proposed for industrial application.
- **HF removal.** The removal of HF from flue gas streams remains insufficiently documented in the scientific literature. Only a few addresses HF separation, highlighting that Ca-based sorbents show high removal efficiency at high temperature (300–800 °C).
- **Competition between hydrogen halides.** Scattered experimental evidence suggests that Ca-based sorbents have a preferential reactivity toward HF compared to HCl, while for Na-based sorbents, the opposite is reported. Notably, the literature offers no insights into the simultaneous sorption behavior of HF or HCl in the presence of HBr.
- **Competition with SO_2.** When SO_2 is also present in the flue gas, experimental data evidence that it competes with HCl for sorption sites on Ca-based sorbents. At high temperatures (over 600 °C), SO_2

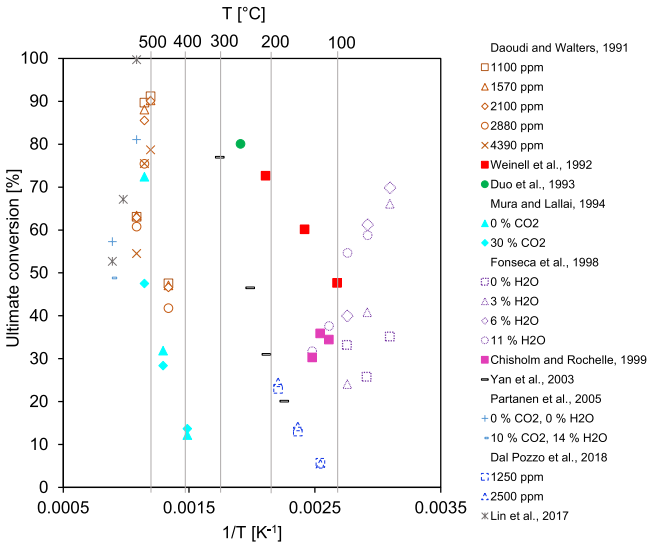

Fig. 12. Ultimate conversion of Ca-based sorbents in HCl removal reported by different authors, in dry conditions or in the presence of H_2O and/or CO_2 (concentration expressed in % v/v), plotted as a function of inverse temperature.

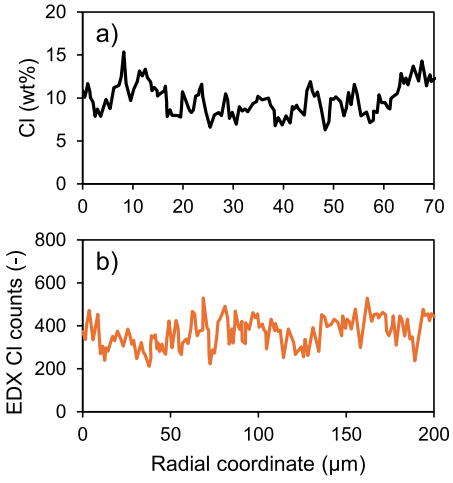

Fig. 13. EDX analysis of the distribution of chlorine in the cross-section of a sorbent particle after exposure to HCl: a) a $Ca(OH)_2$ particle reacted with 1000 ppm HCl at 200 °C (adapted from [74]); b) a CaO particle reacted with 1000 ppm HCl at 850 °C (adapted from [145]).

absorption is enhanced in the presence of HCl due to increased calcium sulfation. However, this simultaneously reduces HCl capture, as calcium is preferentially converted to $CaSO_4$. At low temperatures (< 300 °C), Ca-based sorbents show a higher selectivity for HCl, but SO_2 inhibits HCl sorption by forming dense product layers that block access to the remaining reactive sites. The extent of the inhibition depends on SO_2 concentration and on the presence of oxygen in the gas phase, which favors the formation of sulfate rather than sulfite layers. On Na-based sorbents, HCl generally shows a preferential uptake over SO_2, though some reduction in HCl sorption efficiency is observed with increasing SO_2 concentrations, due to competitive reactions at shared alkaline sites and partial sulfation of sodium chlorides.

- **Competition with CO_2.** CO_2 interacts with Ca-based sorbents through carbonation reactions, forming calcium carbonate and reducing the availability of active sites for HCl sorption. The interference from CO_2 becomes more pronounced at high temperatures (higher than 400 °C), as carbonation kinetics intensifies. At low temperatures (< 300 °C), the extent of carbonation is typically limited, yet some reduction in HCl sorption efficiency still occurs due to pore clogging from carbonate formation. Although only a few studies addressed the topic, the presence of CO_2 in the flue gas is also reported to reduce the efficiency of HCl capture of Na-based sorbents.
- **Reaction process and kinetic modelling.** Most authors agree that the rate of the overall process is governed by diffusional limitations, and, in particular, by diffusional resistance in the layers of solid product. Conventional models, such as the shrinking core model and the grain model, provide a foundational understanding of gas-solid reactions but fail to accurately describe the incomplete conversion of Ca-based sorbents. The random pore model offers enhanced predictive accuracy by considering changes in pore structure during reaction progress, but requires detailed sorbent characterization. Efforts have been devoted to developing advanced fundamental models accounting for the specific phenomena observed in experimental studies, e.g., based on the inclusion of crystallization and fracture mechanisms in the product layer. The use of hybrid modelling approaches, adopting time-dependent diffusion coefficients or lumped reaction parameters, provides an improved accuracy at a lower computational cost but requires case-specific calibration, limiting their general applicability.

The analysis of the literature also allows evidencing the following main knowledge gaps:

- **Validation of fundamental kinetic models for the gas-solid reaction process.** Even if several fundamental kinetic models were proposed for the interpretation of gas-solid reaction experimental

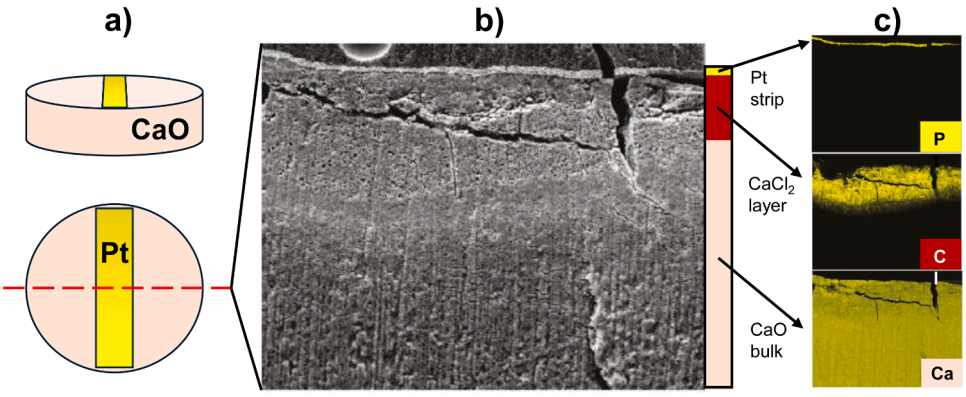

Fig. 14. Inert marker experiment for the elucidation of product layer growth mode: a) positioning of a Pt strip on the surface of a tablet of sintered CaO; b) SEM image of a cross-section of the tablet after reaction with 50 ppm HCl at 500 °C; c) EDX mapping of Pt, Cl, and Ca. Adapted from [168].

data obtained at the laboratory scale, the full-scale validation of such models is still lacking. To date, process design, optimization, and control in the industrial environment are typically carried out by applying empirical data-driven models. This underscores the need of an extended large-scale validation fo fundamental models before they may be proposed for industrial application.

- **Benchmarking of innovative sorbents:** While several recent studies report the development of promising synthetic sorbents for HX removal, systematic studies addressing the comparative assessments of their actual advantages over conventional reactants are still lacking. Performance claims are often based on laboratory-scale results without benchmarking against commercial sorbents under representative operating conditions. Moreover, techno-economic and life cycle aspects are rarely addressed, leaving open questions on the cost competitiveness and environmental sustainability of such materials. Future research should aim to clarify not only the HX removal potential of innovative sorbents but also their practical applicability in terms of cost, scalability, and overall environmental impact.
- **HBr and HF removal**: Notably, no experimental campaign to date has been devoted to clarifying the comparative performance of Ca-based and Na-based sorbents toward HBr and HF, two gases of increasing relevance in industrial flue gas cleaning applications.
- **Competition among halides**: The existing body of research predominantly focuses on the removal of individual acid gases, with limited attention given to the interactions that may arise when multiple acid species are present simultaneously. However, gaining a deeper understanding of such interactions is essential to evaluate potential competitive or synergistic effects that may influence overall removal efficiency. While some studies have explored the interaction between HCl and SO_2, comparative investigations involving multiple hydrogen halides remain scarce. A systematic investigation of the comparative reactivity of the different halides towards the available classes of sorbents is needed to substantiate the currently fragmented information. In particular, the mutual influence between HF, HCl, and HBr during sorption processes has yet to be systematically addressed, representing a notable gap in current knowledge.
- **Understanding/Modelling of the role of humidity**: Humidity in the gas stream represents a critical operational parameter in flue gas treatment, where a non-negligible amount of water vapor is typically present. The influence of moisture on the efficiency of HCl removal has been experimentally investigated by several researchers over a broad temperature range. While qualitatively the effect of moisture is relatively well understood, generally enhancing sorption in the typical temperature range of DSI applications, quantitative modelling remains challenging.
- **Incomplete sorbent conversion:** Despite a wide experimental consensus showing that Ca-based sorbents do not reach full conversion in typical DSI conditions, the underlying mechanisms remain only partially understood. Several hypotheses have been proposed, including pore closure, product layer densification, or thermodynamic limitations to nucleation, but no comprehensive explanation has yet been proved and universally accepted. The issue of incomplete conversion has significant practical implications for the cost-effectiveness and the indirect environmental impacts of dry acid gas treatment, as it leads to excess sorbent consumption and increased generation of solid residues. Understanding the fundamental phenomena leading to incomplete sorbent conversion may allow the identification of operating conditions leading to a higher effectiveness and a lower environmental impact of DSI full-scale applications.

10. Conclusions and future perspectives

In this study, the state-of-the-art concerning gas-solid reaction processes for the removal of hydrogen halides from flue gases was comprehensively examined. The findings of more than 230 articles published from 1980 to date, encompassing experimental and modelling studies, were analyzed. The corpus of research conducted by different authors over three decades was critically examined, combining the experimental data to present a comprehensive characterization of the reactivity of different commercial and synthetic sorbents towards different hydrogen halides (HCl, HF, and HBr) at different operating conditions in terms of temperature and moisture. Knowledge gaps and open issues concerning the fundamental phenomena underlying the acid gas removal reaction process were identified and discussed in light of the different approaches so far adopted.

As discussed above, the main gaps identified are related to the lack of experimental data on the single removal of HBr and HF and their simultaneous removal with HCl. Additionally, understanding the role of humidity is crucial, especially to allow the modelling of gas-solid reactions involved in acid gas removal.

In light of the above, priorities for future research in the field have been identified. On the side of experimental work, there is a pressing need for studies addressing the simultaneous sorption of multiple acid gas compounds, to better elucidate synergic and/or competitive interactions between these species. Relatedly, the significant lack of data on the sorption of halides other than HCl (mainly HF and HBr) needs to be addressed. To date, the WtE sector has been the reference field of application for the removal of hydrogen halides, thus driving the focus of researchers on HCl as a target pollutant. However, stricter emission standards are introduced in other industries (e.g., glass and ceramic tile manufacturing) and novel flue gas cleaning applications emerge (e.g., pyrometallurgical processes for WEEE recycling). Thus, in order to tailor and optimize dry flue gas treatment solutions for these sectors, it is essential to evaluate the performance of solid sorbents under flue gas compositions representative of these emerging environments, where HF and HBr play a relevant role.

High-efficiency advanced synthetic sorbents are also proposed for application. Their higher reactivity and thermal stability with respect to state-of-the-art commercial sorbents make them attractive for prospective use, though currently reported only at limited TRL (typically between 2 and 4). However, as the most effective synthesis routes might be significantly more complex than the production of commercial hydrated lime and sodium bicarbonate, at least a preliminary prospective techno-economic and life cycle analysis is required to identify specific synthetic sorbents that may be considered as potential substitutes for commercial sorbents. Moreover, it is recommended to benchmark the removal performance of novel sorbents to that of representative commercial sorbents, e.g., by using breakthrough curves providing both the rate of HX absorption and the final HX uptake capacity.

On the modelling front, besides the need to address open issues, e.g., regarding the role of water and other gas components in the HX removal process, the analysis of the literature evidenced that fundamental models are currently applied and validated only at laboratory scale (TRL 4). It would be of utmost importance to extend these models to the assessment of full-scale systems, since process design and control of full-scale industrial systems nowadays still mostly rely on empirical or data-driven approaches. Bridging this gap would enhance the predictive power of models and support the development of more efficient and scalable flue gas treatment solutions.

CRediT authorship contribution statement

Carmela Chianese: Writing – original draft, Investigation, Formal analysis, Data curation, Conceptualization. **Valerio Cozzani:** Writing – review & editing, Supervision, Methodology, Investigation, Formal analysis, Conceptualization. **Alessandro Dal Pozzo:** Writing – original draft, Supervision, Methodology, Investigation, Data curation, Conceptualization.

Declaration of Competing Interest

The authors declare that they have no known competing financial interests or personal relationships that could have appeared to influence the work reported in this paper.

Data availability

Data will be made available on request.

References

[1] Zhang, B., Shen, H., Yun, X., Zhong, Q., Henderson, B.H., Wang, X., Shi, L., Gunthe, S.S., Huey, L.G., Tao, S., Russell, A.G., Liu, P., 2022. Global emissions of hydrogen chloride and particulate chloride from continental sources. Environ Sci Technol 56, 3894–3904. https://doi.org/10.1021/acs.est.1c05634.

[2] Zhang, H., Yu, S., Shao, L., He, P., 2019. Estimating source strengths of HCl and SO_2 emissions in the flue gas from waste incineration. J Environ Sci (China) 75, 370–377. https://doi.org/10.1016/j.jes.2018.05.019.

[3] Meynendonckx, W., Ishteva, M., Verbeke, M., Alderweireldt, N., De Greef, J., 2025. Impact of furnace and waste layer control on HCl and SO_2 in combustion gas from a grate-fired Waste-to-Energy boiler. Process Saf Environ Prot 193, 710–720. https://doi.org/10.1016/j.psep.2024.11.051.

[4] Matsukata, M., Takeda, K., Miyatani, T., Ueyama, K., 1996. Simultaneous chlorination and sulphation of calcined limestone. Chem Eng Sci 51, 2529–2534. https://doi.org/10.1016/0009-2509(96)00106-6.

[5] Ma, W., Wenga, T., Frandsen, F.J., Yan, B., Chen, G., 2020. The fate of chlorine during MSW incineration: vaporization, transformation, deposition, corrosion and remedies. Prog Energy Combust Sci 76, 100789. https://doi.org/10.1016/j.pecs.2019.100789.

[6] Zhu, H.M., Jiang, X.G., Yan, J.H., Chi, Y., Cen, K.F., 2008. TG-FTIR analysis of PVC thermal degradation and HCl removal. J Anal Appl Pyrolysis 82, 1–9. https://doi.org/10.1016/j.jaap.2007.11.011.

[7] Ma, W., Hoffmann, G., Schirmer, M., Chen, G., Rotter, V.S., 2010. Chlorine characterization and thermal behavior in MSW and RDF. J Hazard Mater 178, 489–498. https://doi.org/10.1016/j.jhazmat.2010.01.108.

[8] Zhu, H., Chen, W., Jiang, X., Yan, J., Chi, Y., 2015. Study on HCl removal for medical waste pyrolysis and combustion using a TG-FTIR analyzer. Front Environ Sci Eng 9, 230–239. https://doi.org/10.1007/s11783-014-0651-3.

[9] Ren, X., Sun, R., Chi, H.H., Meng, X., Li, Y., Levendis, Y.A., 2017. Hydrogen chloride emissions from combustion of raw and torrefied biomass. Fuel 200, 37–46. https://doi.org/10.1016/j.fuel.2017.03.040.

[10] Tillman, D.A., Duong, D., Miller, B., 2009. Chlorine in solid fuels fired in pulverized fuel boilers-sources, forms, reactions, and consequences: a literature review. Energy Fuels 23, 3379–3391. https://doi.org/10.1021/ef801024s.

[11] Marcantonio, V., Müller, M., Bocci, E., 2021. A review of hot gas cleaning techniques for hydrogen chloride removal from biomass-derived syngas. Energ (Basel) 14, 6519. https://doi.org/10.3390/en14206519.

[12] Jia, Y., Wang, Y., Jiang, C., Wang, X., Hu, Z., Xiao, B., Liu, S., 2022. Simultaneous enhancement of the H_2 yield and HCl removal efficiency from pyrolysis of infusion tube under novel mayenite-based mesoporous catalytic sorbents. Energy 244, 123067. https://doi.org/10.1016/j.energy.2021.123067.

[13] Veksha, A., Giannis, A., Oh, W.Da, Chang, V.W.C., Lisak, G., 2018. Upgrading of non-condensable pyrolysis gas from mixed plastics through catalytic decomposition and dechlorination. Fuel Process Technol 170, 13–20. https://doi.org/10.1016/j.fuproc.2017.10.019.

[14] Micoli, L., Bagnasco, G., Turco, M., 2013. HCl removal from biogas for feeding MCFCs: adsorption on microporous materials. Int J Hydrog Energy 38, 447–452. https://doi.org/10.1016/j.ijhydene.2012.09.102.

[15] Yudovich, Y.E., Ketris, M.P., 2006. Chlorine in coal: a review. Int J Coal Geol 67, 127–144. https://doi.org/10.1016/j.coal.2005.09.004.

[16] Qu, G., Wei, Y., Li, B., Wang, H., 2024. The influence of chlorination additives on metal separation during the pyrometallurgical recovery of spent lithium-ion batteries. Waste Manag 186, 331–344. https://doi.org/10.1016/j.wasman.2024.06.022.

[17] Cossu, R., Lai, T., Pivnenko, K., 2012. Waste washing pre-treatment of municipal and special waste. J Hazard Mater 207–208, 65–72. https://doi.org/10.1016/j.jhazmat.2011.07.121.

[18] Winchell, L.J., Ross, J.J., Wells, M.J.M., Fonoll, X., Norton, J.W., Bell, K.Y., 2021. Per- and polyfluoroalkyl substances thermal destruction at water resource recovery facilities: a state of the science review. Water Environ Res 93, 826–843. https://doi.org/10.1002/wer.1483.

[19] Galán, E., González, I., Fabbri, B., 2002. Estimation of fluorine and chlorine emissions from Spanish structural ceramic industries. The case study of the Bailén area, Southern Spain. Atmos Environ 36, 5289–5298. https://doi.org/10.1016/S1352-2310(02)00645-3.

[20] Boschi, G., Masi, G., Bonvicini, G., Bignozzi, M.C., 2020. Sustainability in Italian ceramic tile production: evaluation of the environmental impact. Appl Sci (Switz) 10, 1–15. https://doi.org/10.3390/app10249063.

[21] Feng, J., Li, K., Ning, P., Wang, C., Sun, X., Wang, F., Gao, P., 2023. Preparation of MgX/Al_2O_3-Y sorbent for highly efficient simultaneous removal of hydrogen fluoride and hydrogen chloride under low-temperature environment. Environ Technol 44, 2230–2243.

[22] Caputo, A.C., Pelagagge, P.M., 1999. Cost-effectiveness analysis of waste gas treatment plants for the glass industry. J Air Waste Manag Assoc 49, 1456–1462. https://doi.org/10.1080/10473289.1999.10463971.

[23] Abdul-Wahab, S., Alsubhi, Z., 2019. Modeling and analysis of hydrogen fluoride pollution from an aluminum smelter located in Oman. Sustain Cities Soc 51, 101802. https://doi.org/10.1016/j.scs.2019.101802.

[24] Chimeh, A.F., Kocaefe, D., Kocaefe, Y., Robert, Y., Bernier, J., 2024. Mathematical modelling of a semi-dry SO_2 scrubber based on a Lagrangian-Eulerian approach. J Hazard Mater 469, 134065. https://doi.org/10.1016/j.jhazmat.2024.134065.

[25] G. Cusano, M.R. Gonzalo, F. Farrell, R. Remus, S. Roudier, L.D. Sancho, Best available techniques (BAT) reference document for the non-ferrous metals industries Industrial Emissions Directive 2010/75/EU (Integrated Pollution Prevention and Control), (2017).

[26] Y, C.X, G.X, C.M, Shen, 2018. Chemical pyrolysis of E-waste plastics: char characterization. J Environ Manag 214, 94–103.

[27] Zhu, J., Huang, T., Huang, Z., Qin, B., Tang, Y., Ruan, J., Xu, Z., 2022. An energy-saving and environment-friendly technology for debromination of plastic waste: novel models of heat transfer and movement behavior of bromine. J Hazard Mater 421, 126814. https://doi.org/10.1016/j.jhazmat.2021.126814.

[28] Ghosh, B., Ghosh, M.K., Parhi, P., Mukherjee, P.S., Mishra, B.K., 2015. Waste Printed Circuit Boards recycling: an extensive assessment of current status. J Clean Prod 94, 5–19. https://doi.org/10.1016/j.jclepro.2015.02.024.

[29] Beccagutti, B., Cafiero, L., Pietrantonio, M., Pucciarmati, S., Tuffi, R., Vecchio Ciprioti, S., 2016. Characterization of some real mixed plastics from weee: a focus on chlorine and bromine determination by different analytical methods. Sustain (Switz) 8, 1–17. https://doi.org/10.3390/su8111107.

[30] Chen, Y., Yang, J., Liang, S., Hu, J., Hou, H., Liu, B., Xiao, K., Yu, W., Deng, H., 2021. New insights into the debromination mechanism of non-metallic fractions of waste printed circuit boards via alkaline-enhanced subcritical water route. Resour Conserv Recycl 165, 105227. https://doi.org/10.1016/j.resconrec.2020.105227.

[31] Thabit, Q., Nassour, A., Nelles, M., 2022. Flue gas composition and treatment potential of awaste incineration plant. Appl Sci 12, 5236.

[32] F, C.G, B.J.G, H.S, R.S. Neuwahl, Best Available Techniques (BAT) Reference Document for Waste Incineration, (2019).

[33] Antonioni, G., Dal Pozzo, A., Guglielmi, D., Tugnoli, A., Cozzani, V., 2016. Enhanced modelling of heterogeneous gas-solid reactions in acid gas removal dry processes. Chem Eng Sci 148, 140–154. https://doi.org/10.1016/j.ces.2016.03.009.

[34] Barba, D., Brandani, F., Capocelli, M., Luberti, M., Zizza, A., 2015. Process analysis of an industrial waste-to-energy plant: theory and experiments. Process Saf Environ Prot 96, 61–73.

[35] Randall, D., Shoraka-Blair, S., 1994. An evaluation of the cost of incinerating wastes containing PVC. ASME Research Report. CRTD, p. 31.

[36] Zhou, C., Xi, W., Yang, L., Li, B., 2022. Chlorine emission characteristics and control status of coal-fired units. Energy Rep 8, 51–58. https://doi.org/10.1016/j.egyr.2021.11.129.

[37] Wolf, C., Stephan, A., Fendt, S., Spliethoff, H., 2017. Measuring gaseous HCl emissions during pulverised co-combustion of high shares of straw in an entrained flow reactor. Energy Procedia 120, 246–253. https://doi.org/10.1016/j.egypro.2017.07.174.

[38] Brough, D., Jouhara, H., 2020. The aluminium industry: a review on state-of-the-art technologies, environmental impacts and possibilities for waste heat recovery. Int J Thermofluids 12, 100007. https://doi.org/10.1016/j.ijft.2019.100007.

[39] Monfort, E., García-Ten, J., Celades, I., Gomar, S., 2010. Monitoring and possible reduction of HF in stack flue gases from ceramic tiles. J Fluor Chem 131, 6–12. https://doi.org/10.1016/j.jfluchem.2009.09.008.

[40] Evans, C.D., Monteith, D.T., Fowler, D., Cape, J.N., Brayshaw, S., 2011. Hydrochloric acid: an overlooked driver of environmental change. Environ Sci Technol 45, 1887–1894. https://doi.org/10.1021/es103574u.

[41] Fan, X., Cai, J., Yan, C., Zhao, J., Guo, Y., Li, C., Dällenbach, K.R., Zheng, F., Lin, Z., Chu, B., Wang, Y., Dada, L., Zha, Q., Du, W., Kontkanen, J., Kurtén, T., Iyer, S., Kujansuu, J.T., Petäjä, T., Worsnop, D.R., Kerminen, V.M., Liu, Y., Bianchi, F., Tham, Y.J., Yao, L., Kulmala, M., 2021. Atmospheric gaseous hydrochloric and hydrobromic acid in urban Beijing, China: detection, source identification and potential atmospheric impacts. Atmos Chem Phys 21, 11437–11452. https://doi.org/10.5194/acp-21-11437-2021.

[42] Radojevic, M., Bashkin, V.N., 2006. Pract Environ Anal.

[43] Damgaard, A., Riber, C., Fruergaard, T., Hulgaard, T., Christensen, T.H., 2010. Life-cycle-assessment of the historical development of air pollution control and energy recovery in waste incineration. Waste Manag 30, 1244–1250. https://doi.org/10.1016/j.wasman.2010.03.025.

[44] Van Caneghem, J., Van Acker, K., De Greef, J., Wauters, G., Vandecasteele, C., 2019. Waste-to-energy is compatible and complementary with recycling in the circular economy. Clean Technol Environ Policy 21, 925–939. https://doi.org/10.1007/s10098-019-01686-0.

[45] Communication from the Commission to the European Parliament, the Council, the European Economic and Social Committee, and the Committee of the Regions, Pathway to a Healthy Planet for All EU Action Plan: "Towards Zero Pollution for Air, Water and Soil", 12.5.2021., (n.d.).

[46] Directive 2010/75/EU of the European Parliament and of the Council on The, emissions (integrated pollution prevention and control) and Council Directive 1999/31/EC on landfill of waste, 1785 (2024) 1–47.

[47] Jiao, X., Liu, X., Gu, Y., Wu, X., Wang, S., Zhou, Y., 2020. Satellite verification of ultra-low emission reduction effect of coal-fired power plants. Atmos Pollut Res 11, 1179–1186. https://doi.org/10.1016/j.apr.2020.04.005.

[48] Zheng, B., Tong, D., Li, M., Liu, F., Hong, C., Geng, G., Li, H., Li, X., Peng, L., Qi, J., Yan, L., Zhang, Y., Zhao, H., Zheng, Y., He, K., Zhang, Q., 2018. Trends in China's anthropogenic emissions since 2010 as the consequence of clean air actions. Atmos Chem Phys 18, 14095–14111. https://doi.org/10.5194/acp-18-14095-2018.

[49] Ma, W., Cui, J., Abdoulaye, B., Wang, Y., Du, H., Bourtsalas, A.C., Chen, G., 2023. Air pollutant emission inventory of waste-to-energy plants in China and prediction by the artificial neural network approach. Environ Sci Technol 57, 874–883. https://doi.org/10.1021/acs.est.2c01087.

[50] Dal Pozzo, A., Abagnato, S., Cozzani, V., 2023. Assessment of cross-media effects deriving from the application of lower emission standards for acid pollutants in waste-to-energy plants. Sci Total Environ 856, 159159. https://doi.org/10.1016/j.scitotenv.2022.159159.

[51] Li, Y., Feng, D., Bai, C., Sun, S., Zhang, Y., Zhao, Y., Li, Y., Zhang, F., Chang, G., Qin, Y., 2022. Thermal synergistic treatment of municipal solid waste incineration (MSWI) fly ash and fluxing agent in specific situation: melting characteristics, leaching characteristics of heavy metals. Fuel Process Technol 233, 107311. https://doi.org/10.1016/j.fuproc.2022.107311.

[52] Yang, D., Kow, K.W., Wang, W., Meredith, W., Zhang, G., Mao, Y., Xu, M., 2024. Co-treatment of municipal solid waste incineration fly ash and alumina-/silica-containing waste: a critical review. J Hazard Mater 479, 135677. https://doi.org/10.1016/j.jhazmat.2024.135677.

[53] Vehlow, J., 2015. Air pollution control systems in WtE units: an overview. Waste Manag 37, 58–74. https://doi.org/10.1016/j.wasman.2014.05.025.

[54] Bal, M., Reddy, T.T., Meikap, B.C., 2019. Removal of HCl gas from off gases using self-priming venturi scrubber. J Hazard Mater 364, 406–418. https://doi.org/10.1016/j.jhazmat.2018.10.028.

[55] Dal Pozzo, A., Muratori, G., Antonioni, G., Cozzani, V., 2021. Economic and environmental benefits by improved process control strategies in HCl removal from waste-to-energy flue gas. Waste Manag 125, 303–315. https://doi.org/10.1016/j.wasman.2021.02.059.

[56] Dal Pozzo, A., Capecci, S., Cozzani, V., 2023. Techno-economic impact of lower emission standards for waste-to-energy acid gas emissions. Waste Manag 166, 305–314. https://doi.org/10.1016/j.wasman.2023.05.013.

[57] Beylot, A., Hochar, A., Michel, P., Descat, M., Menard, Y., Villeneuve, J., 2018. Municipal solid waste incineration in france: an overview of air pollution control techniques, emissions, and energy efficiency. J Ind Ecol 22, 1016–1026.

[58] Dal Pozzo, A., Guglielmi, D., Antonioni, G., Tugnoli, A., 2018. Environmental and economic performance assessment of alternative acid gas removal technologies for waste-to-energy plants. Sustain Prod Consum 16, 202–215. https://doi.org/10.1016/j.spc.2018.08.004.

[59] Sobczyk, A.T., Marchewicz, A., Krupa, A., Śliwiński, Ł., Jaworek, A., 2024. Collection efficiency of hybrid electrostatic filter with in-duct sorbent injection. Fuel 375, 132559. https://doi.org/10.1016/j.fuel.2024.132559.

[60] Katolicky, J., Jicha, M., 2013. Influence of the lime slurry droplet spectrum on the efficiency of semi-dry flue gas desulfurization. Chem Eng Technol 36, 156–166. https://doi.org/10.1002/ceat.201100690.

[61] Saleem, M., Krammer, G., 2007. Effect of filtration velocity and dust concentration on cake formation and filter operation in a pilot scale jet pulsed bag filter. J Hazard Mater 144, 677–681. https://doi.org/10.1016/j.jhazmat.2007.01.094.

[62] Shemwell, B.E., Ergut, A., Levendis, Y.A., 2002. Economics of an integrated approach to control SO_2, NO_x, HCl, and particulate emissions from power plants. J Air Waste Manag Assoc 52, 521–534. https://doi.org/10.1080/10473289.2002.10470805.

[63] Wang, Y., Su, W., Chen, J., Xing, Y., Zhang, H., Qian, D., 2023. A review of hydrogen chloride removal from calcium- and sodium-based sorbents. Environ Sci Pollut Res 30, 73116–73136. https://doi.org/10.1007/s11356-023-27322-5.

[64] Page, M.J., Moher, D., Bossuyt, P.M., Boutron, I., Hoffmann, T.C., Mulrow, C.D., Shamseer, L., Tetzlaff, J.M., Akl, E.A., Brennan, S.E., Chou, R., Glanville, J., Grimshaw, J.M., Hróbjartsson, A., Lalu, M.M., Li, T., Loder, E.W., Mayo-Wilson, E., Mcdonald, S., Mcguinness, L.A., Stewart, L.A., Thomas, J., Tricco, A.C., Welch, V.A., Whiting, P., Mckenzie, J.E., 2021. PRISMA 2020 explanation and elaboration: updated guidance and exemplars for reporting systematic reviews. BMJ 372. https://doi.org/10.1136/bmj.n160.

[65] Harrington, W., Morgenstern, R., Shih, J.S., Bell, M.L., 2012. Did the clean air act amendments of 1990 really improve air quality? Air Qual Atmos Health 5, 353–367. https://doi.org/10.1007/s11869-012-0176-5.

[66] Dong, J., Jeswani, H.K., Nzihou, A., Azapagic, A., 2020. The environmental cost of recovering energy from municipal solid waste. Appl Energy 267, 114792. https://doi.org/10.1016/j.apenergy.2020.114792.

[67] Margallo, M., Taddei, M.B.M., Hernández-Pellón, A., Aldaco, R., Irabien, Á., 2015. Environmental sustainability assessment of the management of municipal solid waste incineration residues: a review of the current situation. Clean Technol Environ Policy 17, 1333–1353. https://doi.org/10.1007/s10098-015-0961-6.

[68] Dal Pozzo, A., Lucquiaud, M., De Greef, J., 2023. Research and Innovation Needs for the Waste-To-Energy Sector towards a Net-Zero Circular Economy. Energ (Basel) 16, 1–14. https://doi.org/10.3390/en16041909.

[69] De Greef, J., Villani, K., Goethals, J., Van Belle, H., Van Caneghem, J., Vandecasteele, C., 2013. Optimising energy recovery and use of chemicals, resources and materials in modern waste-to-energy plants. Waste Manag 33, 2416–2424. https://doi.org/10.1016/j.wasman.2013.05.026.

[70] Tang, L., Qu, J., Mi, Z., Bo, X., Chang, X., Anadon, L.D., Wang, S., Xue, X., Li, S., Wang, X., Zhao, X., 2019. Substantial emission reductions from Chinese power plants after the introduction of ultra-low emissions standards. Nat Energy 4, 929–938. https://doi.org/10.1038/s41560-019-0468-1.

[71] Pollock, W.A., Tomany, J.P., Frieling, G., 1967. Sulfur dioxide and fly ash removal from coal burning power plants. Air Eng 9, 24–28.

[72] S, E.H, B.I, Petrini, 1979. HCl-Absorption durch Kalkstein (in German). Aufbereitungstechnik 6, 309–311.

[73] Foo, R., Berger, R., Heiszwolf, J.J., Reaction Kinetic Modeling of DSI for MATS Compliance., Power Plant Pollutant Control and Carbon Management "MEGA" Symposium (16-19 August 2016), Baltimore, MD (USA). (2016).

[74] Weinell, C.E., Jensen, P.I., Dam-Johansen, K., Livbjerg, H., 1992. Hydrogen chloride reaction with lime and limestone: kinetics and sorption capacity. Ind Eng Chem Res 31, 164–171. https://doi.org/10.1021/ie00001a023.

[75] Moran, D.L., Rostam-Abadi, M., 1996. High Surface Area Hydrated Lime and Method of Removing SO2 from a Gas Stream.

[76] Shin, H.G., Kim, H., Kim, Y.N., Lee, H.S., 2009. Preparation and characterization of high surface area calcium hydroxide sorbent for SO_2 removal. Curr Appl Phys 9, S276–S279. https://doi.org/10.1016/j.cap.2009.01.036.

[77] R. Foo, J. Dickerman, J. Hunt, L. Johnson, J. Heiszwolf, ESP Compatible Calcium Sorbent for SO2 Capture at Great River Energy's Stanton Station. Presented at: Power Plant Pollutant Control and Carbon Management "MEGA" Symposium (16-19 August 2016), Baltimore, MD (USA), (2016).

[78] Jozewicz, W., Gullett, B.K., 1995. Reaction mechanisms of dry Ca-based sorbents with gaseous HCl. Ind Eng Chem Res 34, 607–612. https://doi.org/10.1021/ie00041a022.

[79] Allal, K.M., Dolignier, J.C., Martin, G., 1998. Reaction mechanism of calcium hydroxide with gaseous hydrogen chloride. Rev De l'Inst Fr Du Pet 53, 871–880. https://doi.org/10.2516/ogst:1998074.

[80] Chin, T., Yan, H., Liang, D.T., 2005. Study of the reaction of lime with HCl under simulated flue gas conditions using X-ray diffraction characterization and thermodynamic prediction. Ind Eng Chem Res 44, 8730–8738. https://doi.org/10.1021/ie058021v.

[81] Partanen, J., Backman, P., Backman, R., Hupa, M., 2005. Absorption of HCl by limestone in hot flue gases. Part II: Importance of calcium hydroxychloride. Fuel 84, 1674–1684. https://doi.org/10.1016/j.fuel.2005.02.012.

[82] Dal Pozzo, A., Moricone, R., Antonioni, G., Tugnoli, A., Cozzani, V., 2018. Hydrogen chloride removal from flue gas by low-temperature reaction with calcium hydroxide. Energy Fuels 32, 747–756. https://doi.org/10.1021/acs.energyfuels.7b03292.

[83] Bogush, A.A., Stegemann, J.A., Roy, A., 2019. Changes in composition and lead speciation due to water washing of air pollution control residue from municipal waste incineration. J Hazard Mater 361, 187–199. https://doi.org/10.1016/j.jhazmat.2018.08.051.

[84] Dal Pozzo, A., Armutlulu, A., Rekhtina, M., Müller, C.R., Cozzani, V., 2018. CO_2 uptake potential of Ca-based air pollution control residues over repeated carbonation-calcination cycles. Energy Fuels 32, 5386–5395. https://doi.org/10.1021/acs.energyfuels.8b00391.

[85] Huang, J., Jin, Y., Chu, X., Shu, Z., Ma, X., Liu, J., 2024. Recovery of lead and chlorine via thermal co-treatment of municipal solid waste incineration fly ash and lead-rich waste cathode-ray tubes: analysis of chlorination volatilization mechanism. J Hazard Mater 462, 132752. https://doi.org/10.1016/j.jhazmat.2023.132752.

[86] Samouh, H., Kumar, V., Santiago, H.M., Garg, N., 2023. Enhancing phase identification in waste-to-energy fly ashes: role of Raman spectroscopy, background fluorescence, and photobleaching. J Hazard Mater 460, 132462. https://doi.org/10.1016/j.jhazmat.2023.132462.

[87] Wang, R., Liu, X., Chen, C., Wang, Y., Shen, Z., Meng, L., Gu, X., Sheng, C., Duan, Y., 2023. CaO hydrated with ethanol solution for flue gas HCl immobilization. Part I: Modification & dechlorination. Fuel 348, 128589. https://doi.org/10.1016/j.fuel.2023.128589.

[88] Billen, P., Verbinnen, B., De Smet, M., Dockx, G., Ronsse, S., Villani, K., De Greef, J., Van Caneghem, J., Vandecasteele, C., 2015. Comparison of solidification/stabilization of fly ash and air pollution control residues from municipal solid waste incinerators with and without cement addition. J Mater Cycles Waste Manag 17, 229–236. https://doi.org/10.1007/s10163-014-0292-4.

[89] Kaiser, S., Weigl, K., Spiess-Knafl, K., Aichernig, C., Friedl, A., 2000. Modeling a dry-scrubbing flue gas cleaning process. Chem Eng Process Process Intensif 39, 425–432. https://doi.org/10.1016/S0255-2701(99)00107-5.

[90] Ružovič, T., Svoboda, K., Leitner, J., Pohořelý, M., Hartman, M., 2020. Thermodynamic possibilities of flue gas dry desulfurization, de-HCl, removal of mercury, and zinc compounds in a system with Na_2CO_3, $Ca(OH)_2$, sulfur, and HBr addition. Chem Pap 74, 951–962. https://doi.org/10.1007/s11696-019-00930-7.

[91] Mocek, K., Lippert, E., Erdös, E., 1983. Reactivity of the solid sodium carbonate towards the gaseous hydrogen chloride and the sulphur dioxide. Collect Czechoslov Chem Commun 48, 3500–3507. https://doi.org/10.1135/cccc19833500.

[92] Kimura, J.M., Smith, S., 1987. Kinetics of the sodium carbonate-sulfur dioxide reaction. AIChE J 33, 1522–1532.

[93] Brivio, S., 2007. Depurazione dei fumi e valorizzazione dei prodotti (Flue gas cleaning and by-product valorization) (In Italian). Power Technol 4, 42–44.

[94] Raclavska, H., Matysek, D., Raclavsky, K., Juchelkova, D., 2010. Geochemistry of fly ash from desulphurisation process performed by sodium bicarbonate. Fuel Process Technol 91, 150–157. https://doi.org/10.1016/j.fuproc.2009.09.004.

[95] Decuyper, M., Berteu, P., 2005. NEUTREC overview of the development of dry sodium bicarbonate flue gas cleaning process in Europe. Takuma Tech Rev 13, 16–30.

[96] Hartman, M., Svoboda, K., Pohořelý, M., Šyc, M., Skoblia, S., Chen, P.C., 2014. Reaction of hydrogen chloride gas with sodium carbonate and its deep removal in a fixed-bed reactor. Ind Eng Chem Res 53, 19145–19158. https://doi.org/10.1021/ie503480k.

[97] Hwang, I.H., Matsuo, T., Matsuto, T., Tojo, Y., Sameshima, R., 2021. Dry scrubbing of municipal solid waste incineration flue gas using porous sodium carbonate produced via vacuum thermal treatment of sodium bicarbonate. J Mater Cycles Waste Manag 23, 1609–1616. https://doi.org/10.1007/s10163-021-01241-4.

[98] Dal Pozzo, A., Moricone, R., Tugnoli, A., Cozzani, V., 2019. Experimental investigation of the reactivity of sodium bicarbonate toward hydrogen chloride and sulfur dioxide at low temperatures. Ind Eng Chem Res 58, 6316–6324. https://doi.org/10.1021/acs.iecr.9b00610.

[99] Yasui, S., Shojo, T., Inoue, G., Koike, K., Takeuchi, A., Iwasa, Y., 2012. Gas-solid reaction properties of fluorine compounds and solid adsorbents for off-gas treatment from semiconductor facility. Int J Chem Eng 2012. https://doi.org/10.1155/2012/329419.

[100] Dal Pozzo, A., Lazazzara, L., Antonioni, G., Cozzani, V., 2020. Techno-economic performance of HCl and SO_2 removal in waste-to-energy plants by furnace direct sorbent injection. J Hazard Mater 394, 122518. https://doi.org/10.1016/j.jhazmat.2020.122518.

[101] Moreschi, R., Marras, R., 2014. Method for controlling the emission of polluting substances in a gaseous effluent produced by a combustion process. Int Pat N° WO2014080373A2.

[102] Filitz, R., Kierzkowska, A.M., Broda, M., Müller, C.R., 2012. Highly efficient CO_2 sorbents: development of synthetic, calcium-rich dolomites. Environ Sci Technol 46, 559–565. https://doi.org/10.1021/es2034697.

[103] Biganzoli, L., Racanella, G., Rigamonti, L., Marras, R., Grosso, M., 2015. High temperature abatement of acid gases from waste incineration. Part I: Experimental tests in full scale plants. Waste Manag 36, 98–105. https://doi.org/10.1016/j.wasman.2014.10.019.

[104] Zhou, Z., Chi, Y., Tang, Y., Hu, J., 2021. Effect of calcium-based sorbents on the reduction of chlorinated contaminants during municipal solid waste thermal treatment. Waste Manag Res 39, 1480–1488. https://doi.org/10.1177/0734242X21989793.

[105] Chen, D., Wang, X., Zhu, T., Zhang, H., 2003. HCl dry removal with modified Ca-based sorbents at moderate to high temperatures. J Therm Sci 12. https://doi.org/10.1007/s11630-003-0084-y.

[106] Zhao, Y., Liu, G., Huang, J., Veksha, A., Wu, X., Giannis, A., Lim, T.T., Lisak, G., 2022. Sorbents for high-temperature removal of alkali metals and HCl from municipal solid waste derived syngas. Fuel 321, 124058. https://doi.org/10.1016/j.fuel.2022.124058.

[107] Liang, S., Fan, Z., Zhang, W., Guo, M., Cheng, F., Zhang, M., 2017. Controllable growth of Na_2CO_3 fibers for mesoporous activated alumina ball modification towards the high-efficiency adsorption of HCl gas at low temperature. RSC Adv 7, 53306–53315. https://doi.org/10.1039/c7ra10790k.

[108] Karami, D., Mahinpey, N., 2012. Highly active CaO-based sorbents for CO_2 capture using the precipitation method: preparation and characterization of the sorbent powder. Ind Eng Chem Res 51, 4567–4572. https://doi.org/10.1021/ie2024257.

[109] Kierzkowska, A.M., Poulikakos, L.V., Broda, M., Müller, C.R., 2013. Synthesis of calcium-based, Al_2O_3-stabilized sorbents for CO_2 capture using a co-precipitation technique. Int J Greenh Gas Control 15, 48–54. https://doi.org/10.1016/j.ijggc.2013.01.045.

[110] Pacciani, R., Müller, C.R., Davidson, J.F., Dennis, J.S., Hayhurst, A.N., 2008. Synthetic Ca-based solid sorbents suitable for capturing CO_2 in a fluidized bed. Can J Chem Eng 86, 356–366. https://doi.org/10.1002/cjce.20060.

[111] Wang, Q., O'Hare, D., 2012. Recent advances in the synthesis and application of layered double hydroxide (LDH) nanosheets. Chem Rev 112, 4124–4155. https://doi.org/10.1002/bkcs.12649.

[112] Kameda, T., Uchiyama, N., Yoshioka, T., 2010. Treatment of gaseous hydrogen chloride using Mg-Al layered double hydroxide intercalated with carbonate ion. Chemosphere 81, 658–662. https://doi.org/10.1016/j.chemosphere.2010.07.066.

[113] Kameda, T., Tochinai, M., Kumagai, S., Yoshioka, T., 2020. Treatment of HCl gas by cyclic use of Mg–Al layered double hydroxide intercalated with CO_3^{2-}. Atmos Pollut Res 11, 290–295. https://doi.org/10.1016/j.apr.2019.11.001.

[114] Kameda, T., Takahashi, Y., Kumagai, S., Saito, Y., Fujita, S., Itou, I., Han, T., Yoshioka, T., 2022. Comparison of Mg–Al layered double hydroxides intercalated with OH^- and CO_3^{2-} for the removal of HCl, SO_2, and NO_2. J Porous Mater 29, 723–728. https://doi.org/10.1007/s10934-022-01206-4.

[115] Kameda, T., Uchida, H., Kumagai, S., Saito, Y., Mizushina, K., Itou, I., Han, T., Yoshioka, T., 2021. Regeneration of carbonate-intercalated Mg–Al layered double hydroxides (CO_3·Mg–Al LDHs) by CO_2-induced desorption of anions (X) from X·Mg–Al LDH (X = Cl, SO_4, or NO_3): a kinetic study. Chem Eng Res Des 165, 207–213. https://doi.org/10.1016/j.cherd.2020.10.032.

[116] Cao, J., Chen, T., Jin, B., Huang, Y., Hu, C., 2019. Adsorption of HCl on Calcined Ca and Zn Hydrotalcite-like Compounds (HTLs) at Medium-High Temperature in Flue Gas. Ind Eng Chem Res 58, 18–26. https://doi.org/10.1021/acs.iecr.8b03092.

[117] Cao, J., Zhong, W., Jin, B., Wang, Z., Wang, K., 2014. Treatment of hydrochloric acid in flue gas from municipal solid waste incineration with Ca-Mg-Al mixed oxides at medium-high temperatures. Energy Fuels 28, 4112–4117. https://doi.org/10.1021/ef5008193.

[118] Do, J.L., Friščić, T., 2017. Mechanochemistry: a force of synthesis. ACS Cent Sci 3, 13–19. https://doi.org/10.1021/acscentsci.6b00277.

[119] Sayyah, M., Lu, Y., Masel, R.I., Suslick, K.S., 2013. Mechanical activation of CaO-based adsorbents for CO_2 capture. ChemSusChem 6, 193–198. https://doi.org/10.1002/cssc.201200454.

[120] Wysocki, D., Szymanek, A., 2022. The effectiveness of modified sodium bicarbonate in the purification of exhaust gases from HCl and HF. J Achiev Mater Manuf Eng 114, 57–66. https://doi.org/10.5604/01.3001.0016.2156.

[121] Zhou, X., Tang, W., He, M., Xiao, X., Wang, T., Cheng, S., Zhang, L., 2023. Combined removal of SO_3 and HCl by modified $Ca(OH)_2$ from coal-fired flue gas. Sci Total Environ 857, 1–8. https://doi.org/10.1016/j.scitotenv.2022.159466.

[122] Kurlov, A., Broda, M., Hosseini, D., Mitchell, S.J., Pérez-Ramírez, J., Müller, C.R., 2016. Mechanochemically activated, calcium oxide-based, magnesium oxide-stabilized carbon dioxide sorbents. ChemSusChem 9, 2380–2390. https://doi.org/10.1002/cssc.201600510.

[123] Shen, Z., Liu, X., Ning, X., Wang, R., Yue, P., Shen, A., Meng, L., Wang, Y., Gu, X., Duan, Y., 2023. Investigation on mechanochemically modified calcium-based adsorbent for flue gas HCl removal, Asia-Pacific. J Chem Eng 18, 1–12. https://doi.org/10.1002/apj.2861.

[124] Dou, B., Gao, J., Baek, S.W., Sha, X., 2003. High-temperature HCl removal with sorbents in a fixed-bed reactor. Energy Fuels 17, 874–878. https://doi.org/10.1021/ef010294p.

[125] Dou, B., Chen, B., Gao, J., Sha, X., 2005. Reaction of solid sorbents with hydrogen chloride gas at high temperature in a fixed-bed reactor. Energy Fuels 19, 2229–2234. https://doi.org/10.1021/ef050151t.

[126] Fujita, S., Suzuki, K., Ohkawa, M., Shibasaki, Y., Mori, T., 2001. Reaction of hydrogrossular with hydrogen chloride gas at high temperature. Chem Mater 13, 2523–2527. https://doi.org/10.1021/cm000863r.

[127] Tsubouchi, N., Matsuoka, N., Fukuyama, K., Mochizuki, Y., 2020. Removal of hydrogen chloride gas using honeycomb-supported natural soda ash. Chem Eng Res Des 156, 138–145. https://doi.org/10.1016/j.cherd.2020.01.012.

[128] Wu, W., Wu, Y., Jin, B., Gu, Q., 2019. Synthesis, characterization, and high-temperature HCl capture capacity of different proportions of potassium fluoride-doped CaMgAl layered double hydroxides. ACS Omega 4, 18159–18166. https://doi.org/10.1021/acsomega.9b02069.

[129] Liu, Q., Ehite, E., Houston, R., Li, Y., Pope, C., Labbé, N., Abdoulmoumine, N., 2021. Synthesis and evaluation of layered double hydroxide based sorbent for hot gas cleanup of hydrogen chloride. Mater Sci Energy Technol 4, 46–53. https://doi.org/10.1016/j.mset.2020.12.003.

[130] Cao, S., Cao, J., Zhu, H., Huang, Y., Jin, B., Materazzi, M., 2024. Removal of HCl from gases using modified calcined Mg-Al-CO_3 hydrotalcite: performance, mechanism, and adsorption kinetics. Fuel 355, 129445. https://doi.org/10.1016/j.fuel.2023.129445.

[131] Wajima, T., Takahashi, T., 2021. Synthesis of hydrogrossular and hydroxysodalite from blast furnace slag using alkali fusion for fixation of HCl gas. J Phys Conf Ser 1777. https://doi.org/10.1088/1742-6596/1777/1/012017.

[132] Bhaskar, T., Matsui, T., Nitta, K., Uddin, M.A., Muto, A., Sakata, Y., 2002. Laboratory evaluation of calcium-, iron-, and potassium-based carbon composite sorbents for capture of hydrogen chloride gas. Energy Fuels 16, 1533–1539. https://doi.org/10.1021/ef020094t.

[133] Nunokawa, M., Kobayashi, M., Shirai, H., 2008. Halide compound removal from hot coal-derived gas with reusable sodium-based sorbent. Powder Technol 180, 216–221. https://doi.org/10.1016/j.powtec.2007.03.029.

[134] Liu, X., Wang, R., Geng, X., Shen, A., Chen, C., Xu, Y., Ding, X., Duan, Y., Zhao, S., 2023. Intrinsic reaction selectivity between gaseous HCl and SO_2 over ethanol-hydrated CaO adsorbent in coal-fired flue gas dechlorination. Chem Eng J 473, 145019. https://doi.org/10.1016/j.cej.2023.145019.

[135] Marocco, L., Mora, A., 2013. CFD modeling of the Dry-Sorbent-Injection process for flue gas desulfurization using hydrated lime. Sep Purif Technol 108, 205–214. https://doi.org/10.1016/j.seppur.2013.02.012.

[136] Kavouras, A., Breitschaedel, B., Krammer, G., Garea, A., Marques, J.A., Irabien, A., 2002. SO_2 removal in the filter cake of a jet-pulsed filter: a combined filter and fixed-bed reaction model. Ind Eng Chem Res 41, 5459–5469. https://doi.org/10.1021/ie020281e.

[137] Zach, B., Šyc, M., Svoboda, K., Pohořely, M., Šomplák, R., Brynda, J., Mošťko, J., Punčochár, M., 2021. The influence of SO_2 and HCl concentrations on the consumption of sodium bicarbonate during flue gas treatment. Energy Fuels 35, 5064–5073. https://doi.org/10.1021/acs.energyfuels.0c03655.

[138] Kim, K.D., Jeon, S.M., Hasolli, N., Lee, K.S., Lee, J.R., Han, J.W., Kim, H.T., Park, Y.O., 2017. HCl removal characteristics of calcium hydroxide at the dry-type sorbent reaction accelerator using municipal waste incinerator flue gas at a real site. Korean J Chem Eng 34, 747–756. https://doi.org/10.1007/s11814-016-0306-0.

[139] Fellows, K.T., Pilat, M.J., 1990. HCl sorption by dry $NaHCO_3$ for incinerator emissions control. J Air Waste Manag Assoc 40, 887–893. https://doi.org/10.1080/10473289.1990.10466734.

[140] Gullett, B.K., Jozewicz, W., Stefanski, L.A., 1992. Reaction kinetics of Ca-based sorbents with HCl. Ind Eng Chem Res 31, 2437–2446. https://doi.org/10.1021/ie00011a005.

[141] Ravina, M., Marotta, E., Cerutti, A., Zanetti, G., Ruffino, B., Panepinto, D., Zanetti, M., 2023. Evaluation of Ca-based sorbents for gaseous HCl emissions adsorption. Sustain (Switz) 15. https://doi.org/10.3390/su151410882.

[142] Daoudi, M., Walters, J.K., 1991. A thermogravimetric study of the reaction of hydrogen chloride gas with calcined limestone: determination of kinetic

parameters. Chem Eng J 47, 1–9. https://doi.org/10.1016/0300-9467(91)85001-C.
[143] Yan, R., Chin, T., Liang, D.Tee, Laursen, K., Ong, W.Y., Yao, K., Tay, J.H., 2003. Kinetic study of hydrated lime reaction with HCl. Environ Sci Technol 37, 2556–2562. https://doi.org/10.1021/es020902v.
[144] Bausach, M., Krammer, G., Cunill, F., 2004. Reaction of $Ca(OH)_2$ with HCl in the presence of water vapour at low temperatures. Thermochim Acta 421, 217–223. https://doi.org/10.1016/j.tca.2004.04.011.
[145] Partanen, J., Backman, P., Backman, R., Hupa, M., 2005. Absorption of HCl by limestone in hot flue gases. Part I: The effects of temperature, gas atmosphere and absorbent quality. Fuel 84, 1664–1673. https://doi.org/10.1016/j.fuel.2005.02.011.
[146] Chin, T., Yan, R., Liang, D.T., Tay, J.H., 2005. Hydrated lime reaction with HCl under simulated flue gas conditions. Ind Eng Chem Res 44, 3742–3748. https://doi.org/10.1021/ie040206z.
[147] Karlsson, H.T., Klingspor, J., Bjerle, I., 1981. Adsorption of hydrochloric acid on solid slaked lime for flue gas clean up. J Air Pollut Control Assoc 31, 1177–1180. https://doi.org/10.1080/00022470.1981.10465343.
[148] Byer, S.G., Wong, C., Yang, R.T., Reinhardt, J.R., 1983. Kinetics of the reaction between HF and CaO for fluoride emission control. Environ Sci Technol 17, 84–88. https://doi.org/10.1021/es00108a004.
[149] Kossaya, A.M., Sandrozd, M.K., Kuchma, Z.V., Belyakov, B.P., Vasil, V.G., 1984. 'eva, Kinetics of the reactions of hydrogen fluoride with calcium oxide. Zh Prikl Khimii 59, 162–165.
[150] Mura, G., Lallai, A., 1994. Reaction kinetics of gas hydrogen chloride and limestone. Chem Eng Sci 49, 4491–4500.
[151] Fonseca, A.M., Órfão, J.J., Salcedo, R.L., 1998. Kinetic modeling of the reaction of HCl and solid lime at low temperatures. Ind Eng Chem Res 37, 4570–4576. https://doi.org/10.1021/ie980320f.
[152] Chisholm, P.N., Rochelle, G.T., 1999. Dry absorption of HCl and SO_2 with hydrated lime from humidified flue gas. Ind Eng Chem Res 38, 4068–4080. https://doi.org/10.1021/ie9806601.
[153] Li, M., Shaw, H., Yang, C.L., 2000. Reaction kinetics of hydrogen chloride with calcium oxide by fourier transform infrared spectroscopy. Ind Eng Chem Res 39, 1898–1902. https://doi.org/10.1021/ie990628m.
[154] Dou, B., Gao, J., Baek, S.W., Sha, X., 2003. High-temperature HCl removal with sorbents in a fixed-bed reactor. Energy Fuels 17, 874–878. https://doi.org/10.1021/ef010294p.
[155] Verdone, N., De Filippis, P., 2006. Reaction kinetics of hydrogen chloride with sodium carbonate. Chem Eng Sci 61, 7487–7496. https://doi.org/10.1016/j.ces.2006.08.023.
[156] Chyang, C.S., Han, Y.L., Zhong, Z.C., 2009. Study of HCl absorption by CaO at high temperature. Energy Fuels 23, 3948–3953. https://doi.org/10.1021/ef900234p.
[157] Afzal, S., Rahimi, A., Ehsani, M.R., Tavakoli, H., 2010. Experimental study of hydrogen fluoride adsorption on sodium fluoride. J Ind Eng Chem 16, 147–151. https://doi.org/10.1016/j.jiec.2010.01.004.
[158] Li, C., He, S., Jiang, D., Li, Q., 2012. Hydrogen fluoride adsorption ability of some inorganic compounds. Adv Mat Res 412, 1–4. https://doi.org/10.4028/www.scientific.net/AMR.412.1.
[159] Tan, J., Yang, G., Mao, J., Dai, H., 2014. Laboratory study on high-temperature adsorption of HCl by dry-injection of $Ca(OH)_2$ in a dual-layer granular bed filter. Front Environ Sci Eng 8, 863–870. https://doi.org/10.1007/s11783-013-0618-9.
[160] Lin, G.M., Chyang, C.S., 2017. Removal of HCl in flue gases by calcined limestone at high temperatures. Energy Fuels 31, 12417–12424. https://doi.org/10.1021/acs.energyfuels.7b01830.
[161] Sohn, J.S., Rho, S.G., Sohn, J.Y., Lim, M.H., Sadhasivam, T., Lim, H., Ryi, S.K., Jung, H.Y., 2019. Efficient solid reducing agent CaO/SiO_2 hybrid composite for hydrogen fluoride elimination. Adv Compos Mater 28, 65–77. https://doi.org/10.1080/09243046.2018.1458484.
[162] Iizuka, A., Morishita, Y., Shibata, E., Takatoh, C., Cho, H., 2020. Basic study of the reaction of calcium hydroxide with hydrogen chloride using single crystals. Ind Eng Chem Res 59, 9699–9704. https://doi.org/10.1021/acs.iecr.9b06967.
[163] Ephraim, A., Ngo, L.D., Pham Minh, D., Lebonnois, D., Peregrina, C., Sharrock, P., Nzihou, A., 2019. Valorization of waste-derived inorganic sorbents for the removal of HCl in syngas. Waste Biomass Valoriz 10, 3435–3446. https://doi.org/10.1007/s12649-018-0355-1.
[164] Shemwell, B., Levendis, Y.A., Simons, G.A., 2001. Laboratory study on the high-temperature capture of HCl gas by dry-injection of calcium-based sorbents. Chemosphere 42, 785–796. https://doi.org/10.1016/S0045-6535(00)00252-6.
[165] Lancia, A., Musmarra, D., Pepe, F., 1999. Wet-dry process of HCl removal from flue gas: experimental study on operating parameters. Int J Environ Stud 56, 629–640. https://doi.org/10.1080/00207239908711228.
[166] Liu, K., Pan, W.P., Riley, J.T., 2000. Study of chlorine behavior in a simulated fluidized bed combustion system. Fuel 79, 1115–1124. https://doi.org/10.1016/S0016-2361(99)00247-1.
[167] Wang, Z., Huang, H., Li, H., Wu, C., Chen, Y., Li, B., 2002. HCl formation from RDF pyrolysis and combustion in a spouting-moving bed reactor. Energy Fuels 16, 608–614. https://doi.org/10.1021/ef0101863.
[168] Sun, Z., Yu, F.C., Li, F., Li, S., Fan, L.S., 2011. Experimental study of HCl capture using CaO sorbents: activation, deactivation, reactivation, and ionic transfer mechanism. Ind Eng Chem Res 50, 6034–6043. https://doi.org/10.1021/ie102587s.
[169] Bie, R., Li, S., Yang, L., 2005. Reaction mechanism of CaO with HCl in incineration of wastewater in fluidized bed. Chem Eng Sci 60, 609–616. https://doi.org/10.1016/j.ces.2004.08.022.
[170] Borgwardt, R.H., Bruce, K.R., Blake, J., 1987. An investigation of product-layer diffusivity for CaO sulfation. Ind Eng Chem Res 26, 1993–1998. https://doi.org/10.1021/ie00070a010.
[171] Tang, W., Zhang, L., Luo, H., 2021. Experimental study on the removal of low-concentration SO_3 by trona at medium temperatures. Ind Eng Chem Res 60, 8947–8956. https://doi.org/10.1021/acs.iecr.1c01033.
[172] Ma, M., Su, W., Wang, Y., Xing, Y., Wang, J., Zhang, W., Wang, P., Li, Z., 2024. Absorption of HCl on sodium-based absorbents at medium and high temperatures: the effect of competing absorption of SO_2 and H_2O. Fuel 358, 130007. https://doi.org/10.1016/j.fuel.2023.130007.
[173] Jozewicz, W., Chang, J.C.S., Sedman, C.B., 1990. Bench–scale evaluation of calcium sorbents for acid gas emission control. Environ Prog 9, 137–142. https://doi.org/10.1002/ep.670090312.
[174] Rahaman, A., Grassian, V.H., Margulis, C.J., 2008. Dynamics of water adsorption onto a calcite surface as a function of relative humidity. J Phys Chem C 112, 2109–2115. https://doi.org/10.1021/jp077594d.
[175] Koch, M., Zhang, X., Deng, J., Kavouras, A., Krammer, G., Xu, J., Ge, L., 2005. Reaction mechanism of a single calcium hydroxide particle with humidified HCl. Chem Eng Sci 60, 5819–5829. https://doi.org/10.1016/j.ces.2005.05.035.
[176] Partanen, J., Backman, P., Hupa, M., 2001. Absorption of HCl and HF by Ca-based sorbents at FBC conditions. Proceedings of the 16th International conference on fluidized bed combustion. American Society of Mechanical Engineers, ASME, pp. 194–204.
[177] Frandsen, F.J., van Lith, S.C., Korbee, R., Yrjas, P., Backman, R., Obernberger, I., Brunner, T., Jöller, M., 2007. Quantification of the release of inorganic elements from biofuels. Fuel Process Technol 88, 1118–1128. https://doi.org/10.1016/j.fuproc.2007.06.012.
[178] qi Jin, Y., Tao, L., Chi, Y., Yan, J. hua, 2011. Conversion of bromine during thermal decomposition of printed circuit boards at high temperature. J Hazard Mater 186, 707–712. https://doi.org/10.1016/j.jhazmat.2010.11.050.
[179] S. Hippmann, T. Wolff, U. Singliar, M. Bertau, Bromine recovery from combustion gases of bromine containing plastics (WEEE), in: International Conference on Engineering for Waste and Biomass Valorisation-Waste Eng. Prague, Czech Republic., 2018.
[180] Farshchi Tabrizi, F., Dunker, M., Hiller, A., Beckmann, M., 2020. Maximizing HBr/Br_2 in the flue gas and prevention of secondary pollution during the oxy-combustion of brominated waste electrical and electronic equipment part 1-thermodynamic considerations. Environ Pollut 263, 114410. https://doi.org/10.1016/j.envpol.2020.114410.
[181] Xiao, H., Zhou, Z., Zhou, H., Liu, Q., Ren, W., Lin, H., Zhu, H., He, C., Tian, K., 2017. Conversion of HBr to Br_2 in the flue gas from the combustion of waste printed circuit boards in post-combustion area. J Clean Prod 161, 239–244. https://doi.org/10.1016/j.jclepro.2017.05.117.
[182] Schmal, D., Ligtvoet, A.C.P., Brunia, A., 1989. Some physico-chemical aspects of dry sorbent injection for removal of HCl and HF from waste incinerator flue gases. J Air Pollut Control Assoc 39, 55–57. https://doi.org/10.1080/08940630.1989.10466508.
[183] Gao, P., Feng, J., Xie, Y., Yang, X., Ning, P., Sun, X., Wang, F., Shi, L., Zhao, J., Li, K., 2024. The removal mechanisms of HF and HCl gases using Mg-Al adsorbent prepared by sol-gel synthesis method. J Environ Chem Eng 12, 112380. https://doi.org/10.1016/j.jece.2024.112380.
[184] Ning, H., Tang, R., Li, C., Gu, X., Gong, Z., Zhu, C., Li, J., Wang, K., Yu, J., 2025. Recent advances in process and materials for dry desulfurization of industrial flue gas: an overview. Sep Purif Technol 353, 128425. https://doi.org/10.1016/j.seppur.2024.128425.
[185] Yu, H., Shan, C., Li, J., Hou, X., Yang, L., 2024. Alkaline absorbents for SO_2 and SO_3 removal: a comprehensive review. J Environ Manag 366, 121532. https://doi.org/10.1016/j.jenvman.2024.121532.
[186] Xie, W., Liu, K., Pan, W.P., Riley, J.T., 1999. Interaction between emissions of SO_2 and HCl in fluidized bed combustors. Fuel 78, 1425–1436. https://doi.org/10.1016/S0016-2361(99)00070-8.
[187] Lawrence, A., Bu, J., Gokulakrishnan, P., 1999. The interactions between SO_2, NOx, HCl and Ca in a bench-scale fluidized combustor. J Inst Energy 72, 34–40.
[188] Partanen, J., Backman, P., Backman, R., Hupa, M., 2005. Absorption of HCl by limestone in hot flue gases. Part III: simultaneous absorption with SO_2. Fuel 84, 1685–1694. https://doi.org/10.1016/j.fuel.2005.02.013.
[189] Duo, J., Laursen, W., Lim, K., Grace, J., 2000. Crystallization and fracture: formation of product layers in sulfation of calcined limestone. Powder Technol 111, 154–167.
[190] Boonsongsup, L., Iisa, K., Frederick, W.J., 1997. Kinetics of the sulfation of NaCl at combustion conditions. Ind Eng Chem Res 36, 4212–4216. https://doi.org/10.1021/ie9603225.
[191] Baciocchi, R., Polettini, A., Pomi, R., Prigiobbe, V., Von Zedwitz, V.N., Steinfeld, A., 2006. CO_2 sequestration by direct gas-solid carbonation of air pollution control (APC) residues. Energy Fuels 20, 1933–1940. https://doi.org/10.1021/ef060135b.
[192] Antonioni, G., Guglielmi, D., Cozzani, V., Stramigioli, C., Corrente, D., 2014. Modelling and simulation of an existing MSWI flue gas two-stage dry treatment. Process Saf Environ Prot 92, 242–250. https://doi.org/10.1016/j.psep.2013.02.005.
[193] Dashtestani, F., Nusheh, M., Siriwongrungson, V., Hongrapipat, J., Materic, V., Yip, A.C.K., Pang, S., 2021. Effect of the presence of HCl on simultaneous CO_2 capture and contaminants removal from simulated biomass gasification producer gas by $CaO\text{-}Fe_2O_3$ sorbent in calcium looping cycles. Energ (Basel) 14. https://doi.org/10.3390/en14238167.

[194] Xie, X., Li, Y., Wang, W., Shi, L., 2014. HCl removal using cycled carbide slag from calcium looping cycles. Appl Energy 135, 391–401. https://doi.org/10.1016/j.apenergy.2014.08.098.
[195] Xie, X., Li, Y.J., Liu, C.T., Wang, W.J., 2015. HCl absorption by $CaO/Ca_3Al_2O_6$ sorbent from CO_2 capture cycles using calcium looping. Fuel Process Technol 138, 500–508. https://doi.org/10.1016/j.fuproc.2015.06.028.
[196] Chi, C., Li, Y., Sun, R., Ma, X., Duan, L., Wang, Z., 2016. HCl removal performance of Mg-stabilized carbide slag from carbonation/calcination cycles for CO_2 capture. RSC Adv 6, 104303–104310. https://doi.org/10.1039/c6ra19972k.
[197] Criado, Y.A., Arias, B., Abanades, J.C., 2018. Effect of the carbonation temperature on the CO_2 carrying capacity of CaO. Ind Eng Chem Res 57, 12595–12599. https://doi.org/10.1021/acs.iecr.8b02111.
[198] Duo, W., Kirkby, N.F., Seville, J.P.K., Kiel, J.H.A., Bos, A., 1996. Kinetics of HCl reactions with calcium and sodium sorbents for IGCC fuel gas cleaning. Chem Eng Sci 51, 2541–2546.
[199] Liang, S., Liu, S., Fan, Z., Zhang, W., Guo, M., Cheng, F., Zhang, M., 2020. Enhanced HCl removal from CO_2-rich mixture gases by $CuOx/Na_2CO_3$ porous sorbent at low temperature: Kinetics and forecasting. Chem Eng J 381, 122738. https://doi.org/10.1016/j.cej.2019.122738.
[200] Duo, W., Kirkby, N.F., Seville, J.P.K., Kiel, J.H.A., Bos, A., Den Uil, H., 1996. Kinetics of HCl reactions with calcium and sodium sorbents for IGCC fuel gas cleaning. Chem Eng Sci 51, 2541–2546. https://doi.org/10.1016/0009-2509(96)00111-X.
[201] Pozzo, A.D., Giannella, M., Antonioni, G., Cozzani, V., 2018. Optimization of the economic and environmental profile of HCl removal in a municipal solid waste incinerator through historical data analysis. Chem Eng Trans 67, 463–468. https://doi.org/10.3303/CET1867078.
[202] Tan, Z., Niu, G., Qi, Q., Zhou, M., Wu, B., Yao, W., 2020. Ultralow emission of dust, SO_X, HCl, and NO_X using a ceramic catalytic filter tube. Energy Fuels 34, 4173–4182. https://doi.org/10.1021/acs.energyfuels.9b04480.
[203] Tamascelli, N., Dal Pozzo, A., Scarponi, G.E., Paltrinieri, N., Cozzani, V., 2024. Assessment of safety barrier performance in environmentally critical facilities: bridging conventional risk assessment techniques with data-driven modelling. Process Saf Environ Prot 181, 294–311. https://doi.org/10.1016/j.psep.2023.11.021.
[204] Zach, B., Pohořelý, M., Šyc, M., Svoboda, K., Punčochář, M., 2016. Comparison of sodium and calcium based sorbents for the dry treatment of flue gas from waste-to-energy plants. Energy Prod Manag 21st Century II Quest Sustain Energy 1, 291–299. https://doi.org/10.2495/eq160271.
[205] Dal Pozzo, A., Antonioni, G., Guglielmi, D., Stramigioli, C., Cozzani, V., 2016. Comparison of alternative flue gas dry treatment technologies in waste-to-energy processes. Waste Manag 51, 81–90. https://doi.org/10.1016/j.wasman.2016.02.029.
[206] Yassin, L., Lettieri, P., Simons, S.J.R., Germanà, A., 2007. Study of the process design and flue gas treatment of an industrial-scale energy-from-waste combustion plant. Ind Eng Chem Res 46, 2648–2656. https://doi.org/10.1021/ie060929d.
[207] Poggio, A., Grieco, E., 2010. Influence of flue gas cleaning system on the energetic efficiency and on the economic performance of a WTE plant. Waste Manag 30, 1355–1361. https://doi.org/10.1016/j.wasman.2009.09.008.
[208] Dal Pozzo, A., Guglielmi, D., Antonioni, G., Tugnoli, A., 2017. Sustainability analysis of dry treatment technologies for acid gas removal in waste-to-energy plants. J Clean Prod 162, 1061–1074. https://doi.org/10.1016/j.jclepro.2017.05.203.
[209] Stendardo, P.U., Foscolo, S., 2009. Carbon dioxide capture with dolomite: a model for gas-solid reaction within the grains of a particulate sorbent. Chem Eng Sci 64, 2343–2352.
[210] Fang, F., Li, Z.S., Cai, N.S., Tang, X.Y., Yang, H.T., 2011. AFM investigation of solid product layers of $MgSO_4$ generated on MgO surfaces for the reaction of MgO with SO_2 and O_2. Chem Eng Sci 66, 1142–1149. https://doi.org/10.1016/j.ces.2010.12.014.
[211] Dennis, J.S., Pacciani, R., 2009. The rate and extent of uptake of CO 2 by a synthetic, CaO-containing sorbent. Chem Eng Sci 64, 2147–2157. https://doi.org/10.1016/j.ces.2009.01.051.
[212] Montagnaro, F., Balsamo, M., Salatino, P., 2016. A single particle model of lime sulphation with a fractal formulation of product layer diffusion. Chem Eng Sci 156, 115–120. https://doi.org/10.1016/j.ces.2016.09.021.
[213] Ramachandran, P.A., Doraiswamy, L.K., 1982. Modeling of noncatalytic gas-solid reactions. AIChE J 881–899.
[214] Dou, B.L., Gao, J.S., Sha, X.Z., 2001. A study on the reaction kinetics of HCl removal from high-temperature coal gas. Fuel Process Technol 72, 23–33. https://doi.org/10.1016/S0378-3820(01)00176-X.
[215] Ebrahim, H.A., 2010. Application of random-pore model to SO_2 capture by lime. Ind Eng Chem Res 49, 117–122. https://doi.org/10.1021/ie901077b.
[216] Omidi Bibalani, I., Ale Ebrahim, H., 2022. Kinetic study of low-temperature sulfur dioxide removal reaction by sodium carbonate using random pore model. Environ Sci Pollut Res 29, 6334–6346. https://doi.org/10.1007/s11356-021-16073-w.
[217] Yagi, D., Kunii, S., 1955. Studies on combustion of carbon particles in flames and fluidized beds. Symp (Int) Combust 5, 231–244.
[218] Omidi, I., Ebrahim, H.A., 2021. Kinetic Study of Low Temperature Sulfur Dioxide Removal Reaction By Sodium Carbonate Using Random Pore Model 2. https://doi.org/10.21203/rs.3.rs-324950/v1. Kinetic Study of Low Temperature Sulfur Dioxide Removal Reaction By Sodium Carbonate Using Random Pore Model.
[219] Duo, W., Seville, J.P.K., Kirkby, N.F., Clift, R., 1994. Formation of product layers in solid–gas reactions for removal of acid gases. Chem Eng Sci 49, 4429–4442.
[220] Iisa, M., Hupa, K., 1990. Sulphur absorption by limestone at pressurized fluidized bed conditions. Symp (Int) Combust 23, 943–948.
[221] Simons, A.R., Garman, G.A., 1986. Small pore closure and the deactivation of the limestone sulfation reaction. AIChE J 32, 1491–1499.
[222] Duo, W., Kirkby, N.F., Seville, J.P.K., Clift, R., 1995. Alteration with reaction progress of the rate limiting step for solid-gas reactions of Ca-compounds with HCl. Chem Eng Sci 50, 2017–2027.
[223] Li, S., Bie, R., 2006. Modeling the reaction of gaseous HCl with CaO in fluidized bed. Chem Eng Sci 61, 5468–5475. https://doi.org/10.1016/j.ces.2006.04.014.
[224] Wachtman Jr, J.B., Tefft, W.E., Lam Jr, D.G., Apstein, C.S., 1961. Exponential temperature dependence of Young's modulus for several oxides. Phys Rev 122, 1754.
[225] Wang, N., Teng, B., 2009. Modeling of SO_2 removal in fabric filter. Fuel Process Technol 90, 636–642. https://doi.org/10.1016/j.fuproc.2008.10.003.
[226] Duo, W., Laursen, K., Lim, J., Grace, J., 2004. Crystallization and fracture: product layer diffusion in sulfation of calcined limestone. Ind Eng Chem Res 43, 5653–5662. https://doi.org/10.1021/ie030837d.
[227] Bacci Di Capaci, R., Pannocchia, G., Pozzo, A.D., Antonioni, G., Cozzani, V., 2022. Data-driven models for advanced control of acid gas treatment in waste-to-energy plants. IFACPap 55, 869–874. https://doi.org/10.1016/j.ifacol.2022.07.554.
[228] Birgen, C., Magnanelli, E., Carlsson, P., Becidan, M., 2021. Operational guidelines for emissions control using cross-correlation analysis of waste-to-energy process data. Energy 220, 119733. https://doi.org/10.1016/j.energy.2020.119733.
[229] De Greef, J., Hoang, Q.N., Vandevelde, R., Meynendonckx, W., Bouchaar, Z., Granata, G., Verbeke, M., Ishteva, M., Seljak, T., Van Caneghem, J., Vanierschot, M., 2023. Towards waste-to-energy-and-materials processes with advanced thermochemical combustion intelligence in the circular economy. Energies 16, 1644. https://doi.org/10.3390/en16041644.
[230] Dal Pozzo, A., Capecci, S., Cozzani, V., 2023. Techno-economic impact of lower emission standards for waste-to-energy acid gas emissions. Waste Manag 166, 305–314. https://doi.org/10.1016/j.wasman.2023.05.013.